

Republic of Iraq
Ministry of Higher Education
& Scientific Research
University of Kerbala, College of Science
Department of Chemistry



**Synthesis and Characterization of Binuclear Complexes
with Novel Heterocyclic Ligands Derived from 2,5-
dimercapto-1,3,4-thiadiazolate *Via* Click Chemistry**

A Thesis

*Submitted to the Council of the College of Science,
University of Kerbala as a partial fulfillment
of the requirements for MSc. degree in Chemistry*

By

Atheer Mahdi Madloul

B.Sc. in Chemistry (2003) Al-Mustansiriyah University

Supervised by

Assist. Prof. Dr.

Ashour Hamoad Al-Ghadeer

Assist. Prof. Dr.

Eman Taleb Kareem

1433 A.H.

2012 A.D.

بِسْمِ اللَّهِ الرَّحْمَنِ الرَّحِيمِ

نَرْفَعُ دَرَجَاتٍ مِّنْ نَّشَاءٍ

وَفَوْقَ كُلِّ ذِي عِلْمٍ عَلِيمٌ

(صدق الله العلي العظيم)

(سورة يوسف / الآية ٧٦)

Dedication

To my first and only love “Iraq”

*To my family (my father, my mother, my
brothers: Tha'er, Thamer, Muthanna and my
sisters)*

Acknowledgments

Thanks to Allah the one the single for all this blessing during the pursuit of my academic career.

*I would like to express my sincere thanks and my appreciation to my supervisors Assist. Prof. Dr. **Ashour H. AL-Ghadeer** and Assist. Prof. Dr. **Eman T. Kareem** for their encouragement and guidance throughout the course of this work. I am also grateful thanks to the staff members of the College of Science especially the great human and the best brother Assist. Prof. Dr. **Adnan Al – Sa'adi** for his favor which I will not forget, all words can't express his great role in this stage of my life, so I'll always say to him “thank you”.*

My deep gratitude is due to Dr.Saleh Hadawi, Dr. Ala'a Fraq, Dr. Abbas Matrood, Dr. Zaid Al-A'arajy, Dr. Muneer, Mr. Hatham dallool, Mr. Hassan Faisal, Mr. Hussain Mubarak, Mr. Atheer Hassan, Mr. Naseer, Mr.Ehssan and his wife Mrs. Raghad, and My deep thanks are due to all others who gave me help and sincere cooperation especially my colleagues Atheer, Salam, Mohammad Adnan, Mohammad Hussain and Rajwan Abdul-Jabbar.

*My deep thanks is due to the staff members of the University of Kufa especially to the great human Dr. **Abdullah Mohammad Ali**, my best friends Mr. Haidar Noori and Mr. Haider Abdulrazzaq.*

I am deeply indebted to my family for their support and patience during the years of my study. I wish to express my deepest thanks to my brother Tha'er and his wife for continuous support and encouragement during the whole research period.

Atheer

Certification

We certify that this thesis was prepared under our supervision at the Department of Chemistry, College of Science, University of Kerbala as a partial requirement for the **Degree of Master in Chemistry**.

Signature:

Name: Ashour Hamoad Al-Ghadeer

Title: Assist. Prof.

Address: Al-Mustansiriyah University/

College of Pharmacy

Date : / / 2012

Signature:

Name: Eman Taleb Kareem

Title: Asstis. Prof.

Address: Kerbala University/

Education College of pure and applied Sciences

Date : / / 2012

In view of the available recommendations. I forward this thesis for debate by the examining committee.

Signature:

Assist. Prof. Dr.

Adnan Ibrahim Mohammed

Head of Chemistry Department

Date: / / 2012

Examination Committee Certificate

We, the examination committee, after reading this thesis and examining the student **Atheer Mahdi Madlool**, in its content, have found that it meets the standard and requirements as a thesis in fulfillment for the Degree of MSc. In Chemistry. Date / /2012.

(Chairman)

Signature:

Name: Dr. Abdullah Mohammed Ali

Title: Professor

Address: Kufa University/

(Member)

Signature:

Name: Dr.Khaled Jawad Kadhem

Title: Professor

Address: Al-Qadesyia University/College
of Sciences

Date: / /2012

(Member)

Signature:

Name: Dr. Adnan Ibrahim Mohammed

Title: Assist. Prof.

Address: Kerbala University/College
of Sciences

Date: / /2012

(Member& Supervisor)

Signature:

Name: Dr. Ashour Hamoad Dawood

Title: Assist. Prof.

Address: Al-Mustansiriyah University/
College of Pharmacy

Date: / /2012

(Member& Supervisor)

Signature:

Name: Dr. Eman Taleb Kareem

Title: Assist. Prof.

Address: Kerbala University/
Education College of pure Sciences

Date: / /2012

Approved by the council of the college of science in it's session No.
in / /2012

Signature:

Name: Dr. Ahmed Mahmood Abd Al-latif

Title: Professor

Address: Kerbala Universty / College of Scinces

Date: / /2012

Report of Linguistic Evaluator

I certify that the linguistic evaluation of this thesis was carried out by me and it is accepted linguistically and in expression.

Signature :

Name: Dr. Sabah Wajed Ali

Title: Assist. Prof.

Address: Kerbala University/ College of Education

Date : / / 2012

Report of Scientific Evaluator

I certify that the scientific evaluation of this thesis was carried out by me and it is accepted scientifically.

Signature :

Name: Dr. Hassan Ahmed Hassan

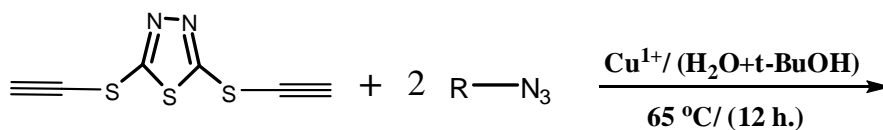
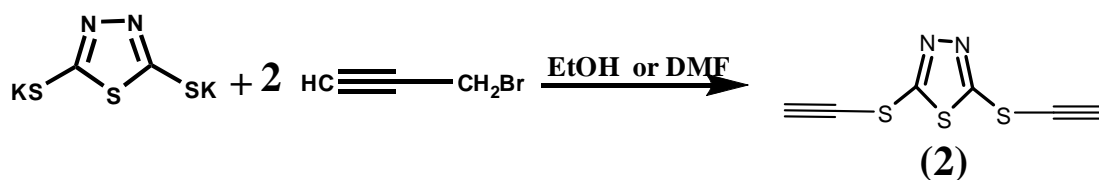
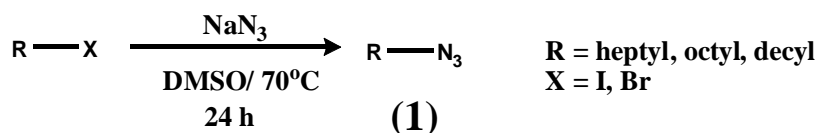
Title: Assist. Prof.

Address:Baghdad University/ Ibn-Elhaitham College of Education

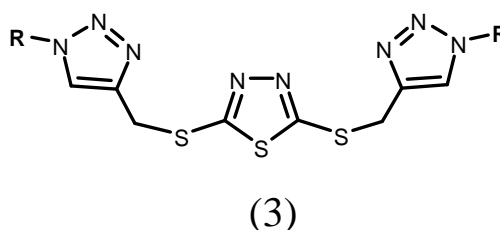
Date : / / 2012

Summary:

The work includes the synthesis and characterization of three ligands that contain three heterocyclic rings, one of these is thiadiazole while the others are two triazoles rings. The preparation of ligands is carried out through synthesis two precursors, the first is alkyl azides, which is prepared from the reaction of alkyl halides with sodium azide and the second is terminal alkyne was prepared by the addition reaction of propargylbromide with 2,5-dimercapto-thiadiazole dipotassium salt, then the collection between two precursors via click chemistry reaction obtained, the general preparation reaction equations summarized by the following scheme:



(3a) when R = Heptyl
(3b) when R = Octyl
(3c) when R = Decyl

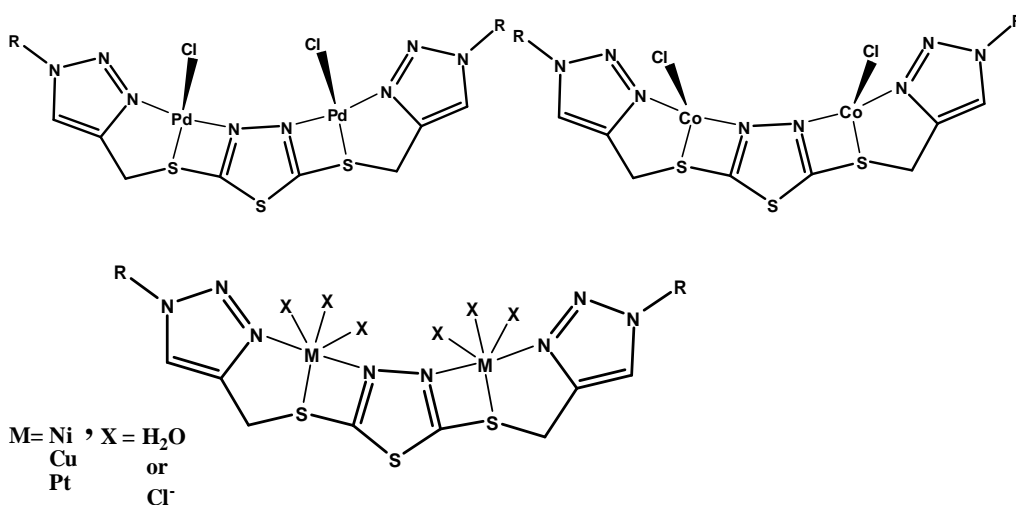


The prepared ligands were characterized by FT-IR, UV-Vis, ^1H , ^{13}C -NMR, Elemental micro analysis of elements C.H.N.S, spectroscopies in addition the solubility in different solvents was tested.

The ligand complexes were prepared by reaction of the titled ligands with Co^{2+} , Ni^{2+} , Cu^{2+} , Pd^{2+} and Pt^{4+} ions, the complexes were characterized by FT-IR, UV-Vis, magnetic susceptibility and Molar conductivity measurements. The solubility of prepared complexes were tested with different solvents.

From the spectroscopies, magnetic moments and molar conductivity the suggested geometry around the metal ions can be described as:

Tetrahedral of cobalt(II) complexes with all ligands, square planar of palladium(II) complexes with all ligands, while the octahedral geometry for nickel(II), copper(II) and platinum(IV) complexes.



List of Contents

Subjects		Page No.
Summary		a-b
List of Contents		I
List of Tables		VII
List of Figures		IX
List of Schemes		XV
List of Abbreviations		XVI
Chapter One	Introduction	1-26
(1)	Introduction	1
(1.1)	2,5-dimercapto-1,3,4-thiadiazole	1
(1.2)	1,2,3-Triazoles	6
(1.3)	N & S donor ligands	7
(1.4)	Metal Complexes Structures and Applications	11
(1.4.1)	Cobalt Complexes Structures and Applications	11
(1.4.2)	Nickel Complexes Structures and Applications	14
(1.4.3)	Copper Complexes Structures and Applications	18
(1.4.4)	Palladium Complexes Structures and Applications	19
(1.4.5)	Platinum Complexes Structures and Applications	23
(1.5)	The Aim of Work	26

Chapter tow		27-38
Experimental Section		
(2)	Experimental Section	27
(2.1)	Chemicals	27
(2.2)	Instruments & Techniques	29
(2.2.1)	Melting point measurement	29
(2.2.2)	Infrared spectra	29
(2.2.3)	Electronic spectra	29
(2.2.4)	Thin layer chromatography (TLC)	29
(2.2.5)	Magnetic Susceptibility Measurements	30
(2.2.6)	Conductivity Measurement	30
(2.2.7)	Elemental microanalysis	30
(2.2.8)	¹ H and ¹³ CNMR spectra	30
(2.2.9)	The Proposed molecular structure	30
(2.3)	Abbreviation of the ligands	31
(2.4)	Synthesis of the ligands and precursors	32
(2.4.1)	Preparation of alkane-azides	32
(2.4.1.1)	Preparation of 1-azido heptane	32
(2.4.1.2)	preparation of n-alkyl azides	33
(2.4.2)	Preparation of [2,5-bis(prop-2-ynylthio)-1,3,4-thiadiazole] terminal alkyne from 2,5-dimercapto -1,3,4-thiadiazole salt	34
(2.4.3)	Preparation of 2,5-bis[1-alkyl-1H-1,2,3-triazol-4-yl] methylthio]-1,3,4-thiadiazole	35
(2.5)	Preparation of complexes	36

Chapter Three		Results and Dissections	39- 121
(3)	Results and discussion		39
(3.1)	Synthesis and characterization of ligands and precursors		39
(3.1.1)	Synthesis and characterization of Alkyl-azid compounds (1a, 1b and 1c)		39
(3.1.2)	Synthesis and characterization of [2,5-bis(prop-2-ynylthio)-1,3,4-thiadiazole]		40
(3.2)	Synthesis and characterization of the ligands (L^1 , L^2 & L^3)		40
(3.3)	FT-IR Spectral data for the ligands and precursors		44
(3.3.1)	FT-IR spectral data for alky-azides		44
(3.3.2)	FT-IR spectral data for 2,5-bis(prop-2-ynylthio)-1,3,4-thiadiazole		46
(3.3.3)	FT-IR spectral data for 2,5-bis[1-alkyl-1H-1,2,3-triazol-4-yl) methylthio]-1,3,4-thiadiazole		47
(3.3.3.1)	FT-IR spectral data for 2,5-bis[1-heptyl-1H-1,2,3-triazol-4-yl) methylthio]-1,3,4-thiadiazole		47
(3.3.3.2)	FT-IR spectral data for 2,5-bis[1-octyl-1H-1,2,3-triazol-4-yl) methylthio]-1,3,4-thiadiazole		48
(3.3.3.3)	FT-IR spectral data for 2,5-bis[1-decyl-1H-1,2,3-triazol-4-yl) methylthio]-1,3,4-thiadiazole		49
(3.4)	(UV-Vis) Spectra of the ligands		52
(3.4.1)	UV-Vis) Spectrum of [L^1] ligand		52
(3.4.2)	UV-Vis) Spectrum of [L^2] ligand		52
(3.4.3)	UV-Vis) Spectrum of [L^3] ligand		53

(3.5)	Nuclear magnetic resonance (NMR) spectra	55
(3.5.1)	^1H , ^{13}C NMR spectra for the ligand $[\text{L}^1]$	55
(3.5.1.1)	^1H NMR spectrum for the ligand $[\text{L}^1]$	55
(3.5.1.2)	^{13}C NMR spectrum for the ligand $[\text{L}^1]$	56
(3.5.2)	^1H , ^{13}C NMR spectra for the ligand $[\text{L}^2]$	58
(3.5.2.1)	^1H -NMR spectrum for the ligand $[\text{L}^2]$	58
(3.5.2.2)	^{13}C NMR spectrum for the ligand $[\text{L}^2]$	59
(3.5.3)	^1H , ^{13}C NMR spectra for the ligand $[\text{L}^3]$	61
(3.5.3.1)	^1H NMR spectrum for the ligand $[\text{L}^3]$	61
(3.5.3.2)	^{13}C NMR spectrum for the ligand $[\text{L}^3]$	62
(3.6)	Synthesis and characterization of the complexes	64
(3.6.1)	Synthesis and characterization of $[\text{L}^1]$ complexes	65
(3.6.2)	Synthesis and characterization of the $[\text{L}^2]$ complexes	65
(3.6.3)	Synthesis and characterization of the $[\text{L}^3]$ complexes	66
(3.7)	FT-IR spectra of synthesis complexes	67
(3.7.1)	FT-IR spectra of $[\text{L}^1]$ metal complexes	67
(3.7.1.1)	FT-IR spectrum of $[\text{Co}_2(\text{L}^1)\text{Cl}_2]\text{Cl}_2$	67
(3.7.1.2)	FT-IR spectrum of $[\text{Ni}_2(\text{L}^1)(\text{H}_2\text{O})_4\text{Cl}_2]\text{Cl}_2$	68
(3.7.1.3)	FT-IR spectrum of $[\text{Cu}_2(\text{L}^1)(\text{H}_2\text{O})_6]\text{Cl}_4$	69

(3.7.1.4)	FT-IR-Spectrum of $[\text{Pd}_2(\text{L}^1)\text{Cl}_2]\text{Cl}_2$	70
(3.7.1.5)	FT-IR-Spectrum of $[\text{Pt}_2(\text{L}^1)(\text{H}_2\text{O})_2\text{Cl}_4]\text{Cl}_4$	72
(3.7.2)	FT-IR spectra of $[\text{L}^2]$ metal complexes	75
(3.7.2.1)	FT-IR spectrum of $[\text{Co}_2(\text{L}^2)\text{Cl}_2]\text{Cl}_2$	75
(3.7.2.2)	FT-IR spectrum of $[\text{Ni}_2(\text{L}^2)(\text{H}_2\text{O})_4\text{Cl}_2]\text{Cl}_2$	76
(3.7.2.3)	FT-IR spectrum of $[\text{Cu}_2(\text{L}^2)(\text{H}_2\text{O})_6]\text{Cl}_4$	77
(3.7.2.4)	FT-IR spectrum of $[\text{Pd}_2(\text{L}^2)\text{Cl}_2]\text{Cl}_2$	79
(3.7.2.5)	FT-IR spectrum of $[\text{Pt}_2(\text{L}^2)(\text{H}_2\text{O})_2\text{Cl}_4]\text{Cl}_4$	80
(3.7.3)	FT-IR spectra of $[\text{L}^3]$ metal complexes	83
(3.7.3.1)	FT-IR spectrum of $[\text{Co}_2(\text{L}^3)\text{Cl}_2]\text{Cl}_2$	83
(3.7.3.2)	FT-IR spectrum of $[\text{Ni}_2(\text{L}^3)(\text{H}_2\text{O})_4\text{Cl}_2]\text{Cl}_2$	84
(3.7.3.3)	FT-IR spectrum of $[\text{Cu}_2(\text{L}^3)(\text{H}_2\text{O})_6]\text{Cl}_4$	85
(3.7.3.4)	FT-IR spectrum of $[\text{Pd}_2(\text{L}^3)\text{Cl}_2]\text{Cl}_2$	87
(3.7.3.5)	FT-IR spectrum of $[\text{Pt}_2(\text{L}^3)(\text{H}_2\text{O})_2\text{Cl}_4]\text{Cl}_4$	88
(3.8)	UV-Vis spectral data of synthesized complexes	91
(3.8.1)	UV-Vis spectral data of $[\text{L}^1]$ complexes	91
(3.8.1.1)	UV-Vis spectrum of $[\text{Co}_2(\text{L}^1)\text{Cl}_2]\text{Cl}_2$ complex	91
(3.8.1.2)	UV-Vis spectrum of $[\text{Ni}_2(\text{L}^1)(\text{H}_2\text{O})_4\text{Cl}_2]\text{Cl}_2$ complex	92
(3.8.1.3)	UV-Vis spectrum of $[\text{Cu}_2(\text{L}^1)(\text{H}_2\text{O})_6]\text{Cl}_4$ complex	93
(3.8.1.4)	UV-Vis spectrum of $[\text{Pd}_2(\text{L}^1)\text{Cl}_2]\text{Cl}_2$ complex	94

(3.8.1.5)	UV-Vis spectrum of $[\text{Pt}_2(\text{L}^1)(\text{H}_2\text{O})_2\text{Cl}_4]\text{Cl}_4$ complex	95
(3.8.2)	UV-Vis spectral data of $[\text{L}^2]$ complexes	97
(3.8.2.1)	UV-Vis spectrum of $[\text{Co}_2(\text{L}^2)\text{Cl}_2]\text{Cl}_2$ complex	97
(3.8.2.2)	UV-Vis spectrum of $[\text{Ni}_2(\text{L}^2)(\text{H}_2\text{O})_4\text{Cl}_2]\text{Cl}_2$ complex	98
(3.8.2.3)	UV-Vis spectrum of $[\text{Cu}_2(\text{L}^2)(\text{H}_2\text{O})_6]\text{Cl}_4$ complex	99
(3.8.2.4)	UV-Vis spectrum of $[\text{Pd}_2(\text{L}^2)\text{Cl}_2]\text{Cl}_2$ complex	100
(3.8.2.5)	UV-Vis spectrum of $[\text{Pt}_2(\text{L}^2)(\text{H}_2\text{O})_2\text{Cl}_4]\text{Cl}_4$ complex	101
(3.8.3)	UV-Vis spectral data of $[\text{L}^3]$ complexes	103
(3.8.3.1)	UV-Vis spectrum of $[\text{Co}_2(\text{L}^3)\text{Cl}_2]\text{Cl}_2$ complex	103
(3.8.3.2)	UV-Vis spectrum of $[\text{Ni}_2(\text{L}^3)(\text{H}_2\text{O})_4\text{Cl}_2]\text{Cl}_2$ complex	104
(3.8.3.3)	UV-Vis spectrum of $[\text{Cu}_2(\text{L}^3)(\text{H}_2\text{O})_6]\text{Cl}_4$ complex	105
(3.8.3.4)	UV-Vis spectrum of $[\text{Pd}_2(\text{L}^3)\text{Cl}_2]\text{Cl}_2$ complex	106
(3.8.3.5)	UV-Vis spectrum of $[\text{Pt}_2(\text{L}^3)(\text{H}_2\text{O})_2\text{Cl}_4]\text{Cl}_4$ complex	107
(3.9)	Magnetic susceptibility of synthesized complexes	109
(3.10)	Molar conductivity for the synthesized complexes	111
(3.11)	Suggested structures of ligands & complexes	113
(3.11.1)	Suggested structure of ligands	113
(3.11.2)	Suggested structures of the ligands	114
References		118

Table		Page No.
(2-1)	Chemicals used and their supplier	27
(2-2)	Abbreviations, structure and nomenclature of the synthesized ligands	31
(2-3)	Quantities and reaction conditions to prepare compounds	33
(2-4)	Quantities and reaction conditions to prepare ligands	36
(2-5)	Quantity of ligands and metal salts to prepare complexes	37
(3-1)	Melting point and C.H.N.S elemental analysis of compounds (3a), (3b) & (3c)	41
(3-2)	Solubility of Compound (2), [L ¹], [L ²] & [L ³]	42
(3-3)	FT-IR spectrum of 2,5-bis[1-alkyl-1H-1,2,3-triazol-4-yl) methylthio]-1,3,4-thiadiazole	51
(3-4)	Electronic spectral data for the ligands	54
(3-5)	solubility of [L ¹] complexes in different solvents	65
(3-6)	solubility of [L ²] complexes in different solvents	66
(3-7)	solubility of [L ³] complexes in different solvents	66
(3-8)	The FT-IR bands of [L ¹] ligand and Co(II), Ni(II), Cu(II), Pd(II) and Pt(IV) complexes	74
(3-9)	FT-IR of (L2) ligand and its Co(II), Ni(II), Cu(II), Pd(II) and Pt(IV) complexes	82
(3-10)	FT-IR spectrum of [L ³] and its Co(II), Ni(II), Cu(II), Pd(II) and Pt(IV) complexes	90

Table		Page No.
(3-11)	Electronic spectral data of [L ¹] and its metal complexes	96
(3-12)	Electronic spectral data of [L ²] and its metal complexes	102
(3-13)	Electronic spectral data of [L ³] and its metal complexes	108
(3-14)	Magnetic susceptibility of synthesized complexes	110
(3-15)	Molar conductivity of different complex solutions	111
(3-15)	conductivity of complexes dissolved in (DMF)	112

Figure		Page No.
(1-1)	Isomeric forms of thiadiazoles	2
(1-2)	Metal 5-(2-aminoethyl)-2-amino-1,3,4-thiadiazole complex	3
(1-3)	Resonance shapes of 1,3,4-thiadiazole-2,5-dimercapto	4
(1-4)	X-ray crystallography of Re(I) complex containing 1,3,4-thiadiazole-2,5-dithiolate	4
(1-5)	Square-pyramidal structure for Cu(II) complex	5
(1-6)	Iridium(III) triazole complexes	7
(1-7)	Schiff Base ligand diverted from 1,3,4-thiadiazole	9
(1-8)	Crystal structure of Pd(II) pyrrolo pyridine complex	9
(1-9)	Aqua bis[2,5-bis(pyridin-2-yl) 1,3,4-thiadiazole κ_2 N2,N3] (trifluoromethanesulfonato κ_0)copper(II)trifluoromethanesulfonate	10
(1-10)	Theoretical structure (octahedral geometry) of Cu(II) complex	10
(1-11)	five-membered ring of cobalt complex & its X-ray crystallography	12
(1-12)	Cobalt complex and H-bonding between ligands	12
(1-13)	X-ray crystallography of [Co(Phca2en)Cl ₂] complex	13
(1-14)	Perspective view of the [Co ^{II} ₂ (L)(NCO) ₃] ⁺ cation	14
(1-15)	X-ray of the complex cation [Ni(AEPyz)] ⁺	15
(1-16)	X-ray of [(L4c) ₄ Ni ₂] complex	16

Figure		Page No.
(1-17)	ORTEP plot of the molecular structure of Ni(II) complex	16
(1-18)	A perspective view of complete coordination around Ni(II)	17
(1-19)	X-ray structure of [Cu(meophdpa)Cl(H ₂ O)](ClO ₄).H ₂ O	18
(1-20)	Representative structures of copper complex	19
(1-21)	Palladium(II) complexes with ethylenediamine ligand	20
(1-22)	structure of palladium (II) complexes with thiosemicarbazone derivatives	22
(1-23)	X-ray crystallography of Pd complexes	22
(1-24)	Binuclear platinum complexes containing two linked cisplatin centers	24
(1-25)	Molecular structures of the investigated Pt(II) and Pt(IV) complexes	24
(1-26)	The crystal structure of trans-Pt ₂ (μ-Cl) ₂ Cl ₂ (CO) ₂	25
(1-27)	The crystal structure of trans-Pt ₂ (μ-X) ₂ X ₂ (CO) ₂ , X= Br, I	25
(3-1)	C.H.N.S graph of ligand [L ¹]	42
(3-2)	C.H.N.S graph of ligand [L ²]	43
(3-3)	C.H.N.S graph of ligand [L ³]	43
(3-4)	FT-IR spectrum of 1-Azido heptane	44
(3-5)	FT-IR spectrum of 1-Azido octane	45

Figure		Page No.
(3-6)	FT-IR spectrum of 1-Azido decane	45
(3-7)	FT-IR spectrum of 2,5-bis(prop-2-ynylthio)-1,3,4-thiadiazole	46
(3-8)	FT-IR spectrum of [L ¹] ligand	48
(3-9)	FT-IR spectrum of [L ²] ligand	49
(3-10)	FT-IR spectrum of [L ³] ligand	50
(3-11)	UV-Vis spectrum of [L ¹] ligand	52
(3-12)	UV-Vis spectrum of [L ²] ligand	53
(3-13)	UV-Vis spectrum of [L ³] ligand	54
(3-14)	¹ H NMR spectrum of ligand [L ¹]	55
(3-15)	¹³ C NMR of ligand [L ¹]	57
(3-16)	¹ H NMR of ligand [L ²]	58
(3-17)	¹³ C NMR of ligand [L ²]	60
(3-18)	¹ H NMR of the ligand [L ³]	61
(3-19)	¹³ C NMR of the ligand [L ³]	63
(3-20)	FT-IR spectrum of [Co ₂ (L ¹)Cl ₂]Cl ₂ complex	68
(3-21)	FT-IR spectrum of [Ni ₂ (L ¹)(H ₂ O) ₄ Cl ₂]Cl ₂ complex	69
(3-22)	FT-IR spectrum of [Cu ₂ (L ¹)(H ₂ O) ₆]Cl ₄ complex	70

Figure		Page No.
(3-23)	FT-IR spectrum of $[\text{Pd}_2(\text{L}^1)\text{Cl}_2]\text{Cl}_2$ complex	71
(3-24)	FT-IR spectrum of $[\text{Pt}_2(\text{L}^1)(\text{H}_2\text{O})_2\text{Cl}_4]\text{Cl}_4$ complex	73
(3-25)	FT-IR spectrum of $[\text{Co}_2(\text{L}^2)\text{Cl}_2]\text{Cl}_2$ complex	76
(3-26)	FT-IR spectrum of $[\text{Ni}_2(\text{L}^2)(\text{H}_2\text{O})_4\text{Cl}_2]\text{Cl}_2$ complex	77
(3-27)	FT-IR spectrum of $[\text{Cu}_2(\text{L}^2)(\text{H}_2\text{O})_6]\text{Cl}_4$ complex	78
(3-28)	FT-IR spectrum of $[\text{Pd}_2(\text{L}^2)\text{Cl}_2]\text{Cl}_2$ complex	79
(3-29)	FT-IR spectrum of $[\text{Pt}_2(\text{L}^2)(\text{H}_2\text{O})_2\text{Cl}_4]\text{Cl}_4$ complex	81
(3-30)	FT-IR spectrum of $[\text{Co}_2(\text{L}^3)\text{Cl}_2]\text{Cl}_2$ complex	84
(3-31)	FT-IR spectrum of $[\text{Ni}_2(\text{L}^3)(\text{H}_2\text{O})_4\text{Cl}_2]\text{Cl}_2$ complex	85
(3-32)	FT-IR spectrum of $[\text{Cu}_2(\text{L}^3)(\text{H}_2\text{O})_6]\text{Cl}_4$ complex	86
(3-33)	FT-IR spectrum of $[\text{Pd}_2(\text{L}^3)\text{Cl}_2]\text{Cl}_2$ complex	87
(3-34)	FT-IR spectrum of $[\text{Pt}_2(\text{L}^3)(\text{H}_2\text{O})_2\text{Cl}_4]\text{Cl}_4$ complex	89
(3-35)	UV-Vis spectrum of $[\text{Co}_2(\text{L}^1)\text{Cl}_2]\text{Cl}_2$ complex	91
(3-36)	UV-Vis spectrum of $[\text{Ni}_2(\text{L}^1)(\text{H}_2\text{O})_4\text{Cl}_2]\text{Cl}_2$ complex	92
(3-37)	UV-Vis spectrum of $[\text{Cu}_2(\text{L}^1)(\text{H}_2\text{O})_6]\text{Cl}_4$ complex	93
(3-38)	UV-Vis spectrum of $[\text{Pd}_2(\text{L}^1)\text{Cl}_2]\text{Cl}_2$ complex	94

Figure		Page No.
(3-39)	UV-Vis spectrum of $[\text{Pt}_2(\text{L}^1)(\text{H}_2\text{O})_2\text{Cl}_4]\text{Cl}_4$ complex	95
(3-40)	UV-Vis spectrum of $[\text{Co}_2(\text{L}^2)\text{Cl}_2]\text{Cl}_2$ complex	97
(3-41)	UV-Vis spectrum of $[\text{Ni}_2(\text{L}^2)(\text{H}_2\text{O})_4\text{Cl}_2]\text{Cl}_2$ complex	98
(3-42)	UV-Vis spectrum of $[\text{Cu}_2(\text{L}^2)(\text{H}_2\text{O})_6]\text{Cl}_4$ complex	99
(3-43)	UV-Vis spectrum of $[\text{Pd}_2(\text{L}^2)\text{Cl}_2]\text{Cl}_2$ complex	100
(3-44)	UV-Vis spectrum of $[\text{Pt}_2(\text{L}^2)(\text{H}_2\text{O})_2\text{Cl}_4]\text{Cl}_4$ complex	101
(3-45)	UV-Vis spectrum of $[\text{Co}_2(\text{L}^3)\text{Cl}_2]\text{Cl}_2$ complex	103
(3-46)	UV-Vis spectrum of $[\text{Ni}_2(\text{L}^3)(\text{H}_2\text{O})_4\text{Cl}_2]\text{Cl}_2$ complex	104
(3-47)	UV-Vis spectrum of $[\text{Cu}_2(\text{L}^3)(\text{H}_2\text{O})_6]\text{Cl}_4$ complex	105
(3-48)	UV-Vis spectrum of $[\text{Pd}_2(\text{L}^3)\text{Cl}_2]\text{Cl}_2$ complex	106
(3-49)	UV-Vis spectrum of $[\text{Pt}_2(\text{L}^3)(\text{H}_2\text{O})_2\text{Cl}_4]\text{Cl}_4$ complex	107
(3-50)	$[\text{L}^1]$ ligand structure	113
(3-51)	$[\text{L}^2]$ ligand structure	113
(3-52)	$[\text{L}^3]$ ligand structure	114
(3-53)	structure of $[\text{Co}_2\text{L}^1\text{Cl}_2]^{+2}$ complex	115
(3-54)	structure of $[\text{Ni}_2\text{L}^1(\text{H}_2\text{O})_4\text{Cl}_2]^{+2}$ complex	115
(3-55)	structure of $[\text{Cu}_2\text{L}^1(\text{H}_2\text{O})_6]^{+4}$ complex	116

Figure		Page No.
(3-56)	structure of $[\text{Pd}_2\text{L}^1\text{Cl}_2]^{+2}$ complex	116
(3-57)	structure of $[\text{Pt}_2\text{L}^1(\text{H}_2\text{O})_2\text{Cl}_4]^{+4}$ complex	117

List of Schemes

Scheme		Page No.
(1-1)	Preparation of 2,5-Dimecapto-1,3,4-Thiadiazole	2
(1-2)	Preparation of 1,4N-Substituted-1,2,3-Triazole (<i>Click Chemistry</i>)	6
(1-3)	Pd enolate as a key intermediate for the enantioselective reactions	21
(2-1)	preparation of 1-azido heptane	32
(2-2)	preparation of n-alkyl azides	33
(2-3)	preparation of 2,5-bis(prop-2-ynylthio)-1,3,4-thiadiazole	34
(2-4)	Preparation of 2,5-bis[(1-alkyl-1H-1,2,3-triazol-4-yl)methylthio]-1,3,4-thiadiazole	35
(3-1)	the method to prepare alkyl-azides compounds (1a, 1b & 1c)	39
(3-2)	prepare of 2,5-bis(prop-2-ynylthio)-1,3,4-thiadiazole compound (2)	40
(3-3)	General method to prepare 2,5-bis[1-alkyl-1H-1,2,3-triazol-4-yl) methylthio]-1,3,4-thiadiazole, compounds: (3a), (3b) & (3c)	41
(3-4)	preparation of (Oh) complexes	64
(3-5)	preparation of (Td or Sp) complexes	64

List of Abbreviations

λ	Wave length
ϵ_{\max}	Molar absorptivity
nm	Nanometer
mol.	Mole
g	Gram
wt.	Weight
m.w	Molecular weight
m.p	Melting point
Dec.	Decomposed
MeOH	Methanol
EtOH	Ethanol
t-BuOH	Tertiary butanol
DCM	Dichloromethane
DMF	Dimethyl form amide
DMSO	Dimethyl sulphoxide
TLC	Thin layer chromatography
UV-Vis	Ultra violet and Visible
IR	Infrared
NMR	Nuclear magnetic resonance
TGA	Thermo gravimetric analysis
DTA	Differential thermal analysis
afmt	4-amino-3-trifloromethyl
meophdpa	4-methoxy-N,N-bis(pyridine-2-yl-methyl)aniline
STSC	Steroidal thiosemicarbazones
IP	Ionic position

HRMS	High resolution mass spectroscopy
ORTEP	Oak Ridge Thermal Ellipsoid Plot program for crystal structure illustrations
EPR	Electron Paramagnetic Resonance
FAB mass	Fast-atom bombardment mass spectroscopy
MTT dye	Colorimetric assay for measuring the activity of cellular enzymes that reduce the tetrazolium dye in tumor cells
k N	Coordination between N atom from the ligand and metal
k O	Coordination between O atom from the ligand and metal
[L ¹]	2,5-bis[1-heptyl-1H-1,2,3-triazol-4-yl) methylthio]-1,3,4-thiadiazole
[L ²]	2,5-bis[1-octyl-1H-1,2,3-triazol-4-yl) methylthio]-1,3,4-thiadiazole
[L ³]	2,5-bis[1-decyl-1H-1,2,3-triazol-4-yl) methylthio]-1,3,4-thiadiazole
HOMO	Highest Occupied Molecular Orbital
LUMO	Lowest Unoccupied Molecular Orbital



Chapter One

INTRODUCTION

(1).Introduction:

Heterocyclic compounds occupy a central position among those molecules that makes life possible. The chemistry of heterocyclic compounds has been an interesting field of study for a long time⁽¹⁾. The vital interest of the pharmaceutical and agrochemical industries in heterocycles is often connected with their natural occurrence, among the approximately 20 million chemical compounds identified by the end of the second millennium; more than two-thirds are heterocyclic⁽²⁾. Synthetic chemistry provides cornucopia of heterocyclic systems. More than 90% of new drugs contain heterocycles and then interface between chemistry and biology⁽²⁾. So that heterocycles were have a big distance in applications as ligands in the inorganic chemistry filed. A lot of applications and uses of complexes which often contain from heterocycles and metal ions have been known⁽²⁾.

(1.1)2,5-dimercapto-1,3,4-thiadiazole:

Thiadiazole is a heterocyclic compound featuring both two nitrogen and one sulfur atoms as a part of the aromatic five-membered ring. Thiadiazole and related compounds are called 1,3,4-thiadiazole (two nitrogen and one other heteroatom in a five-membered ring). They occur in nature in four isomeric forms as: **A.** 1,2,3-thiadiazole; **B.** 1,2,5-thiadiazole; **C.** 1,2,4-thiadiazole and **D.** 1,3,4-thiadiazole^(1,3,4) **Fig.(1-1)** illustrated the isomeric forms of thiadiazoles. Chemical properties of 1,3,4-thiadiazole have been reviewed in the last few years. So that, the interesting of 1,3,4-thiadiazole as a privileged system in medicinal chemistry has prompted the advances on the therapeutic potential of this system⁽⁵⁾.

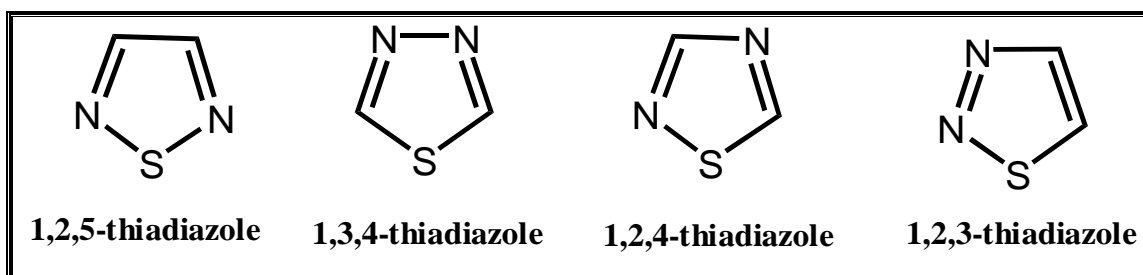
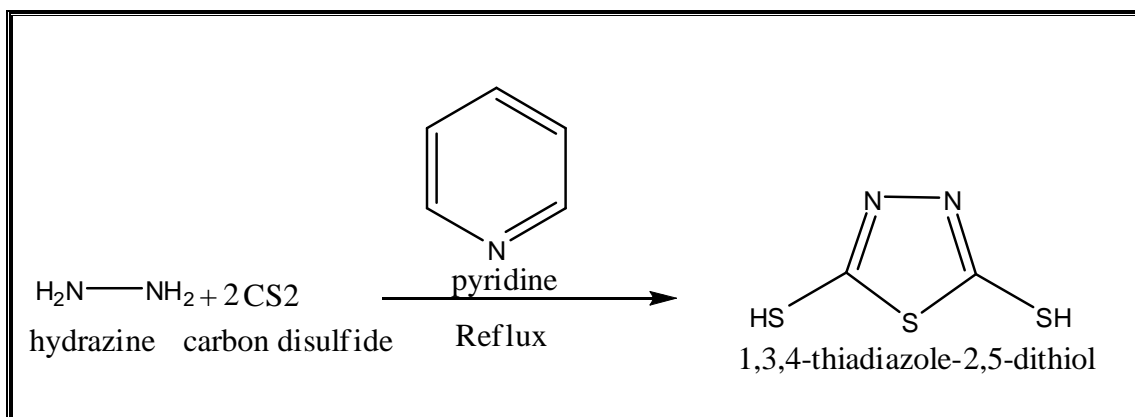


Fig. (1-1) Isomeric forms of thiadiazole

2,5-Dimercapto-1,3,4-thiadiazole is one of the family of five members heterocyclic compounds, two nitrogen atoms containing heterocycles with three sulfur atoms are considered as an important class of compounds in medicinal, industrial, biological chemistry because of their interesting diversified biological application^(3,6). It used in several applications as organic compound or as a ligand in inorganic compounds, the best method to produce it was reported by Salimon and coworkers⁽⁶⁾

Scheme (1:1)



Scheme (1:1) Preparation of 2,5-Dimercapto-1,3,4-Thiadiazole

Supumn and coworkers⁽⁷⁾ reported a study of synthesis and biological activity of metal complexes of 5-(2-aminoethyl)-2-amino-1,3,4-thiadiazole. The complexes were containing Co(II), Ni(II), and Cu(II) metal ions, it was prepared and characterized by elemental analysis, IP electronic spectroscopy and conductimetry. The new derivatives, possessing the following formulae, $[\text{CuL}_2(\text{OH})_2]$, $[\text{NiL}_2\text{Cl}_2]$,

and $[\text{Co}_2\text{LCl}_4]_n$ showed *in vitro* antifungal activity against *Aspergillus* and *Candida spp.* The structures of complexes which have been prepared belong to pseudo octahedral geometry system **Fig. (1-2)**

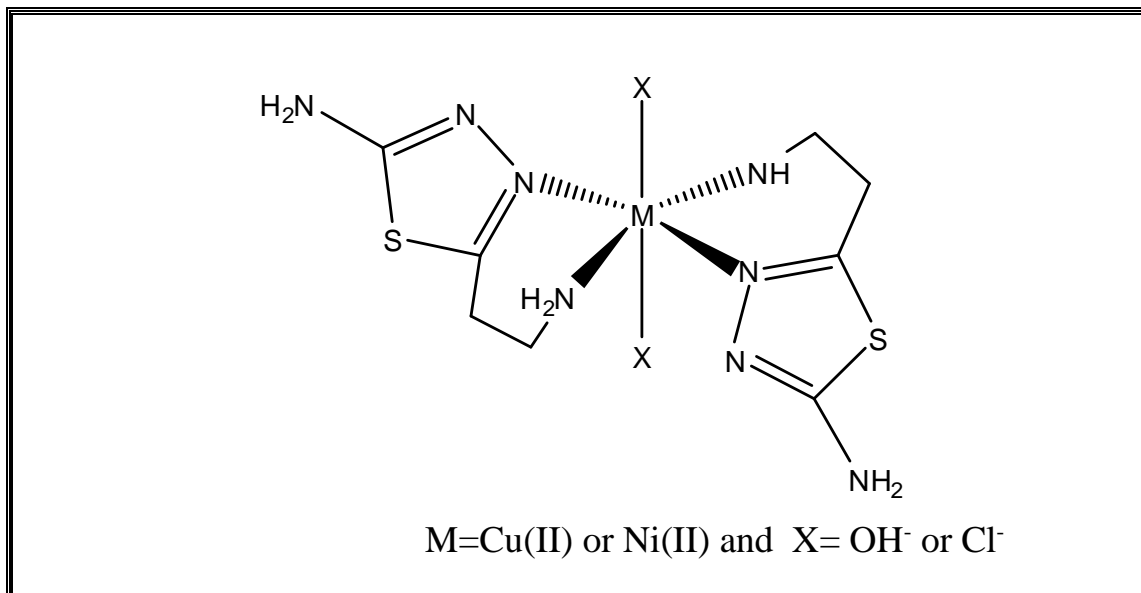


Fig.(1-2) Metal 5-(2-aminoethyl)-2-amino-1,3,4-thiadiazole complex

In 2007 Tzeng and coworkers⁽⁸⁾ reported a study of [Novel trinuclear Re(I) complex containing 1,3,4-thiadiazole-2,5-dithiolate], found that due to the three resonance states of 1,3,4-thiadiazole-2,5-dimercapto **Fig.(1-3)** the ligand was tridentate so the state **(B)** was the most stable when it forming a complex with Re(I), this complex is belong to type NS_2 donor ligand complexes. X-ray crystallography shown that the coordination bonds in the complex were created between two (S) atoms from dimercapto and the third from (N) atom with Re(I) metal ion. **Fig.(1-4)**

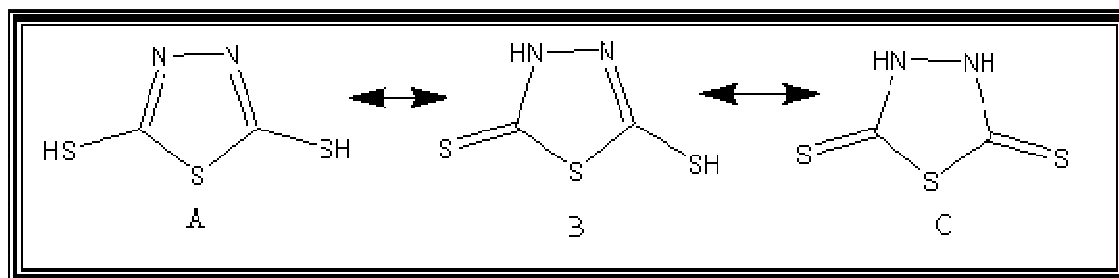


Fig.(1-3) Resonance shapes of 1,3,4-thiadiazole-2,5-dimercapto

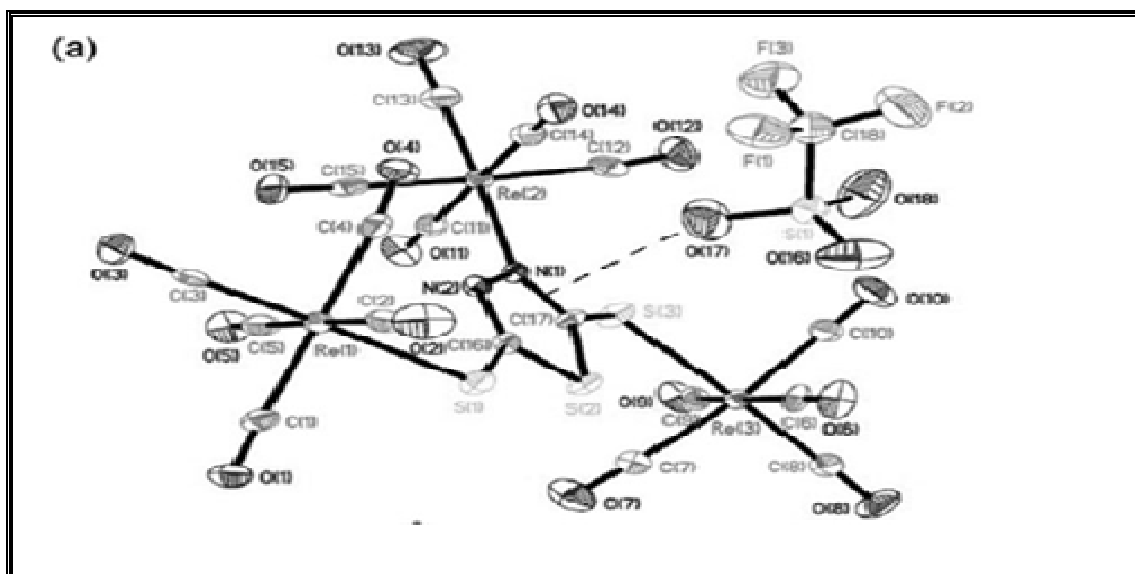


Fig.(1-4) X-ray crystallography of Re(I) complex containing 1,3,4-thiadiazole-2,5-dithiolate

In 2010 Turan and coworkers⁽⁹⁾ were reported the study of preparation and characterization complexes of thiadiazole derivatives with Co(II), Ni(II), Cu(II) and Zn(II) metal ions, the ligand (L) and its metal complexes have been characterized by elemental analyses, UV-Vis, IR, ¹H-NMR spectroscopies, magnetic susceptibility and thermo gravimetric differential thermal analysis (TGA, DTA). The suggested structure of these complexes are octahedral for Zn (II) complex, tetrahedral for Ni (II) complex, square planar for Co(II) complex and square-pyramidal for Cu (II) complex. **Fig. (1-5)**

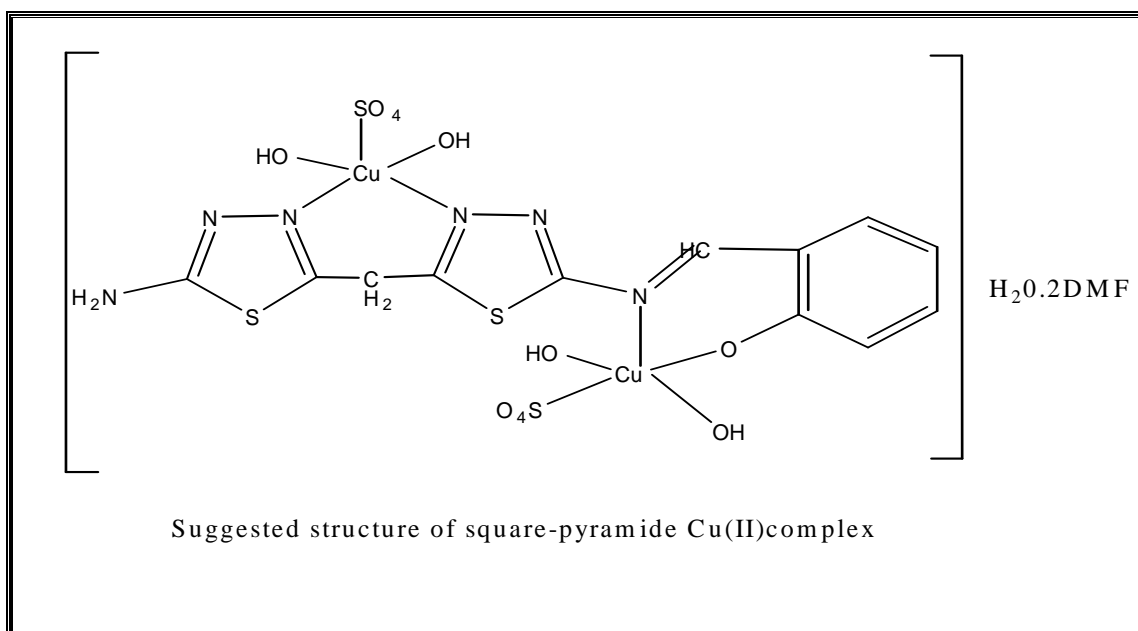
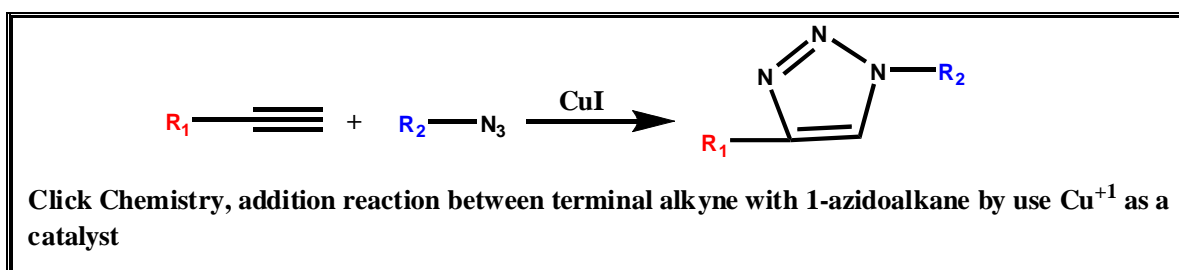


Fig.(1-5) Square-pyramidal structure for Cu(II) complex

In 2011 Adediji and coworkers⁽¹⁰⁾ were synthesized and studied the biological activities on metal complexes of 2,5-diamino-1,3,4-thiadiazole derived from semicarbazide hydrochloride. The metal complexes were prepared and characterized using elemental analysis, infra-red, UV-Vis, magnetic moment, atomic absorption, thin layer chromatography and molar conductance measurements. The IR data revealed that the ligand behaved as tridentate neutral ligand. It coordinated to the metal ion *via* sulfur and nitrogen of the amines, the UV-Vis spectra and magnetic moment data, shown that the complexes were had octahedral geometrical structure⁽¹⁰⁾.

(1.2)1,2,3-Triazoles:

1,2,3-Triazole ring system has been the subject of considerable research mainly due to its usefulness in synthetic organic chemistry and also because of the pharmacological properties shown by some of its derivatives^(11, 12). In 2002, Sharpless and Meldal⁽¹³⁾ improved the regioselectivity of the cycloaddition reactions by using Cu(I)-catalyzed ligation (*click chemistry*) of organic azides and terminal alkynes.

Scheme(1:2)

Scheme (1:2) Preparation of 1,4N-Substituted-1,2,3-Triazole (*Click Chemistry*)

Preparation of regioselective of 1,4-N-substituted 1,2,3-triazole by using this mechanism was one of marvelous methods which can produce these compounds by using Cu(I) ion as a catalyst to this reaction. Many methods can be used to obtain Cu(I) ion, the Cu(I) species can be generated by oxidation of Cu(0) or reduction of Cu(II) species⁽¹¹⁾, or by direct use of Cu(I) ion found in CuI or CuCl salts⁽¹⁴⁾, so it can be used in cycloaddition reaction as a catalyst, another indirect method to obtain Cu(I) ion instant in solution by reducing Cu(II) ion of copper sulfate to Cu(I) ion by sodium-L-ascorbate in aqueous environment^(11,13,15).

In 2009 Gonzalez and coworkers⁽¹⁶⁾ reported a study of Phenyl-1H-1,2,3-triazoles as new cyclometalating ligands for Iridium(III) complexes, the triazoles were synthesized *via* “click chemistry” method, as a new type of cyclometalating ligand. The photophysical and electrochemical

properties of these complexes were investigated experimentally as well as theoretically by using density functional theory. The properties of these new complexes were compared to their known 2-phenylpyridinato analogues. The emission of the described complexes was clearly influenced by the applied ancillary ligand and can be adjusted over a broad range of frequencies **Fig.(1-6)**

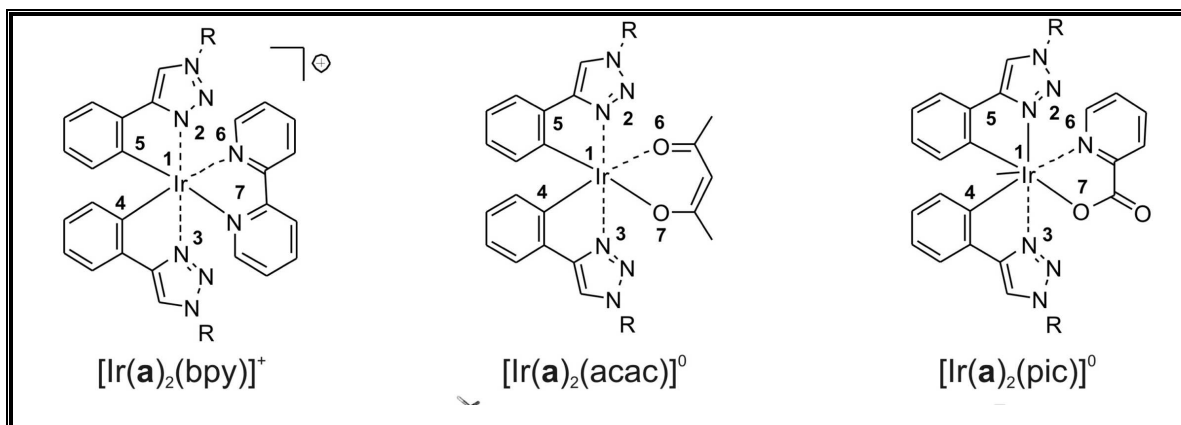


Fig. (1-6) Iridium(III) triazole complexes

(1.3) N & S donor ligands:

Chemistry of metal complexes containing both nitrogen and sulfur donor ligands has grown rapidly, largely due to the discovery of metals in mixed nitrogen/sulfur environments as the active sites of many important enzymes⁽¹⁷⁾. Macrocyclic ligands are considerably attractive in the quest for new chemistry, because they offer a wide variety of donor atoms, ionic charges, coordination numbers and geometry of the resultant complexes⁽¹⁸⁾. In the literature survey 1,3,4-thiadiazole, 1,2,3-triazole, amino acids, Schiff bases, semi and thiosemicarbazide had been divided as organic compounds having N,O and S donor atoms^(1,2,19), these compounds were largely used as antibacterial, antifungal, antitumor and anti-leukemia agents⁽²⁰⁾. As ligands, they also provide many potential binding sites for complexation and have obtained a diversified biological activity, by the result of such chelation⁽¹⁹⁾. Metal complexes of

semicarbazones and thiosemicarbazones have aroused considerable interest in view of their industrial and biological importance⁽²¹⁾.

In 2003 Kuzmanović⁽²²⁾ was prepared complexes of Ni(II) and Co(II) with 2-phenyl-2-imidazoline. Complexes were synthesized and characterized by elemental analysis of the metal, molar conductivity, magnetic susceptibility measurements, UV-Vis and IR spectra. The room temperature effective magnetic moments, UV-Vis and IR data of the complexes suggest that all Ni(II) and Co(II) complexes have a tetrahedral configuration, which is realized by participation of the pyridine nitrogen of two organic ligand molecules, and two chloride or nitrate anions, typical for these classes of organic ligands.

In 2008 Hussain and coworkers⁽²³⁾ reported a study of synthesis and antimicrobial activities of 1,2,4-Triazole and 1,3,4-Thiadiazole derivatives of 5-amino-2-hydroxybenzoic acid, the structures of the compounds were assigned on the basis of IR, ¹H NMR spectral data. The study interested to the synthesis of some triazole, thiadiazole derivatives and evaluation of their antimicrobial activities. Compounds 1,2,4-triazoles and 1,3,4-thiadiazoles were screened for their antibacterial activity against *S.aureus* (gram-positive) and *E. coli* (gram-negative) bacteria, compounds were found to have moderate antimicrobial activity⁽²³⁾.

In 2010 Salimon and coworkers⁽²⁴⁾ were reported a study of synthesis, characterization and biological activity of Schiff Bases of 2,5-dimercapto-1,3,4-thiadiazole, the compound were elucidated by elemental analysis, electronic absorption, infrared, ¹H and ¹³C NMR spectral measurements. The structural formula of prepared compound had shown in **Fig.(1-7)**

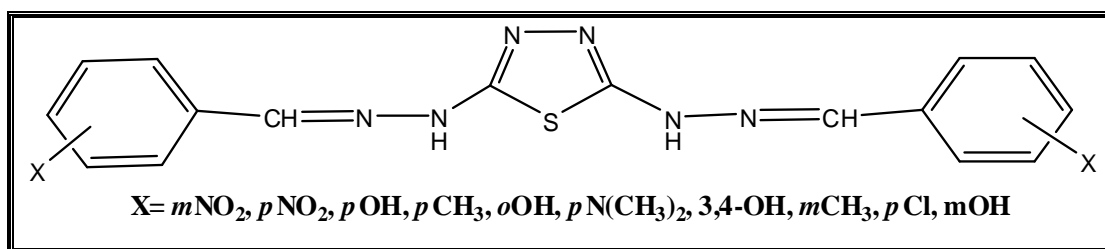
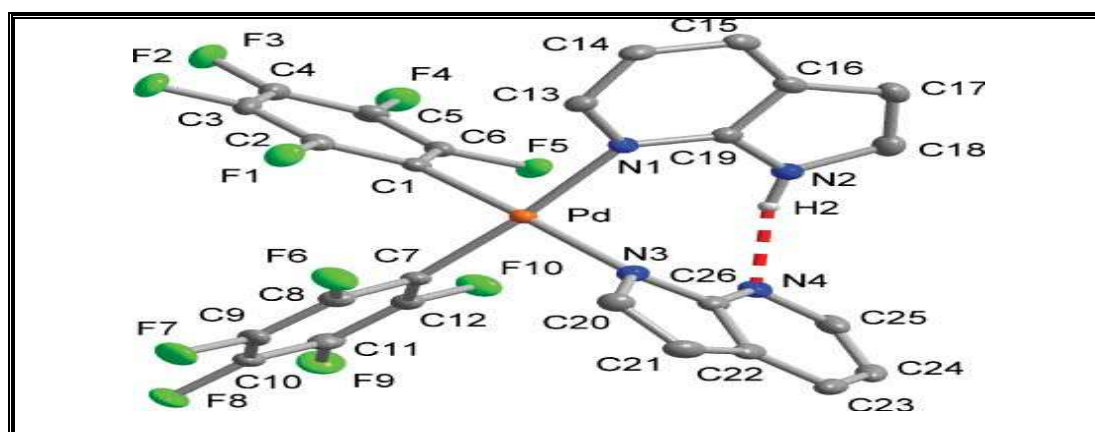


Fig. (1-7) Schiff Base ligand diverted from 1,3,4-thiadiazole

In 2010 Ruiz and coworkers⁽²⁵⁾ were reported a study of new 7-azaindole palladium and platinum complexes, crystal structures, theoretical calculations and *in vitro* anticancer activity of the platinum compounds. The X-ray structure determinations of $[\text{NBu}_4][\text{M}(\text{C}_6\text{F}_5)_2(\text{Haza-N}_7)(\text{aza-N}_1)] \cdot \text{Haza}$ [$\text{M} = \text{Pd}, \text{Pt}$; Haza = 7-azaindolate (*1H*-pyrrolo[2,3-*b*]pyridinate)] have established for the first time the coordination to the same metal center of both neutral and anionic forms of the ligand. Theoretical calculations were supported the observed coordination and H-bonding interaction of the pyrrolo and pyridine moieties of the neutral and deprotonated heterocyclic ligands. **Fig. (1-8)**



Fig(1-8) Crystal structure of Pd(II) pyrrolo pyridine complex

In 2012 Bentiss and coworkers⁽²⁶⁾ were reported a study of preparation of Aqua bis[2,5-bis(pyridin-2-yl)1,3,4-thiadiazole $\kappa_2\text{N}_2, \text{N}_3$] (trifluoromethane-sulfonato- κ_O)copper(II) trifluoro-methanesulfonate, the complex shows a distorted octahedral coordinated copper(II) cation

which is linked to two thiadiazole ligands, one water molecule and one trifluoromethanesulfonate anion. The second trifluoromethanesulfonate anion does not coordinate with Cu(II) cation. Each thiadiazole ligand uses one N pyridyl and one N thiadiazole atoms for coordination with copper ion. N atom of the second non-coordinating pyridin substituent is found on the same side of the 1,3,4-thiadiazole ring as the S atom, as it shown in **Fig.(1-9)**

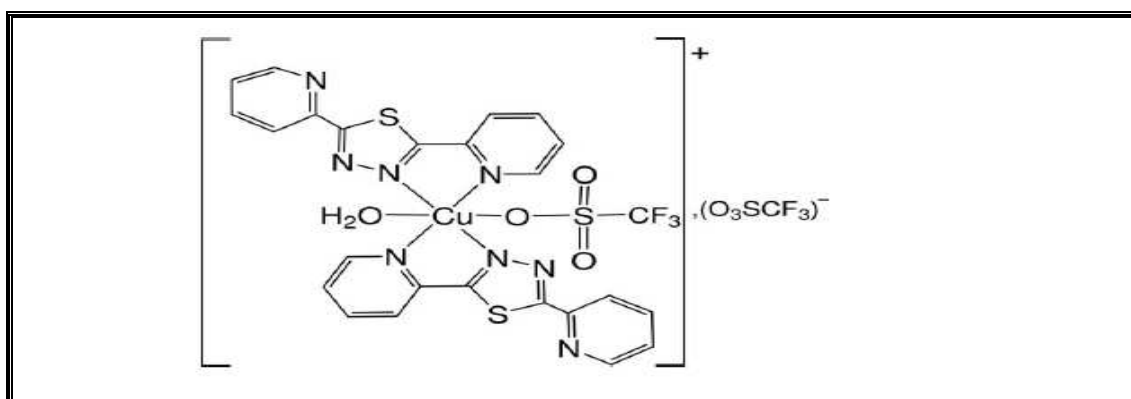


Fig. (1-9) Aqua bis[2,5-bis(pyridin-2-yl) 1,3,4-thiadiazole κ_2N_2,N_3] (trifluoromethanesulfonato κ_o)copper(II)trifluoromethanesulfonate

Theoretical data collection and calculation of this complex by several chemical computer programs⁽²⁶⁾ shown that ligand groups will be arrange around central metal ion in octahedral geometry. **Fig.(1-10)**

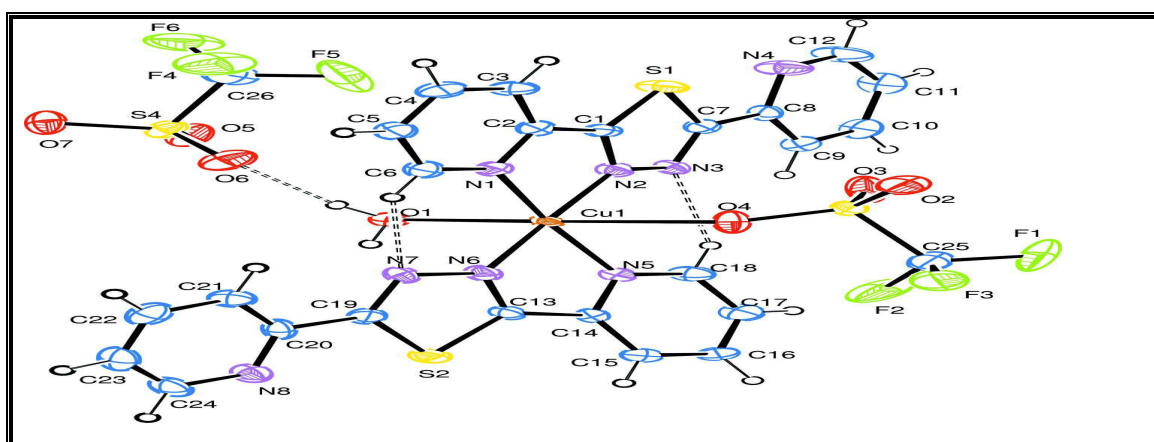


Fig.(1-10)Theoretical structure (octahedral geometry) of Cu(II) complex

(1.4) Metal Complexes Structures and Applications:

Metal complexes play an essential role in several fields and applications chemistry such as agriculture, pharmaceutical and industrial chemistry⁽²⁷⁾. So that, scientific research centers, big medicine companies, physical and chemical colleges around the world have a great interesting to study these compounds and its applications in all of life fields. The studied of complexes have a potential to be used as drugs and these would further enable us to evaluate their utility in agriculture and industry⁽²⁸⁾. The cognition of potential employment of metal complexes and chelates in therapeutic application provides useful outlets for basic research in transition metal chemistry⁽²⁹⁾.

(1.4.1) Cobalt Complexes Structures and Applications:

Cobalt complexes have been interesting in our life, some of vital compounds were divided as cobalt complexes, simple example of these compounds was B₁₂ Vitamin. As it known Vitamin B₁₂ (cobaloxime) is a cobalt complex containing a glyoxime ligand⁽³⁰⁾. Cobalt complexes were found to act as catalysts in cross-coupling and Mizoroki–Heck reactions⁽³¹⁾.

In 2001 Squattrito⁽³²⁾ was studied crystal structures of the cobalt complexes of 4-amino-3-trifluoromethyl-1,2,4-triazole-5-thione, he found that in the bis natural bidentate ligand of 4-amino-3-trifluoromethyl-1,2,4-triazole-5-thione, SN₄C₃H₃F₃ (afmt) of the divalent cobalt ion, the triazole bonds to the metal ion through the amine and thione substituents on the five-membered ring **Fig.(1-11)**. Two water molecules complete the octahedral coordination sphere [Co(afmt)₂(H₂O)₂](NO₃)₂

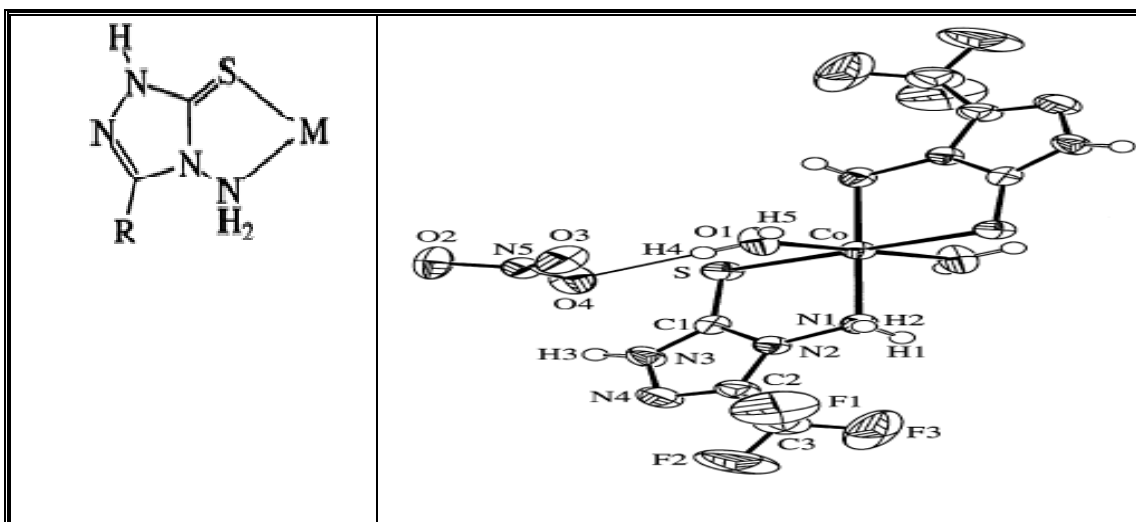


Fig.(1-11) five-membered ring of cobalt complex & its X-ray structure crystallography

In 2002 Nayak and coworkers⁽³³⁾ were reported a study of synthesis and characterization of some Cobalt(III) complexes containing heterocyclic nitrogen donor ligands. These compounds were belong to the type $\text{trans-[Co(DH)}_2\text{LCl]}$ where DH = dimethylglyoximate anion, L=heterocyclic nitrogen donor ligand(pyridine, piperidine). The complexes have been characterized by FT-IR, ^1H , ^{13}C NMR spectra, conductivity and thermal decomposition studies. The structure of these complexes shows that the geometry was octahedral and hydrogen bonding was formed between ligands in complexes **Fig. (1-12)**

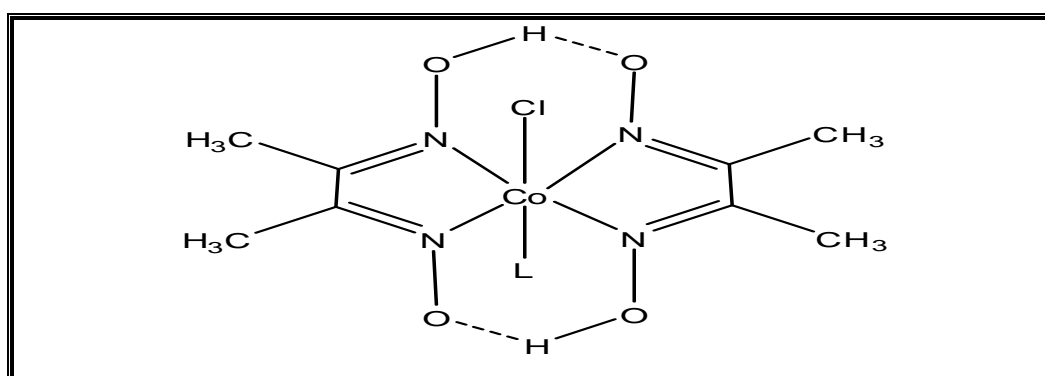


Fig. (1-12) Cobalt complex and H-bonding between ligands

In 2002 Amirasr and coworkers⁽³⁴⁾ were prepared and characterized a series of complexes of the type $M(\text{Phca}_2\text{en})\text{X}_2$, where $\text{Phca}_2\text{en} = \text{N,N}'\text{-bis}(\beta\text{-phenyl-cinnamaldehyde})\text{-1,2-diiminoethane}$. In the study the crystal and molecular structures of $[\text{Co}(\text{Phca}_2\text{en})\text{Cl}_2]$ **Fig.(1-13)** was determined by X-ray crystallography from single-crystal data, the coordination polyhedron about the central cobalt ion is distorted tetrahedron with Cl-Co-Cl , $110.17(6)^\circ$; and N-Co-N , $84.16(13)^\circ$. This structure consists of intermolecular hydrogen bonds of the type $\text{C-H}\cdots\text{X}$. The formation of the $\text{C-H}\cdots\text{M}$ weak intramolecular hydrogen bonds due to the trapping of C-H bonds in the vicinity of the metal atoms.

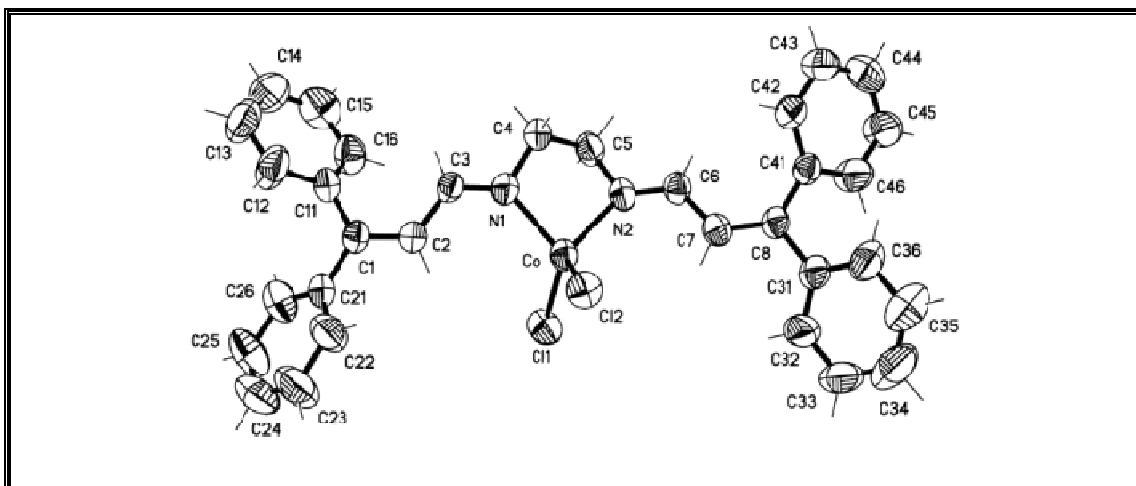


Fig.(1-13) X-ray crystallography of $[\text{Co}(\text{Phca}_2\text{en})\text{Cl}_2]$ complex

In 2003 Brooker and Udo Beckmann⁽³⁵⁾ were synthesized and characterize many of di and tri nuclear cobalt complexes with many of triazoles, the complexes were characterized by X-ray crystallography and the geometry of all complexes was octahedral. **Fig.(1-14)**

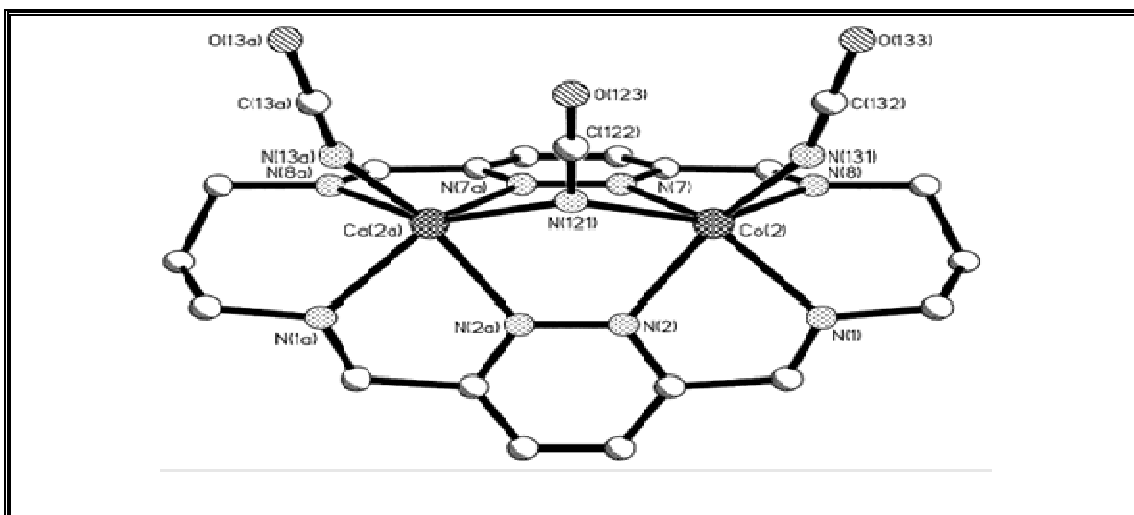


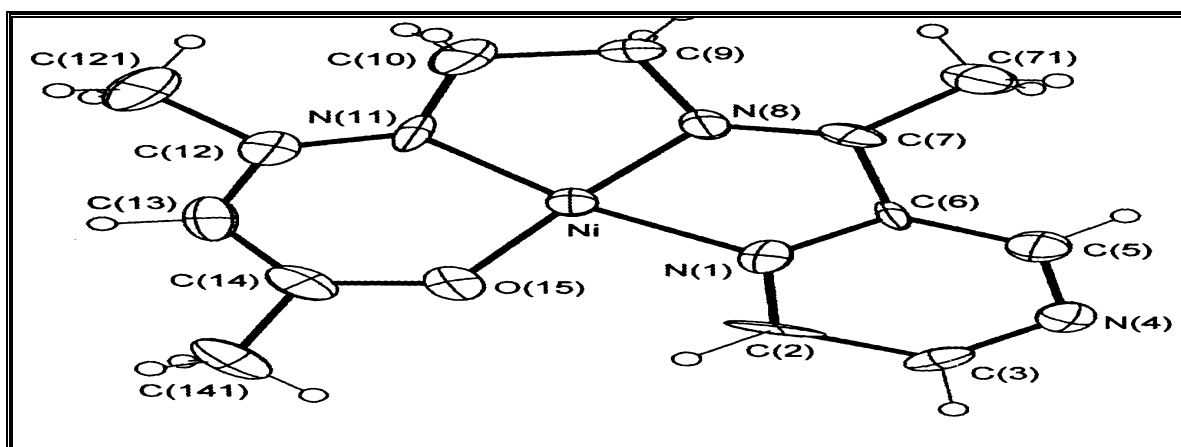
Fig.(1-14) Perspective view of the $[\text{Co}^{\text{II}}_2(\text{L})(\text{NCO})_3]^+$ cation

In 2010 Chang and coworkers⁽³⁰⁾ were reported an interview and study of cobalt complexes as antiviral and antibacterial agents, the cobalt complexes were containing polydentate donor ligands, the study was focus on the *antimicrobial* activity of the homoleptic $[\text{Co}(\text{NH}_3)_6]^{3+}$ ion. So the study was review the current status of the biological activities of Co(III) complexes formed with mono and polydentate ligands.

(1.4.2) Nickel Complexes Structures and Applications:

Nickel was found in its compounds in several oxidation states; the divalent ion seems to be the most important for both organic and inorganic substances. Water-insoluble nickel compounds may dissolve in biological fluids. Particles of the same chemical entity (oxides and sulfides) have different biological activity depending on crystalline structure and surface properties⁽³⁶⁾.

In 2000 Bermejo and coworkers⁽³⁷⁾ were synthesized and studied of Mono- and di- nuclear Ni(II) complexes with N₃O Schiff base ligands and crystal structure of [Ni(AEPyz)]ClO₄ (HAEPyz derived from 7-amino-4-methyl-5-aza-3-hepten-2-one and 2-acetylpyrazine). In the study mono- and di- nuclear Ni(II) complexes with N₃O asymmetrical Schiff bases have been prepared and characterized, physicochemical data indicate that all the complexes were quasi square-planar. The X-ray crystal structure of [Ni(AEPyz)]ClO₄ was reported, whose NiN₃O chromophore is remarkably square planar. **Fig(1-15)**



Fig(1-15) X-ray of the complex cation [Ni(AEPyz)]⁺

In 2007 Santillan and Carrano⁽³⁸⁾ were reported a research of synthesized new binuclear complexes of Ni(II) derived from a diatopic hetero -scorpionateligand,(4-carboxyphenyl) bis(3,5dimethyl -pyrazolyl) methane, the complexes have been synthesized and characterized by X-ray diffraction, ¹H NMR, IR, UV-Vis spectroscopies, and magnetic susceptibility. These building blocks have been subsequently used for the construction of higher order metallosupramolecular architectures. **Fig. (1-16)**

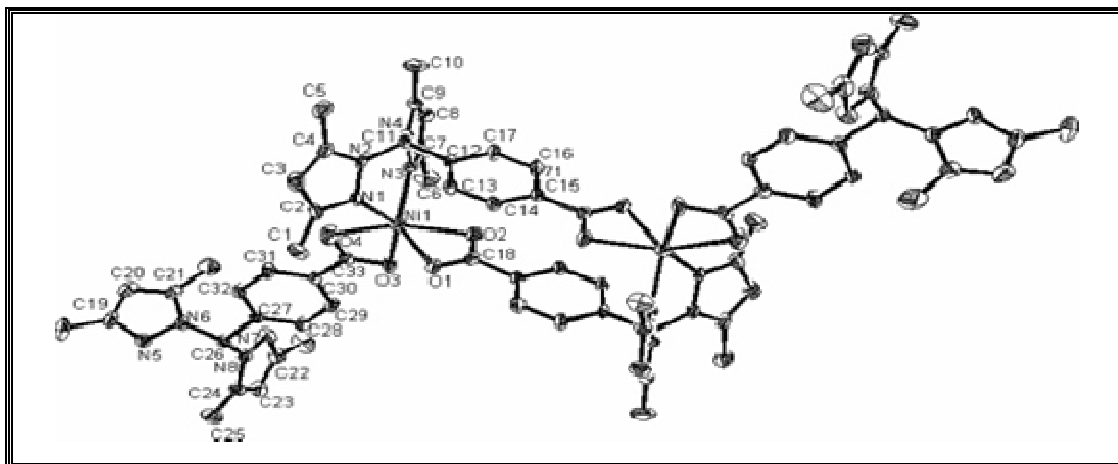
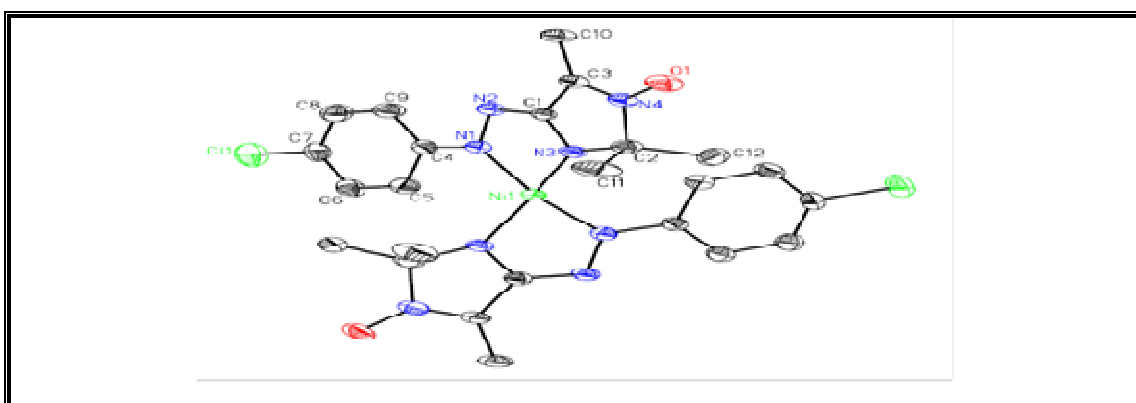


Fig (1-16) X-ray of [Ni₂ (L4c)₄] complex

In 2005 Boese and coworkers⁽³⁹⁾ were reported a study of ring transformation and complex formation of (3-acetyl-4,5-dihydro-1,2,4-triazole oximes). The reaction of the ligands with Ni(II) and Pd(II) acetates in ethanol at room temperature yielded the respective square planar complexes. X-ray structure determination of one of these complexes revealed that metallation led to unexpected ring transformation of the triazole ligand. It is probable that such ring transformation generated the imidazole-N-oxide intermediate which coordinated to Ni(II) ion. The complexes were characterized by elemental analysis, FT-IR, ¹H-NMR, ¹³C-NMR and HRMS spectroscopies. Complex theoretical structure was in square-planar geometry, it was draw by ORTEP plot. **Fig.(1-17)**



Fig(1-16) ORTEP plot of the molecular structure of Ni(II) complex

In 2010 Al-Amiery and coworkers⁽⁴⁾ were reported a study of synthesis, characterization and *antibacterial* study of some metal complexes derived from bis(5-(benzylthio)-1,3,4-thiadiazol-2-yl)methane, one of these complexes was containing Ni(II) metal ion, these complexes were characterized by C.H.N.M. elemental analysis, FTIR spectroscopy, Electronic spectra (UV–Vis), in addition to molar conductance of complexes solution in DMF solvent , and evaluation the magnetic moments *via* Gouy’s method .The *antibacterial* activity for the ligand and their metal complexes were studied against three selected micro-organisms *Staphylococcus aureus*, *Pseudomonas*, and *Klebsiella* complexes were more effective than alone ligand.

In 2012 Aly and coworkers⁽⁴⁰⁾ they are study of synthesis and characterization of transition metal coordination polymers derived from 1,4-benzenedicarboxylate and certain azoles. A series of coordination polymers of Co(II), Ni(II), and Cu(II) were prepared and characterized based on elemental analysis, infrared and electronic spectral studies, magnetic measurements, molar conductance, thermal analysis, X-ray diffraction, scanning electron microscopy, and biological activity.

Fig(1-18)

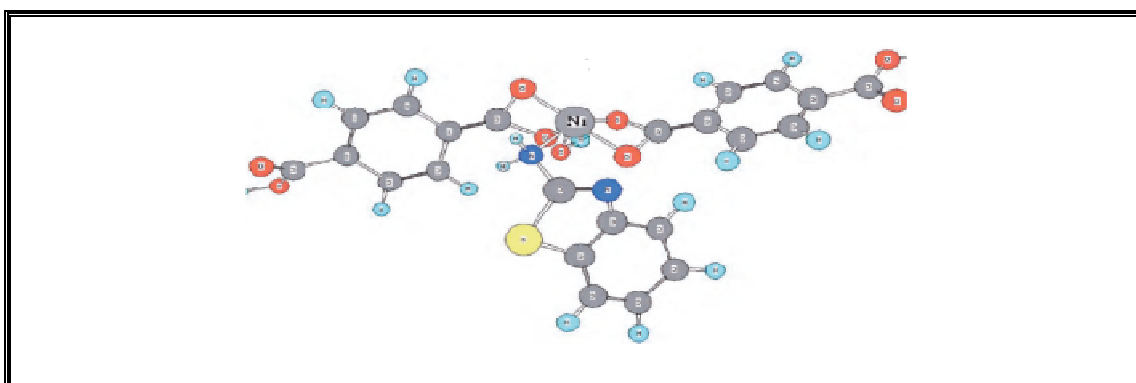
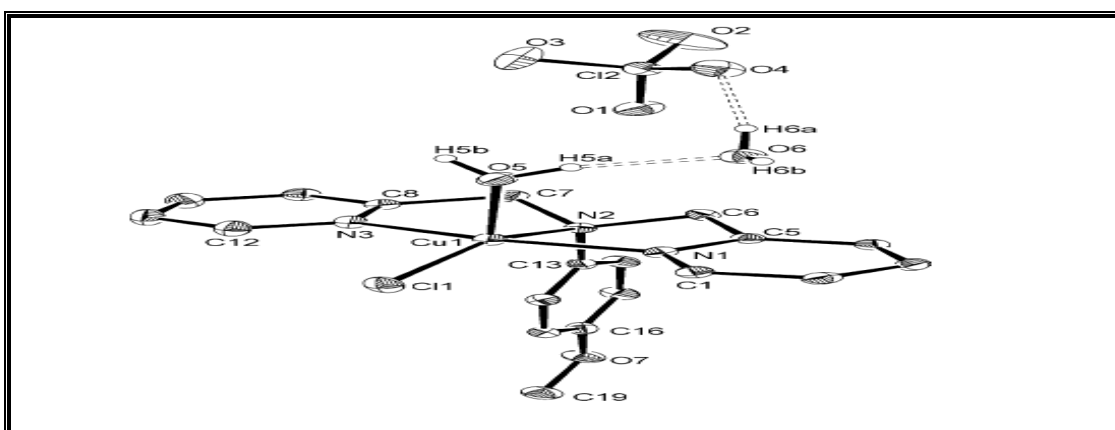


Fig. (1-18) A perspective view of complete coordination around Ni(II)

(1.4.3)Copper Complexes Structures and Applications:

It has been established that the properties of copper-coordinated compounds are largely determined by the nature of ligands and donor atoms bound to the metal ion. The most remarkable achievements in the design and development of Cu(I) and Cu(II) complexes as *antitumor*, *anticancer* agents, industrial and agriculture applications⁽⁴¹⁾.

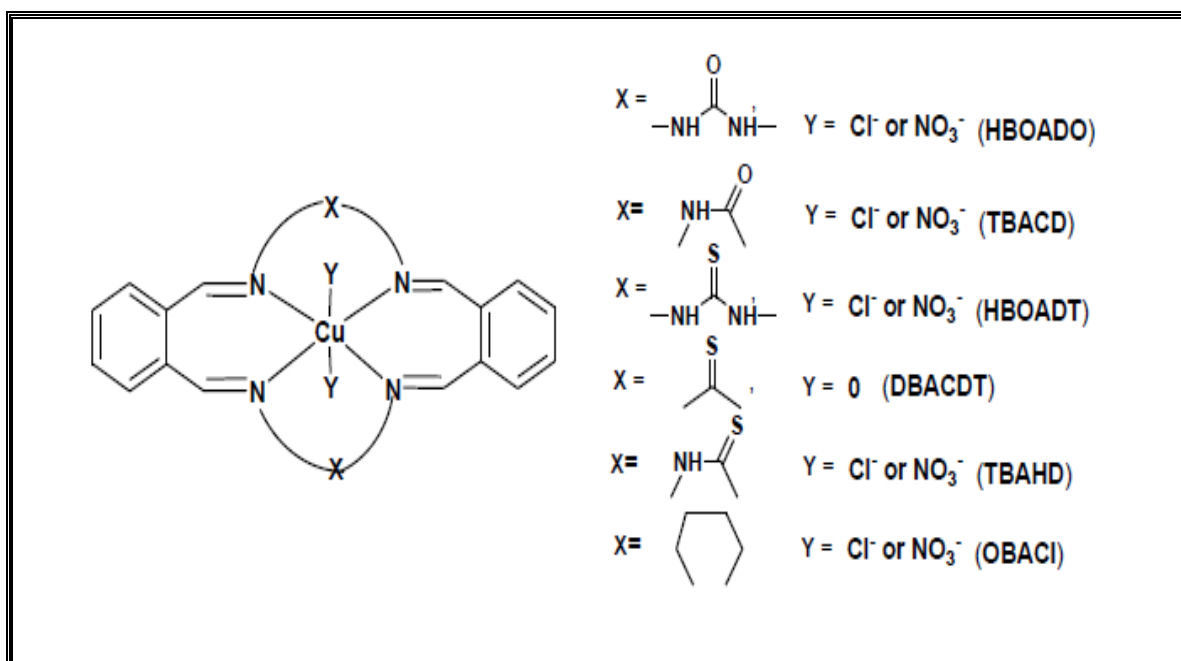
In 2006 McGinley and coworkers⁽⁴²⁾ were reported a study of Copper(II) complex of a tridentate N-donor ligand with unexpected Cu–H interaction. The new pyridine amine ligand, meophdpa -bis(dipyridylmethyl)-4-methoxyaniline) was synthesized and reacted with copper(II) perchlorate. The X-ray crystal structure of the resulting complex revealed a monomeric copper(II) site, with the copper bound to the three ligands nitrogen in a relatively unusual meridional fashion, as well as a chloride and a water molecule. The sixth coordination site was, unexpectedly, occupied by a phenyl ring hydrogen atom. **Fig (1-19)**



Fig(1-19)X-ray structure of $[\text{Cu}(\text{meophdpa})\text{Cl}(\text{H}_2\text{O})](\text{ClO}_4)\cdot\text{H}_2\text{O}$

In 2012 Ravinder and coworkers⁽¹⁸⁾ were synthesized and studied spectral and antibacterial of Copper(II)tetra-aza macrocyclic complexes. In the study a novel family of tetra-aza macrocyclic Cu(II) complexes

[CuLX₂] (where L = N₄ donor macrocyclic ligands) and (X = Cl⁻, NO₃⁻) have been synthesized and characterized by elemental analysis, magnetic moments, FT- IR, EPR, mass, electronic spectra and thermal studies. The magnetic moments and electronic spectral studies suggest square-planar geometry for [Cu(DBACDT)]Cl₂ and [Cu(DBACDT)](NO₃)₂ complexes [where (DBACDT) = 7,16-dihydrodibenzo(*e,l*) [1,3,8,10]-tetraazacyclo tetradecine-7,16-dithione] and distorted octahedral geometry to the rest of the complexes. The biological activity of all these complexes against gram-positive and gram-negative bacteria was compared with the activity of existing commercial antibacterial compounds . **Fig(1-20)**



Fig(1-20) Representative structures of copper complex

(1.4.4) Palladium Complexes Structures and Applications:

Palladium complexes have been interested in many application fields: research, industry, chemotherapy and agriculture. The significant similarity between the coordination chemistry of palladium(II) and platinum(II) compounds has advocated studies of Pd(II) complexes as antitumor drugs; but the hydrolysis in palladium complexes is too rapid

about 10^5 times faster than for their corresponding platinum analogues, so that, several research groups have focused on the preparation of Pd(II) complexes bearing bidentate ligands as a way to stabilize these compounds and to prevent any possible *cis-trans* isomerism⁽⁴³⁾ **Fig.(1-21)**

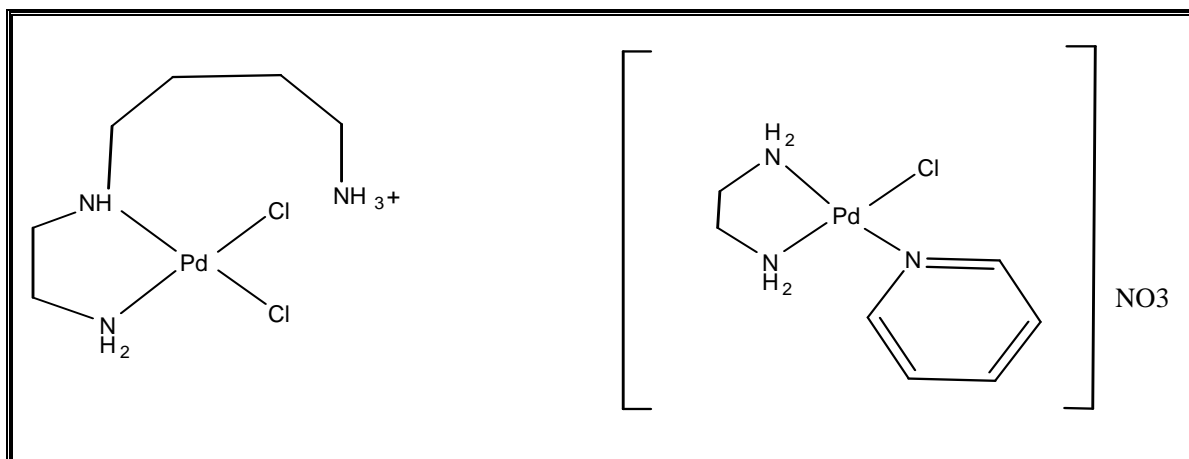
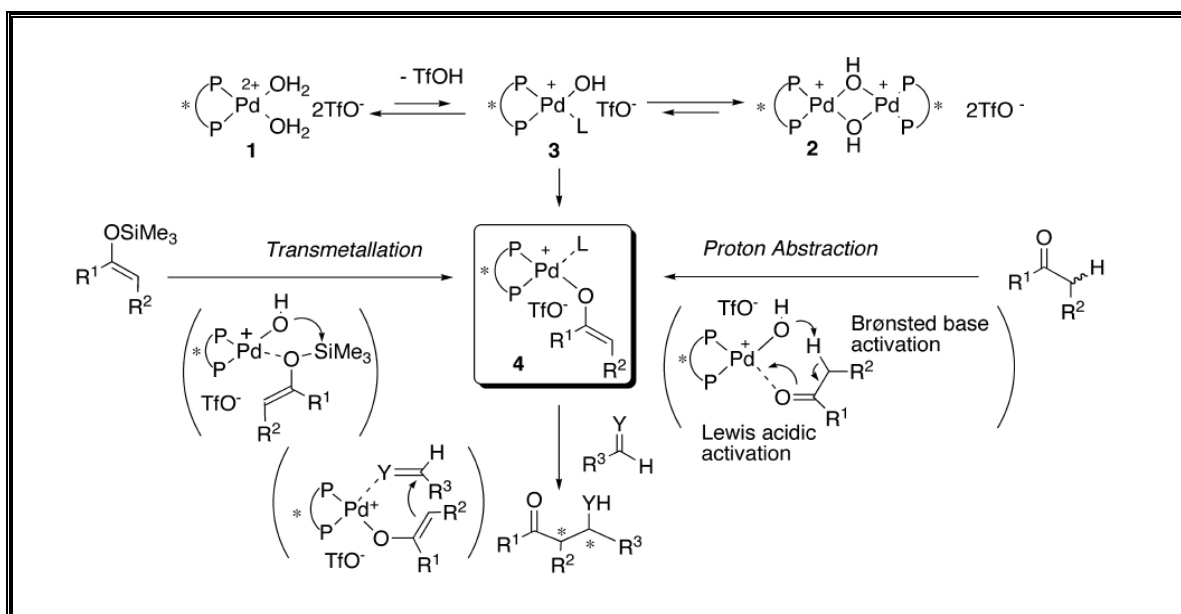


Fig. (1-21) Palladium(II) complexes with ethylenediamine ligand

In 2006 Sodeoka and Hamashima⁽⁴⁴⁾ were reported a study of acid–base catalysis using chiral palladium complexes. In the study chiral Pd aqua and μ -hydroxo complexes were found to act as mild Brønsted acids and bases, and chiral Pd enolates were generated from these complexes even under acidic conditions. Highly enantioselective Michael addition, Mannich-type reaction, fluorination, and conjugate addition of amines have been developed based on the acid–base character of these Pd (II) complexes. **Scheme (1-3)** shown Pd enolate as a key intermediate for the enantioselective reactions:



Scheme (1-3) Pd(II) enolate as a key intermediate for the enantioselective reactions

In 2010 Asiri and Khan⁽⁴⁵⁾ were reported a study of Palladium(II) complexes of N and S donor ligands derived from steroidal thiosemicarbazones as *antibacterial* agents. In the study they were reported synthesis, characterization and *antibacterial* activity of Pd (II) complexes of steroidal thiosemicarbazones (STSC) against two Gram-positive and Gram-negative bacteria. The structures of these compounds were elucidated by IR, ¹H NMR, ¹³C NMR, FAB mass spectroscopic methods, elemental analyses and TGA analysis. The *antibacterial* activity of these compounds were tested *in vitro* by the disk diffusion assay against two Gram-positive and two Gram-negative bacteria. The results showed that steroidal complexes are better inhibitors of both types of the bacteria as compared to steroidal thiosemicarbazones. **Fig. (1-22)**

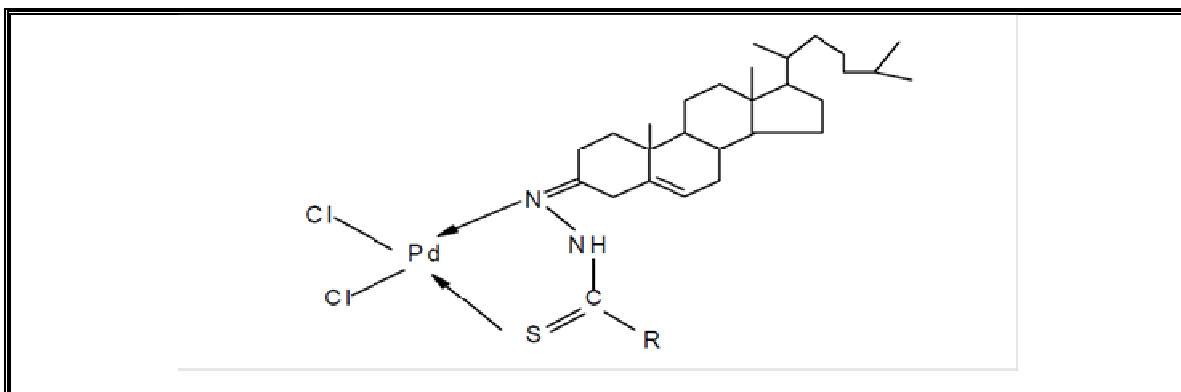


Fig. (1-22) structure of palladium (II) complexes with thiosemicarbazone derivatives

In 2011 Mirica and coworkers⁽⁴⁶⁾ were reported a study of binuclear palladium(III) complexes with a single unsupported bridging halide ligand and reversible formation from mononuclear palladium(II) or palladium(IV) precursors. In the study they were reported novel cationic binuclear Pd(III) and mono-nuclear Pd(IV) complexes supported by a common tridentate nitrogen donor ligand, N,N',N''-trimethyl-1,4,7-triazacyclononane (Me₃tacn). The X-ray structure analysis of complex reveals a square-planar arrangement of two Cl⁻ ions and two N atoms around Pd, while the third N atom of Me₃tacn is not in close proximity to the metal center. **Fig. (1-23)**

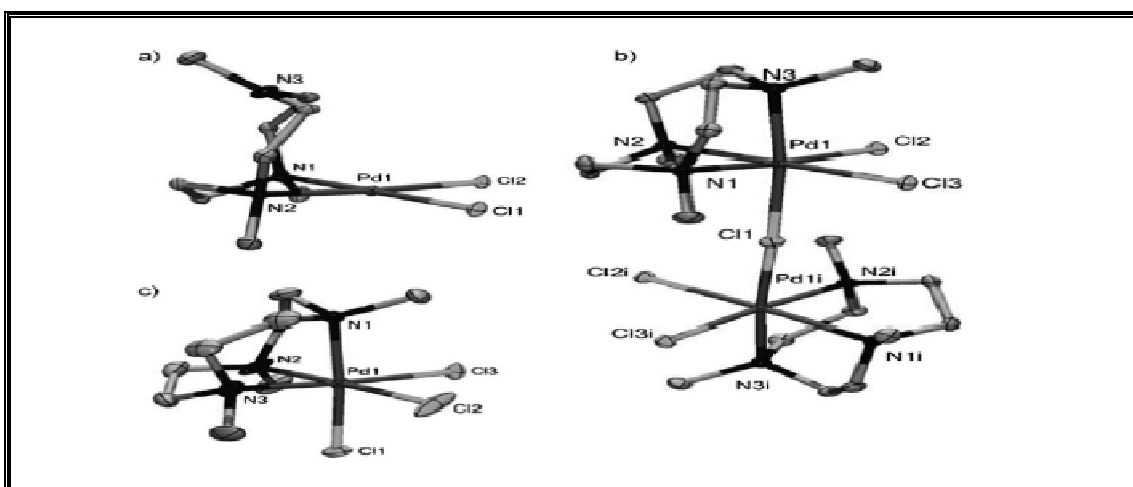


Fig. (1-23) X-ray crystallography of Pd(II) complexes

(1.4.5) Platinum Complexes Structures and Applications:

Chemical, pharmacological and clinical research on anticancer coordination complexes has yielded remarkable anticancer agents such as cisplatin, carboplatin, and oxaliplatin^(47, 48). Many of studies had been prepared to explain the mechanism of platinum complexes activity as anticancer and *antitumor* agents⁽⁴⁹⁻⁵²⁾.

In 2002 De Almeida and coworkers⁽⁵¹⁾ were reported a study about synthesis of platinum complexes from N-Benzyl-1,3-propanediamine derivatives, potential antineoplastic agents. They were described the synthesis of seven new platinum complexes having N-benzyl-1,3-propanediamine derivatives as ligands. Complexes were prepared by the reaction of $K_2[PtCl_4]$ with the appropriate ligand in water. The complexes were analogs of cisplatin, so they were characterized by FT-IR, 1H -, ^{13}C - and ^{195}Pt NMR spectroscopies.

In 2003 Collins and Wheate⁽⁵²⁾ were reported a study of binuclear platinum complexes as *anticancer* drugs. In the study it has been found that the multi-nuclear platinum complexes exhibit excellent anti-cancer activity, the associated toxicity could limit their clinical use. Given that these complexes derive their activity from the novel adducts they form with DNA, three important aspects of their binding are discussed; their DNA pre-association, the DNA adducts formed and the DNA conformational changes induced. **Fig (1-24)**

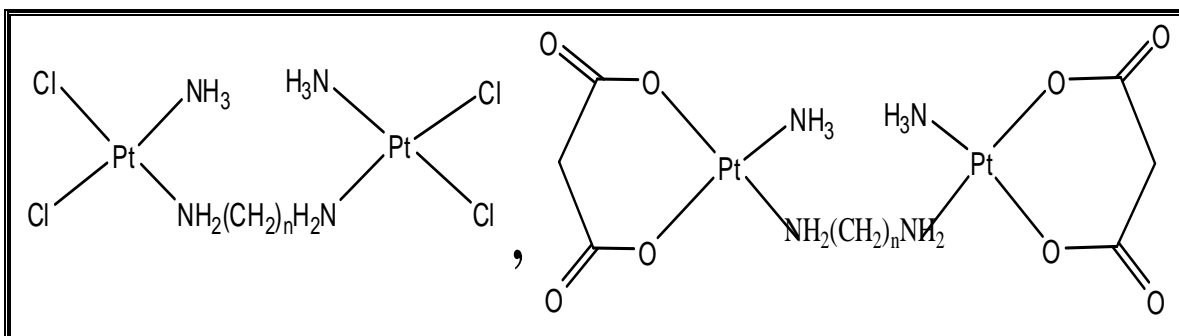


Fig. (1-24) Binuclear platinum complexes containing two linked cisplatin centers

In 2011 Bakalova and coworkers⁽⁵³⁾ were reported a study of platinum complexes with 5-methyl-5(4-pyridyl)hydantoin and its 3-methyl derivatives, synthesis and cytotoxic activity quantitative structure activity relationships. The novel complexes were characterized by elemental analysis, IR, ^1H , ^{13}C , ^{195}Pt NMR spectroscopies and molar conductivity. The cytotoxic effects of these complexes were examined on three human tumor cell lines by MTT-dye reduction assay. **Fig. (1-25)** shown molecular structures of the investigated Pt(II) and Pt(IV) complexes:

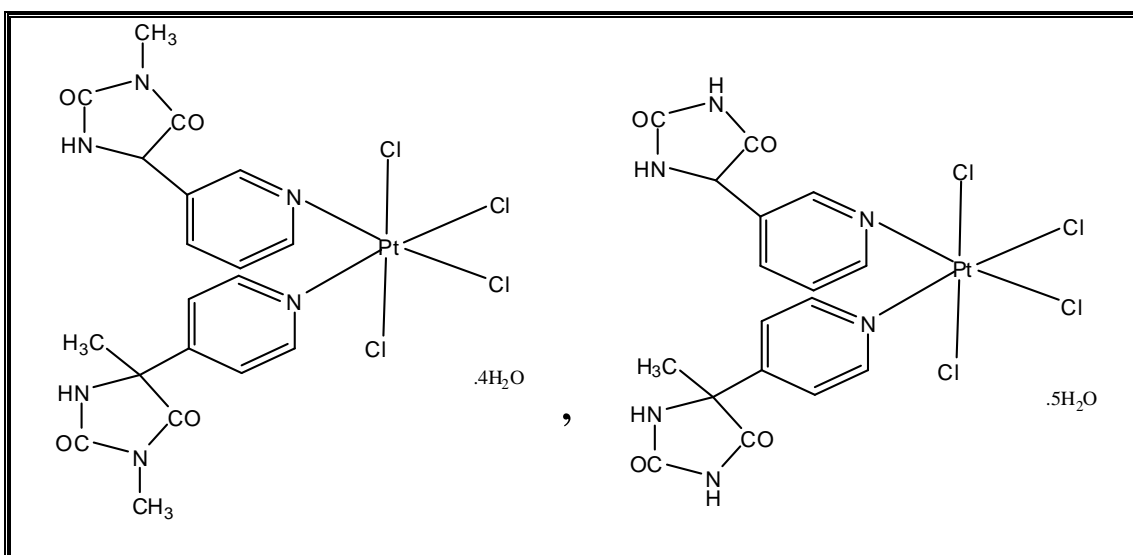


Fig.(1-25) Molecular structures of the investigated Pt(IV) complexes

In 2011 Dell'Amico and coworkers⁽⁵⁴⁾ were reported a study of bent binuclear platinum (II) halo-bridged carbonyl complexes. The study appeared that binuclear platinum (II) complexes have two square-planar planes, so the bent (angle) between these planes decrease belong to the decrease of electronegativity of halo-bridge atom, so it was in(I) less than (Br) and in (Br) less than (Cl), when the halo-bridge atom was (Cl) there was not found bent, the angle in this case is equal 180°. **Fig.(1-26)** the crystal structure of $trans-[Pt_2(\mu-Cl)_2Cl_2(CO)_2]$ and **Fig.(1-27)** the crystal structure of $trans-[Pt_2(\mu-X)_2X_2(CO)_2]$ X= Br, I

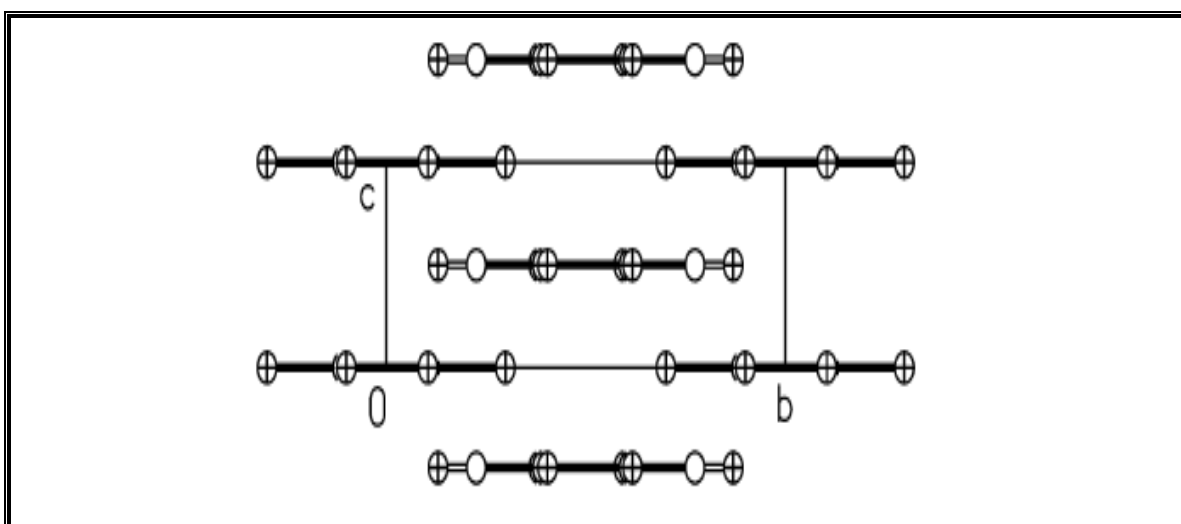


Fig.(1-26) The crystal structure of $trans-Pt_2(\mu-Cl)_2Cl_2(CO)_2$

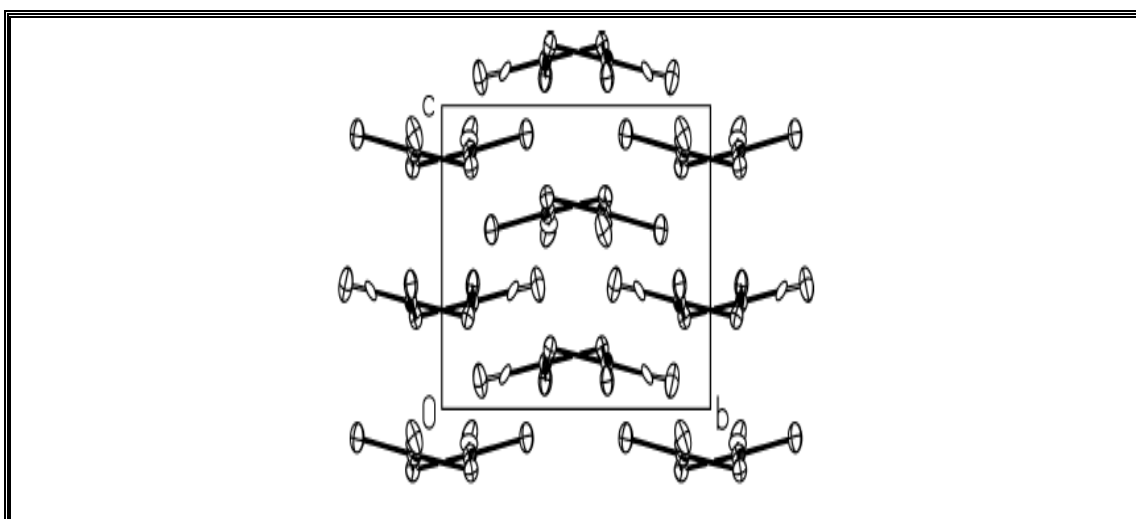


Fig.(1-27) The crystal structure of $trans-Pt_2(\mu-X)_2X_2(CO)_2$, X= Br, I

(1.5) The Aim of Work:

Literature show that 2,5-Dimercapto1,3,4-thiadiazoles, 1,4-substituted 1,2,3-triazoles and there complexes have a general role in analytical, industrial, agriculture and pharmacological applications^(1, 8, 11, 13). According to these facts, the aim of this work could be summarized:

- 1- Synthesis and characterization of a series of polydentate (2,5-bis((1-alkyl-1H-1,2,3triazole-4-yl)methylthio)-1,3,4-thiadiazole) ligands type N_4S_2 that may be used in medical application as *antibacterial*, *antifungal*, and *antiviral* agents.
- 2- Synthesis complexes of ligands with some metal ions of potential medicinal, industrial, agriculture and analytical applications.
- 3- Study the coordination positions of the prepared ligands with various metal ions.
- 4- Study the chemistry and structure of the prepared complexes.

(2) Experimental Section:**(2.1) Chemicals:**

All common laboratory chemicals and reagents are listed in **Table (2-1)**. It has been used without further purification.

Table (2-1) Chemicals used and their supplier

No.	Material	Company source of supply	Purity %
1	1-Iodooctane	Aldrich	98.00
2	1-Iododecane	Aldrich	98.00
3	1-Bromoheptane	Aldrich	99.00
4	Sodium azide	B.D.H	99.00
5	Dimethylsulfoxide (DMSO)	Qualikems	99.00
6	Diethyl ether	Scharlau	99.50
7	Ethyl acetate	Sigma-Aldrich	99.50
8	N-N Dimethyl form amide (DMF)	Qualikems	99.00
9	Methanol	Fluka	99.90
10	Absolute Alcohol (Ethanol)	Hyman	99.90
11	n-Hexane	G C C	95.00
12	Dichloromethane (DCM)	Lab-Scan	99.80
13	Acetonitrile	Sigma-Aldrich	99.50

No.	Material	Company source of supply	Purity %
14	Sodium sulfate	Sigma	99.90
15	Sodium-L-ascorbate	Sigma	98.00
16	Propargylbromide	Aldrich	80.00
17	1,3,4-Thiadiazole-2,5-dithiol dipotassium salt	Aldrich	98.00
18	Platinum tetrachloride	Fluka	99.00
19	Palladium chloride	B.D.H	99.00
20	Nickel (II) chloride hexahydrate	Fluka	99.00
21	Cobalt (II) chloride hexahydrate	Riedel. De Hean	99.00
22	Copper (II) chloride dihydrate	Merck	99.00
23	Copper sulfate pentahydrate	B.D.H	99.00
24	t-Butanol	G.C.C	99.50
25	Acetone	G.C.C	99.00
26	Sodium Chloride	Trade	99.00

(2.2) Instruments & Techniques:

The following measurements were used to characterize the ligands and their complexes.

(2.2.1) Melting point measurement:

Melting points of the complexes were measured determined in open glass capillary tubes using an electro thermal 9300 digital melting point apparatus with an Electro-thermal Stuart melting point apparatus.

(2.2.2) Infrared spectra:

Infrared spectra were recorded as (KBr) and (CsI) discs using (8300) (FT-IR) Shimadzu spectrophotometer in the range (4000–400) cm^{-1} , at University of Kufa / Iraq.

(2.2.3) Electronic spectra:

The electronic spectra of the compounds were obtained using a (UV-Visible) spectrophotometer type Shimadzu 160 in the range (800–200) nm, using quartz cell of (1.0) cm length with concentration (10^{-3}) mol.L^{-1} solution in DMF at 25°C of sample.

(2.2.4) Thin layer chromatography (TLC):

TLC was performed on ready-to-use silica-gel G-plates (Mesh 60) to monitor the reactions and test the purity of the new synthesized compounds, staining solution was KMnO_4 in basic media.

(2.2.5) Magnetic Susceptibility Measurements:

Magnetic susceptibility measurements determined by Balance Magnetic Susceptibility, Model (MSB-Mk1) at University of Al-Nahrain / Iraq.

(2.2.6) Conductivity Measurement:

Electrical conductivity measurements of the complexes were recorded at 25°C for solutions of samples in DMF using a PW 9526 digital Conductivity meter.

(2.2.7) Elemental microanalysis:

Elemental microanalysis for the ligands were performed on a (C.H.N.S) analyser from EuroEA elemental analyser at University of Kufa / Iraq.

(2.2.8) ^1H and ^{13}C NMR spectra:

^1H and ^{13}C NMR spectra for ligands and some complexes were recorded in DMSO- d_6 using a Jeol EX270 MHz, and BRUKER-400 MHz instruments with a tetramethylsilane (TMS) as an internal standard at Ahl-Albait University / Amman-Jordan.

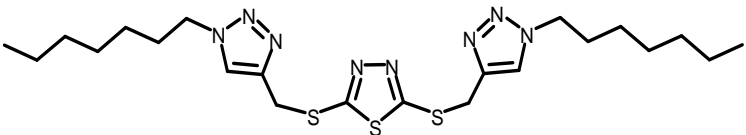
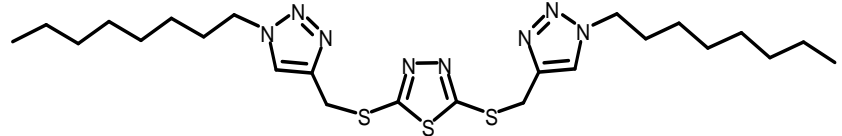
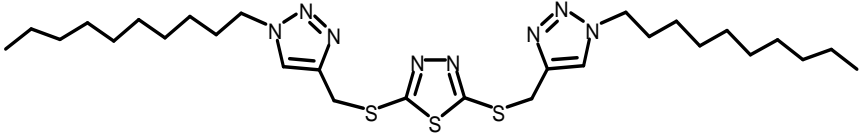
(2.2.9) The Proposed molecular structure:

The molecular structures of the complexes were suggested by using chem. Office 2003, ultra draw and ultra pro3DX program.

(2.3) Abbreviation of the ligands

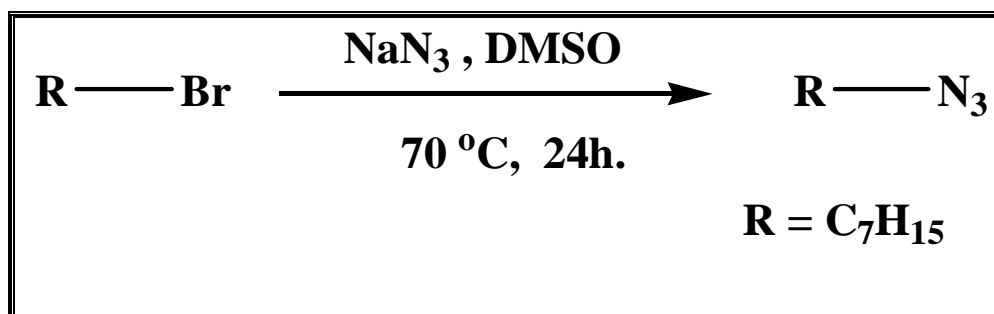
Table (2-2): describes the suggested abbreviation, structure and nomenclature of the synthesized ligands.

Table (2-2): Abbreviations, structure and nomenclature of the synthesized ligands

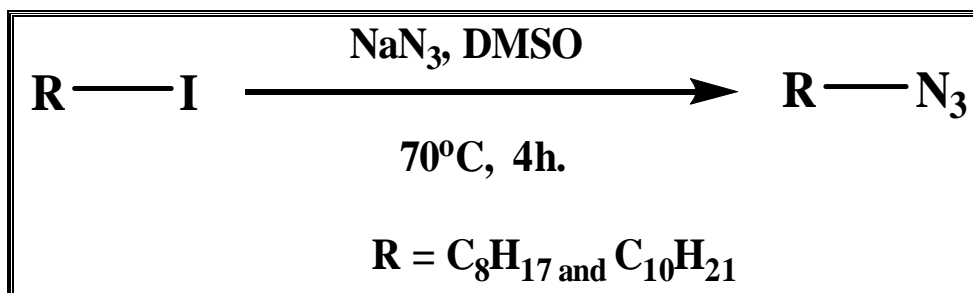
Symbol	Structure	M.W & Empirical formula
L¹	 <p>2,5-bis((1-heptyl-1H-1,2,3-triazol-4-yl)methylthio)-1,3,4-thiadiazole</p>	508.77 C₂₂H₃₆N₈S₃
L²	 <p>2,5-bis((1-octyl-1H-1,2,3-triazol-4-yl)methylthio)-1,3,4-thiadiazole</p>	536.82 C₂₄H₄₀N₈S₃
L³	 <p>2,5-bis((1-decyl-1H-1,2,3-triazol-4-yl)methylthio)-1,3,4-thiadiazole</p>	592.93 C₂₈H₄₈N₈S₃

(2.4) Synthesis of the ligands and precursors:

The compounds of 2,5-bis[(1-alkyl-1H-1,2,3-triazol-4-yl)methylthio]-1,3,4-thiadiazole (alkyl = heptyl-, octyl- and decyl) were synthesized by a method containing multi step reactions as well as using starting materials to produce the precursor compounds then preparing final products. The methods are listed below

(2.4.1) Preparation of 1-azidoalkane:**(2.4.1.1) Preparation of 1-azidoheptane:****Scheme (2:1) preparation of 1-azidoheptane**

Sodiumazide (2.93 g, 45 mmol) was added to the stirred solution of 1-bromoheptane (2.686 g, 15 mmol) in DMSO (50 mL), the suspension was stirred at 70 °C for 24 h., the reaction mixture was diluted with water (50 mL), extracted with Et₂O (3 × 50 mL). the combined organic layer was washed with saturated solution of NaCl (50 mL), dried over Na₂SO₄ and evaporated to dryness under reduced pressure to give 1-azidoheptane as a colorless liquid (1.485g, 70%).

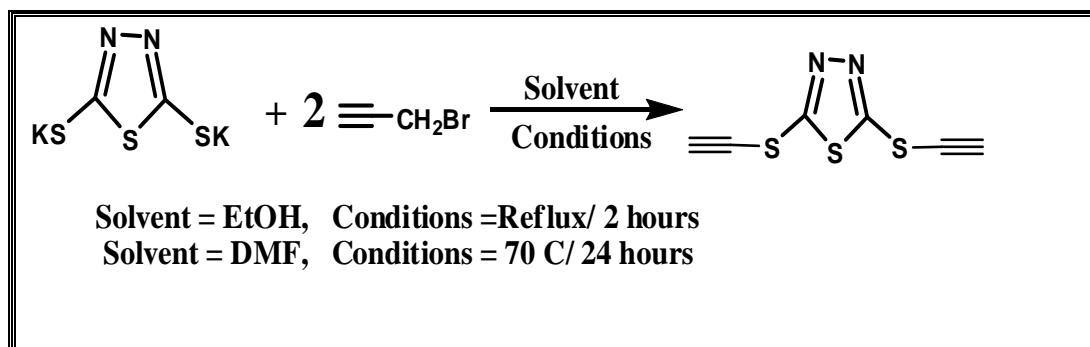
(2.4.1.2) preparation of *n*-alkylazides:Scheme (2-2) preparation of *n*-alkyl azides

Sodium azide (2.93 g, 45 mmol) was added to the stirred solution of alkyl iodide (15 mmol) in DMSO (50 mL), the suspension was stirred at 70°C for (4 h.), the reaction mixture was poured in water (100 mL) and extracted with Et₂O (3 × 50 mL), the combined organic layers were washed with saturated solution of NaCl (50 mL), dried over Na₂SO₄ and evaporated under reduced pressure to give *n*-alkylazides as a colorless liquids. **Table (2-3)** states the quantities, reaction conditions to prepare compounds.

Table (2-3) Quantities & reaction conditions to prepare compounds

Compound	Starting alkylhalide	Alkylhalide (mmol. & wt.)	Sodiumazide (mmol. & wt.)	Time & Temp.	%of yield
1-Azido octane	1-Iodooctane	(15 mmol, 3.600 g)	(45 mmol, 2.925 g)	4 hours 70 °C	59.30
1-Azido decane	1-Iododecane	(15 mmol, 4.022 g)	(45 mmol, 2.925 g)	4 hours 70 °C	53.13

(2.4.2) Preparation of [2,5-bis(prop-2-ynylthio)-1,3,4-thiadiazole] terminal alkyne derivatives from 2,5-dimercapto -1,3,4-thiadiazole salt :



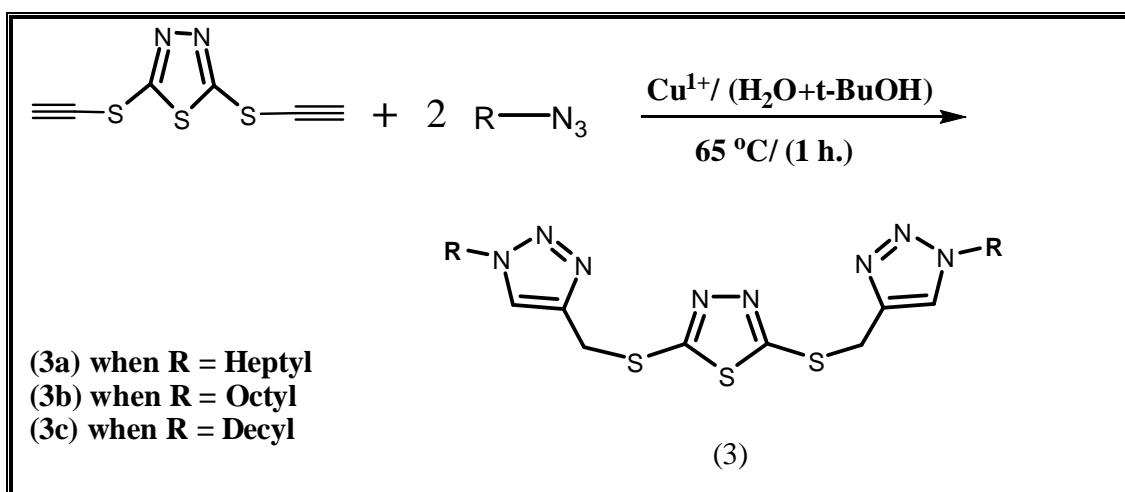
Scheme (2-3) preparation of terminal alkyne

Two different methods had been used to prepare this compound: First, propargylbromide (24 mmol, 2.856 g) was added to the stirred solution of 1,3,4-Thiadiazole-2,5-dithiol dipotassium salt (24 mmol, 2.856 g) in EtOH (40 mL), the mixture was stirred and reflux for (2 h.), the mixture was poured in ice water (80 mL) and extracted with Et₂O (3 × 40 mL), the combined organic layers were washed with saturation solution of NaCl (50 mL), dried over Na₂SO₄ and evaporated under reduced pressure to give 2,5-bis(prop-2-ynylthio)-1,3,4-thiadiazole. Recrystallized by n-Hexane the product was precipitated as white needle crystals in yield (0.485 g) %17.

Second, propargylbromide (24 mmol, 2.856 g) was added to the stirred solution of 1,3,4-Thiadiazole-2,5-dithiol dipotassium salt (24 mmol, 2.856 g) in DMF (40 mL), the mixture was stirred at 70 °C for (24 h.), the reaction mixture was poured in ice water (80 mL) and extracted with Et₂O (3 × 40 mL), the combined organic layers were washed with saturation

solution of NaCl (50 mL), dried over Na₂SO₄ and evaporated under reduced pressure to give 2,5-bis(prop-2-ynylthio)-1,3,4-thiadiazole. Recrystallized by n-Hexane the product was precipitated as white needle crystals in yield (1.085 g) %38.

(2.4.3) Preparation of 2,5-bis[1-alkyl-1H-1,2,3-triazol-4-yl)methylthio]-1,3,4-thiadiazole:



Scheme (2-4) Preparation of 2,5-bis[(1-alkyl-1H-1,2,3-triazol-4-yl)methylthio]-1,3,4-thiadiazole

Click chemistry reaction was used in the end step to prepare 2,5-bis[(1-alkyl-1H-1,2,3-triazol-4-yl)methylthio]-1,3,4-thiadiazole by cycloaddition reaction between (1.0 mmol.) of 2,5-bis(prop-2-ynylthio)-1,3,4-thiadiazole dissolved in (9 mL, mixture solution of distilled water with t-Butanol (2:1) in ratio) with (2.5 mmol.) of alkyl-azide by used Cu¹⁺ as a catalyst (this ion was formed instant in solution by reduce Cu²⁺ to Cu¹⁺ ion in reaction between (0.1 mmol, 0.0250 g) of copper sulfate with (0.2 mmol, 0.0396 g) of sodium-L-ascorbate), stirred at 60°C for (1 h.), white precipitate was formed, dissolved by (10 mL) DCM, dried over Na₂SO₄,

purification by column made of silica gel (mesh 60) dissolved in DCM and evaporated partitions of product under reduced pressure to give 2,5-bis[(1-alkyl-1H-1,2,3-triazol-4-yl)methylthio]-1,3,4-thiadiazole. **Table(2-4)** stated the quantities, reaction conditions to prepare ligands:

Table (2-4) Quantities and reaction conditions to prepare ligands

Ligand	1.0 mmol of alkyne	2.5 mmol of alky- azide	0.2 mmol (Sodium-L-ascorbate)	0.1 mmol (Copper sulfate)	V(mL) mixture (H ₂ O+t-Butanol) (2:1)	% yield
L ¹	0.226 g	0.4570 g	0.039 g	0.025 g	9 mL	83.21
L ²	0.226 g	0.388 g	0.039 g	0.025 g	9 mL	85.44
L ³	0.226 g	0.457 g	0.039 g	0.025 g	9 mL	83.78

(2.5) Preparation of complexes:

All metal complexes were prepared by the same method, (5 mL) solution of metal salt dissolved in MeOH added to (5 mL) solution of ligand dissolved in MeOH in the mole ratio (2:1) respectively, reflux for (2 h.) a precipitate was formed, separated by filtration, washed by (5 mL) of Et₂O and (5 mL) of cold MeOH. Finally, recrystallized the complex by

acetonitrile. **Table (2-5)** listed quantity of ligands, metal salts to prepare complexes and some physical properties of the prepared complexes.

Table (2-5) Quantity of ligands & metal salts to prepare complexes

Complex	Ligand	ligand (wt. & mmol.)	Metal salt	Wt. & mmol of metal salt	Color	M.p °C
[Co ₂ L ¹ mH ₂ OxCl]	L ¹	(0.03 g) (0.0589) mmol	CoCl ₂ .6H ₂ O	(0.0199 g) (0.1179) mmol	Deep blue	176
[Co ₂ L ² mH ₂ OxCl]	L ²	(0.03 g) (0.0558) mmol	CoCl ₂ .6H ₂ O	(0.0188g) (0.1117)mmol	Blue	192
[Co ₂ L ³ mH ₂ OxCl]	L ³	(0.03 g) (0.0505) mmol	CoCl ₂ .6H ₂ O	(0.0171 g) (0.10119) mmol	Pale-blue	221
[Ni ₂ L ¹ mH ₂ OxCl]	L ¹	(0.03 g) (0.0589) mmol	NiCl ₂ .6H ₂ O	(0.0199 g) (0.1179) mmol	Yellowish- green	228 Dec.
[Ni ₂ L ² mH ₂ OxCl]	L ²	(0.03 g) (0.0558) mmol	NiCl ₂ .6H ₂ O	(0.0188 g) (0.1117) mmol	Yellowish- green	235 Dec.
[Ni ₂ L ³ mH ₂ OxCl]	L ³	(0.03 g) (0.0505) mmol	NiCl ₂ .6H ₂ O	(0.0170 g) (0.10119) mmol	Yellowish- green	242 Dec.
[Cu ₂ L ¹ mH ₂ OxCl]	L ¹	(0.03 g) (0.0589) mmol	CuCl ₂ .2H ₂ O	(0.0188 g) (0.1179) mmol	Green	101
[Cu ₂ L ² mH ₂ OxCl]	L ²	(0.03 g) (0.0558) mmol	CuCl ₂ .2H ₂ O	(0.0178 g) (0.1117) mmol	Greenish- yellow	107

$[\text{Cu}_2\text{L}^3\text{mH}_2\text{OxCl}]$	L^3	(0.03 g) (0.0505) mmol	$\text{CuCl}_2 \cdot 2\text{H}_2\text{O}$	(0.0161 g) (0.10119) mmol	Yellowish-green	119
-------------------------------------------------	--------------	----------------------------------	-------------------------------------------	-------------------------------------	-----------------	-----

Complex	Ligand	Wt. of ligand & mmol	Metal salt	Wt. & mmol of metal salt	Color	M.p °C
$[\text{Pd}_2\text{L}^1\text{mH}_2\text{OxCl}]$	L^1	(0.03 g) (0.0589) mmol	PdCl_2	(0.0209 g) (0.1179) mmol	Deep brown	108
$[\text{Pd}_2\text{L}^2\text{mH}_2\text{OxCl}]$	L^2	(0.03 g) (0.0558) mmol	PdCl_2	(0.0198 g) (0.1117) mmol	Brown	111
$[\text{Pd}_2\text{L}^3\text{mH}_2\text{OxCl}]$	L^3	(0.03 g) (0.0505) mmol	PdCl_2	(0.0179 g) (0.10119) mmol	Pale brown	122
$[\text{Pt}_2\text{L}^1\text{mH}_2\text{OxCl}]$	L^1	(0.03 g) (0.0589) mmol	PtCl_4	(0.0397 g) (0.1179) mmol	Orangish-yellow	201 Dec.
$[\text{Pt}_2\text{L}^2\text{mH}_2\text{OxCl}]$	L^2	(0.03 g) (0.0558) mmol	PtCl_4	(0.0376 g) (0.1117) mmol	Orangish-yellow	218 Dec.
$[\text{Pt}_2\text{L}^3\text{mH}_2\text{OxCl}]$	L^3	(0.03 g) (0.0505) mmol	PtCl_4	(0.03408 g) (0.10119) mmol	Yellowish-orange	239 Dec.

Dec. = decomposed



Chapter Two

EXPERIMENTAL SECTION

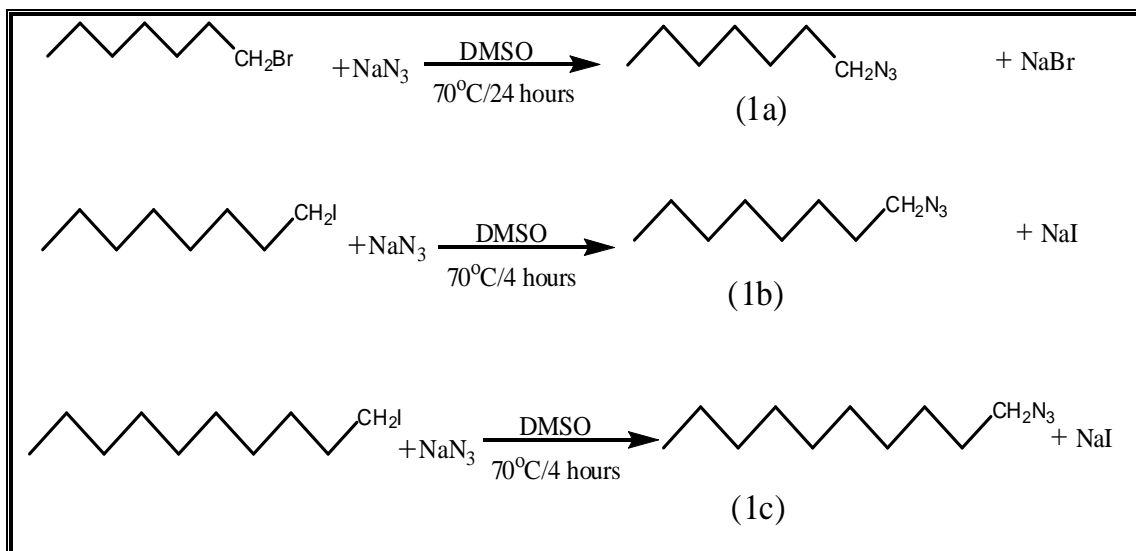
(3) Results and discussion

(3.1) Synthesis and characterization of ligands and precursors:

New polydentate ligands with (N & S) donor type atoms have been synthesised. In general the ligands contain three heterocyclic five membrane rings, one of [1,3,4-thiadiazole] central ring and two of [1,4-N substituted 1,2,3-triazole] rings.

(3.1.1) Synthesis and characterization of Alkyl-azid compounds (1a, 1b and 1c):

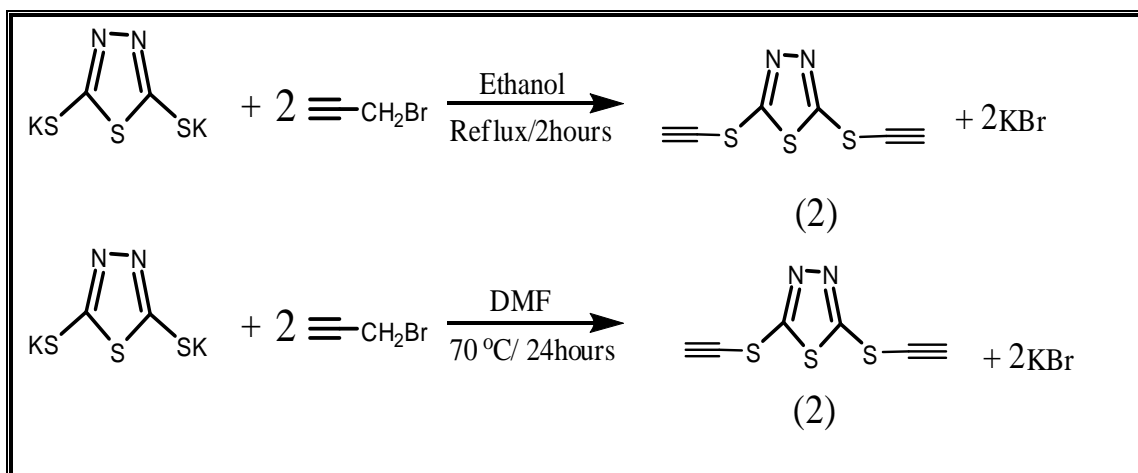
Compounds (1a, 1b and 1c) were prepared by a classical method, **scheme (3:1)**. The compounds were prepared from the reaction of halo-alkane with sodium azide. The reaction belongs to SN2 mechanism, the azide group will be substituted with halogen. Compounds (1a, 1b & 1c) were characterized by FT-IR spectra.



Scheme (3:1) the method to prepare compounds (1a, 1b & 1c)

(3.1.2) Synthesis and characterization of [2,5-bis(prop-2-ynylthio)-1,3,4-thiadiazole] compound (2):

Compound (2) was prepared by substitution reaction between [1,3,4-thiadiazole,2,5-dithiol potassium salt] with [propargylbromide] **Scheme (3:2)** Compound (2) was characterized by FT-IR spectra and C.H.N.S elemental analysis. Solubility of compound (2) is summarized in **Table (3-2)**

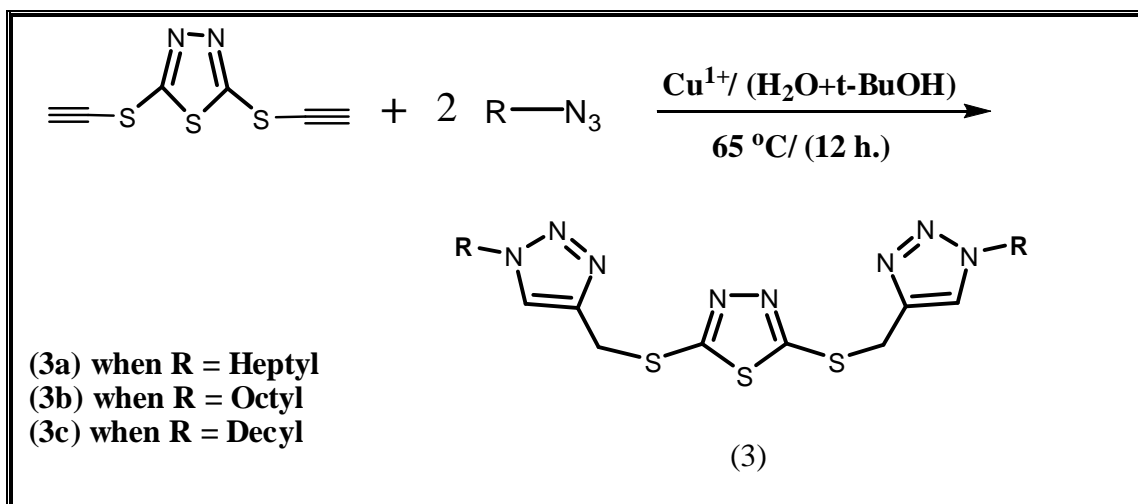


Scheme (3:2) prepare of compound (2)

(3-2) Synthesis and characterization of the ligands (L¹, L² & L³):

Compounds (3a), (3b) and (3c) were prepared by cycloaddition reaction between compound (2) with compounds (1a), (1b) and (1c) respectively. The cycloaddition reaction of alky-azide with [2,5-bis(prop-2-ynylthio)-1,3,4-thiadiazole] by use Cu(I) ion as a catalyst “Click Chemistry” resulted to prepare compounds (3a, 3b and 3c) the ligands [L¹], [L²] and [L³] respectively according to the general method shown in **Scheme (3:3)**. Compounds (3a), (3b) and (3c) were characterized by FT-IR, ¹HNMR, ¹³CNMR spectra and C.H.N.S elemental analysis.

Table (3-1) summarized melting point and C.H.N.S elemental analysis of compounds **(3a)**, **(3b)** & **(3c)** **Figs. (3-1)**, **(3-2)** and **(3-3)**. **Table (3-2)** summarised solubility of compounds **(3a)**, **(3b)** and **(3c)** in different solvents.



Scheme (3:3) General method to prepare **(3a)**, **(3b)** & **(3c)**

Table (3-1) Melting point and C.H.N.S elemental analysis of compounds **(3a)**, **(3b)** & **(3c)**

Compound	Empirical Formula	M.W	Yield %	m.p	Colour	Found, (calc.) %			
						C	H	N	S
L¹	C₂₂H₃₆N₈S₃	508.77	83.21	108.0°C	Off white	51.427	7.192	21.025	18.601
						(51.94)	(7.13)	(22.02)	(18.91)
L²	C₂₄H₄₀N₈S₃	536.82	85.44	109.5°C	Off white	53.326	7.366	20.474	17.808
						(53.70)	(7.51)	(20.87)	(17.92)
L³	C₂₈H₄₈N₈S₃	592.93	83.78	113.0°C	White	56.380	7.586	18.431	15.891
						(56.72)	(8.16)	(18.90)	(16.22)

() calculated.

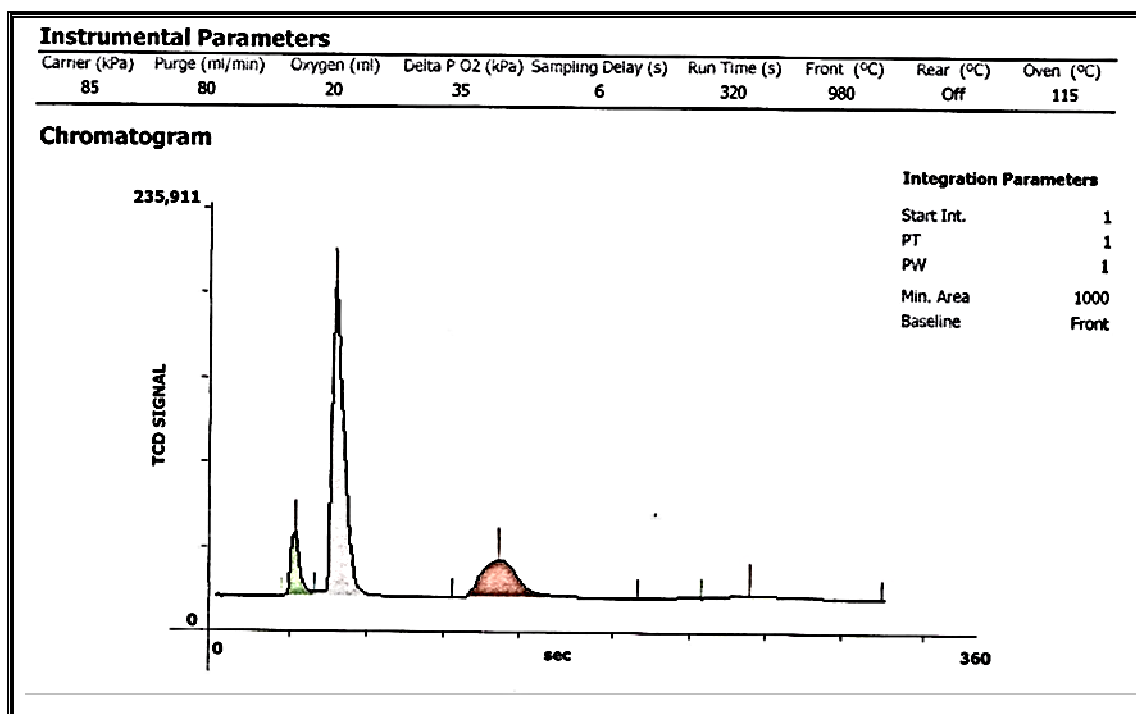
Table (3-2): Solubility of Compound (2), [L¹], [L²] & [L³]

Solvent	Compound (2)	[L ¹]	[L ²]	[L ³]
H ₂ O	÷	-	-	-
n-Hexane	÷	-	-	-
Ethyl acetate	+	-	-	-
Diethyl ether	+	÷	÷	÷
DCM	+	+	+	+
t-Butanol	+	-	-	-
Methanol	+	+	+	+
Acetonitrile	+	+	+	+
DMSO	+	+	+	+
DMF	+	+	+	+
Acetone	+	+	+	+

(+) Soluble

(-) Insoluble

(÷) Sparingly

Fig.(3-1) C.H.N.S graph of ligand [L¹]

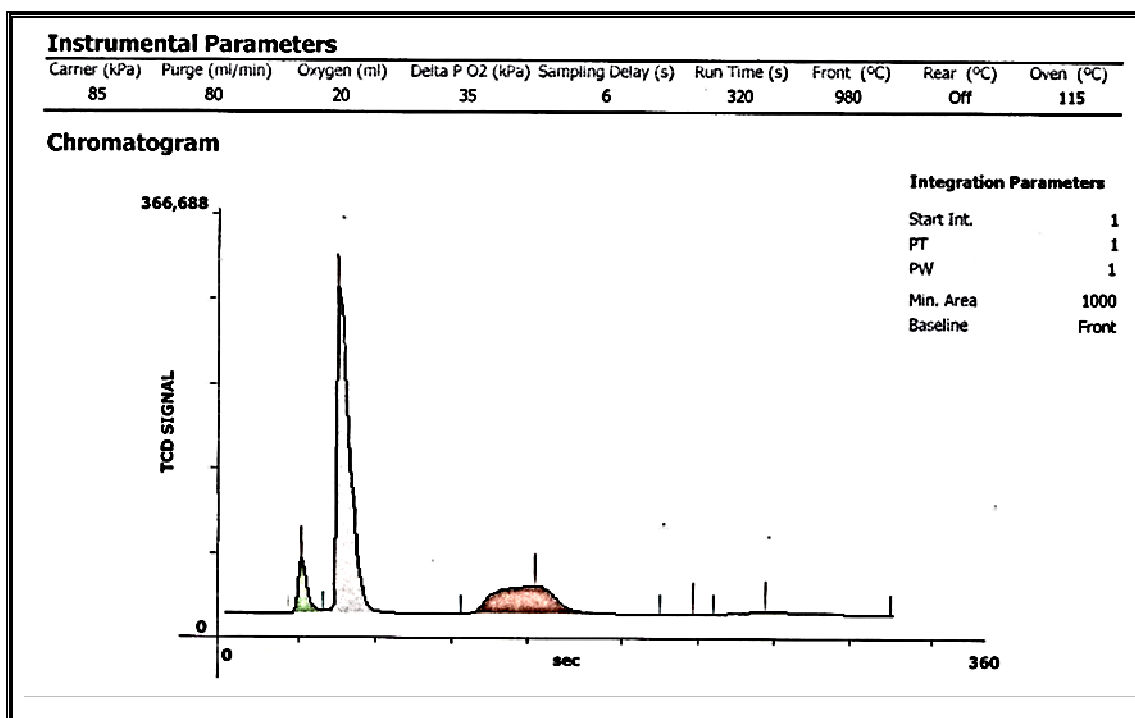


Fig.(3-2) C.H.N.S graph of ligand [L²]

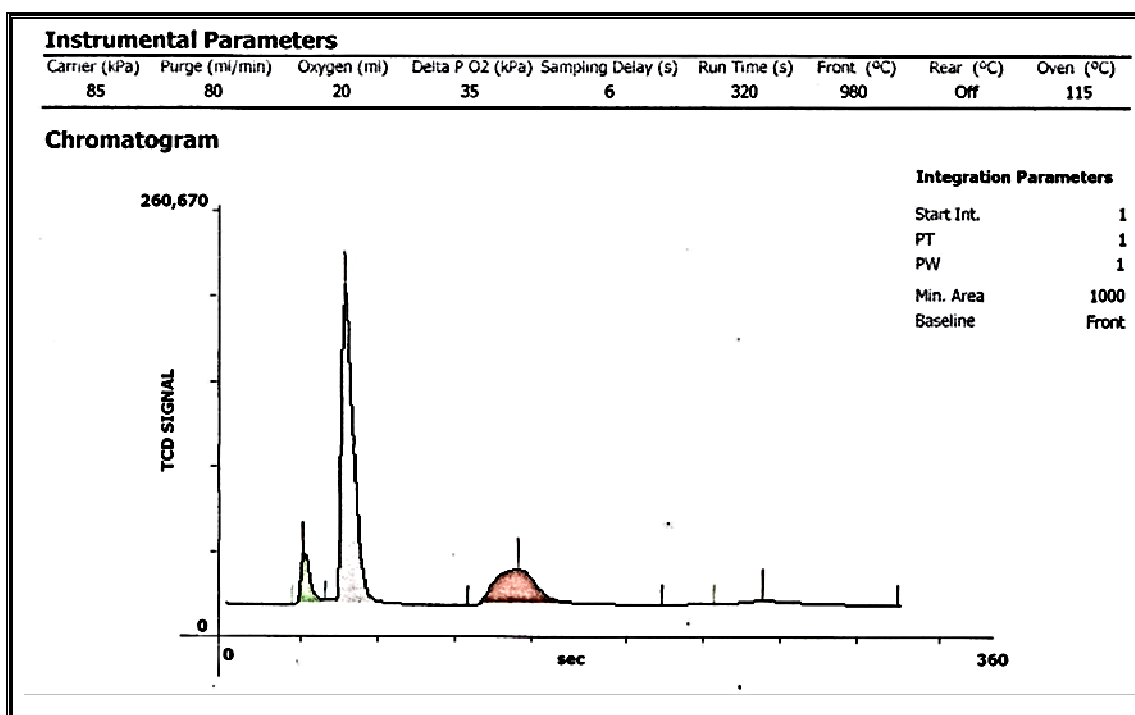


Fig.(3-3) C.H.N.S graph of ligand [L³]

(3.3) FT-IR Spectral data for the ligands and precursors:

(3.3.1) FT-IR spectral data for alky-azides:

The FT-IR spectra of 1-Azidoheptane, 1-Azidooctane and 1-Azidodecanen **Figs.(3-4), (3-5), (3-6)** respectively display the same characteristic bands, since the bands in the region ($2965, 2850 \text{ cm}^{-1}$) attributed to the $\nu(\text{C-H})$ and $\nu(\text{C-H})$ stretching of methyl and methylene groups in the aliphatic chain respectively. While the characteristic band at ($2096-2094 \text{ cm}^{-1}$) assigned to $\nu(\text{N}_3)$ stretching referred a good evidence to the alkylazides were obtained. The $\delta(\text{C-H})$ bending bands appeared at the region between ($1458-1377 \text{ cm}^{-1}$). The bands at the region ($1259, 1120 \text{ cm}^{-1}$) attributed to $\nu(\text{C-N})$ and $\nu(\text{C-C})$ stretching respectively^(55, 56).

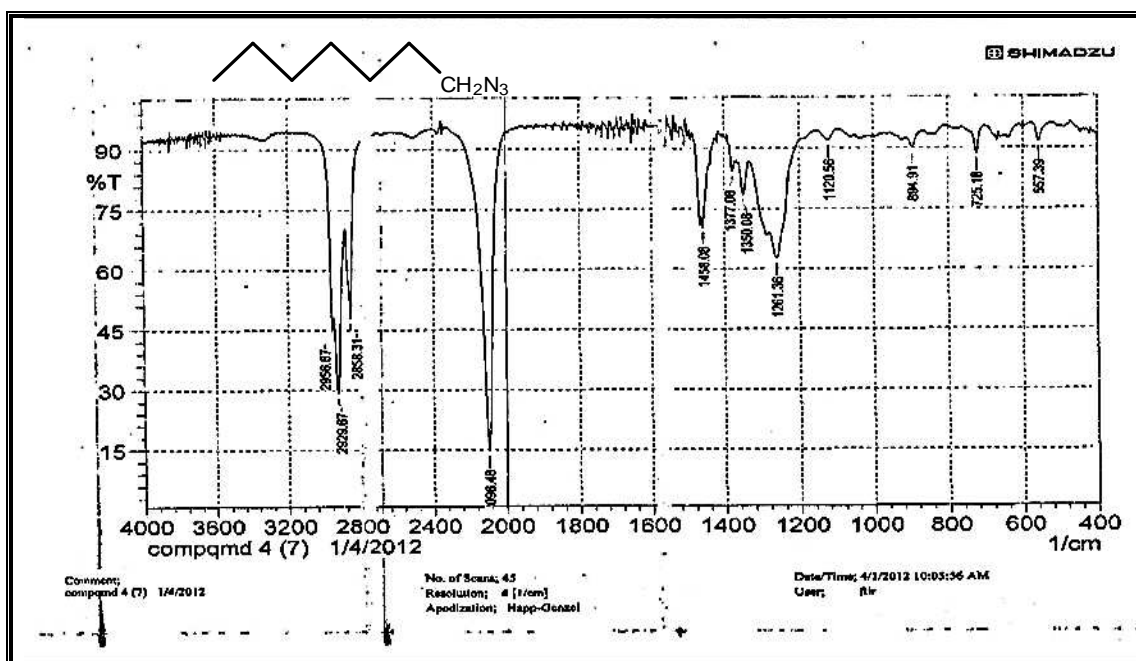


Fig. (3- 4) FT-IR spectrum of 1-Azido heptane

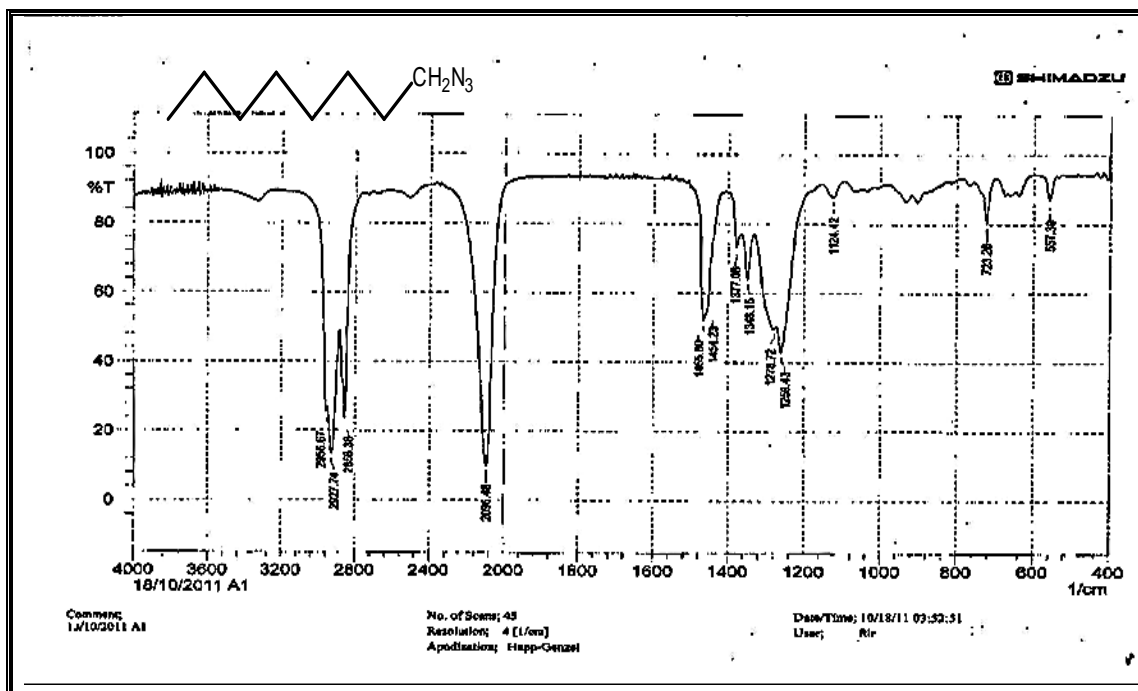


Fig. (3- 5) FT-IR spectrum of 1-Azido octane

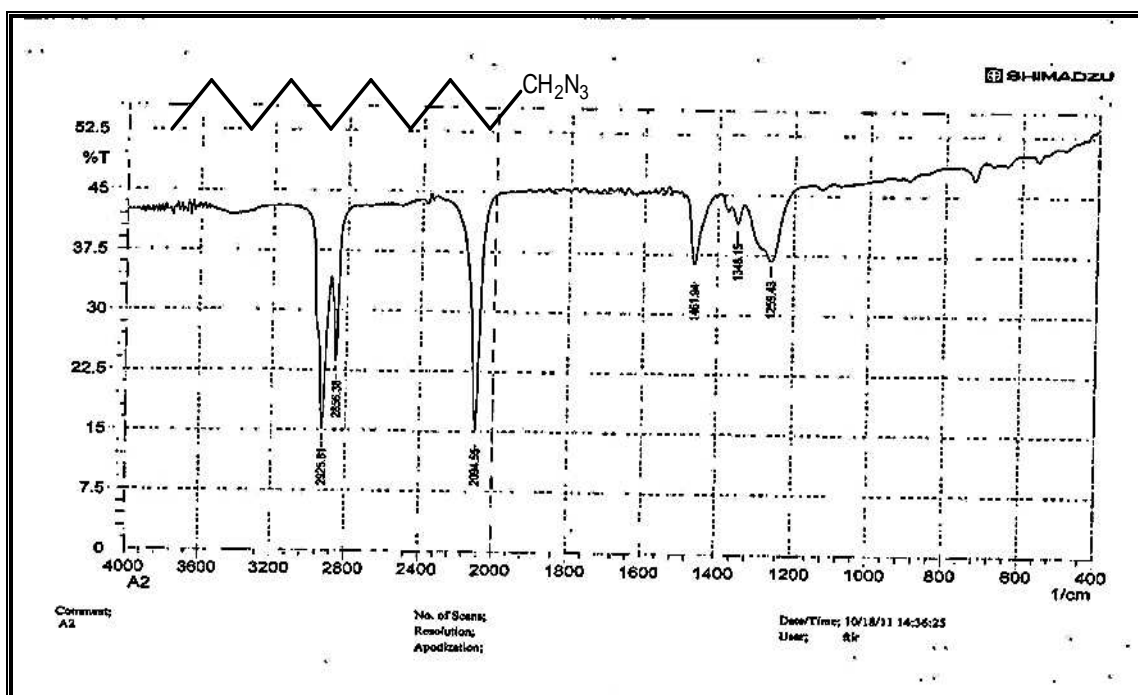


Fig. (3-6) FT-IR spectrum of 1-Azido decane

(3.3.2) FT-IR spectral data for 2,5-bis(prop-2-ynylthio)-1,3,4-thiadiazole:

The FT-IR spectrum of 2,5-bis(prop-2-ynylthio)-1,3,4-thiadiazole **Fig.(3-7)** exhibits band at (3210 cm^{-1}) assigned to stretching of $\nu(\text{C-H})$ band in terminal alkyne group. While the band at (2950 cm^{-1}) assigned to $\nu(\text{C-H})$ stretching of methylene group. The band at (2111 cm^{-1}) characterized with symmetry reduces intensity of $\nu(\text{C}\equiv\text{C})$. While the bands at (1396 cm^{-1}), (1375 cm^{-1}) due to $\delta(\text{C-H})$ bending of aliphatic chain, the bands at (1058 cm^{-1}), (952 cm^{-1}) and (865 cm^{-1}) assigned to $\nu(\text{N-N})$ stretching, $\delta(\text{C-H})$ bending in plane and out of plan of alkyne respectively, and the band at (698 cm^{-1}) assigned to $\nu(\text{C-S})$ of thiadiazole ring^(55,56).

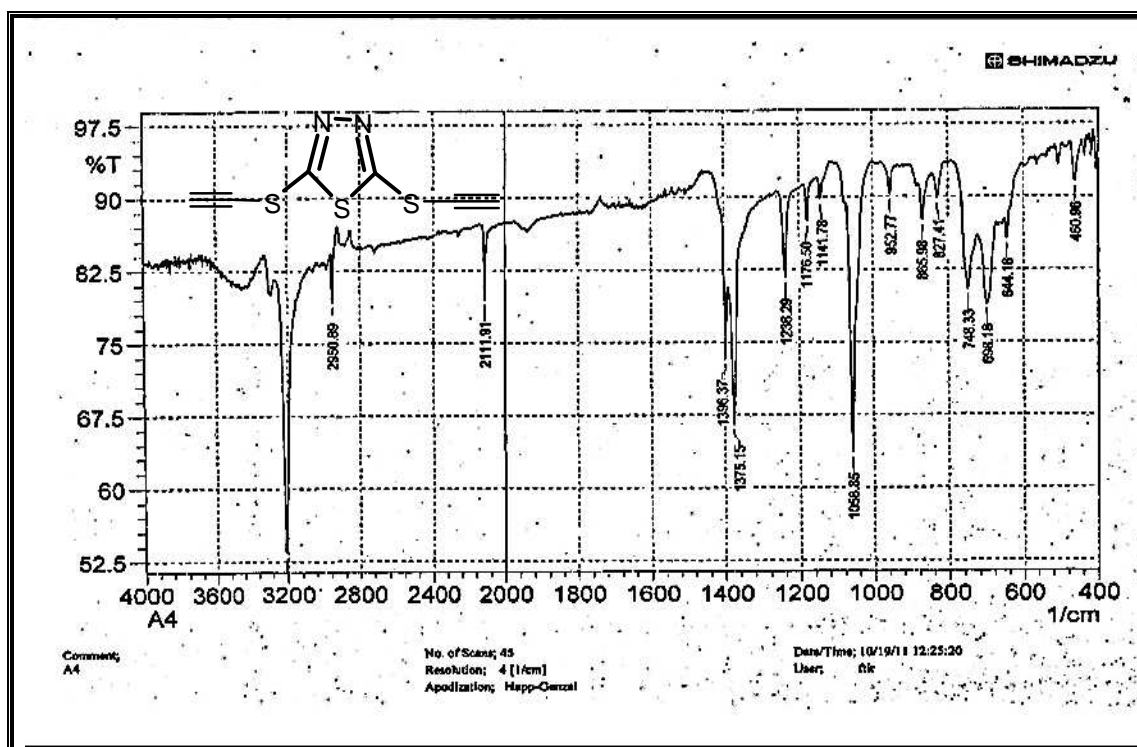


Fig. (3-7) FT-IR spectrum of 2,5-bis(prop-2-ynylthio)-1,3,4-thiadiazole

(3.3.3) FT-IR spectral data for 2,5-bis[1-alkyl-1H-1,2,3-triazol-4-yl) methylthio]-1,3,4-thiadiazole:

(3.3.3.1) FT-IR spectral data for 2,5-bis[1-heptyl-1H-1,2,3-triazol-4-yl) methylthio]-1,3,4-thiadiazole:

The FT-IR spectrum of 2,5-bis[1-heptyl-1H-1,2,3-triazol-4-yl) methylthio]-1,3,4-thiadiazole [**L**¹] ligand **Fig.(3-8)** shows bands at (3128 cm⁻¹) and (3116 cm⁻¹) assigned to $\nu(\text{C-H})$ stretching of aromatic ring. While the bands at (2954 cm⁻¹), (2924 cm⁻¹) and (2850 cm⁻¹) due to $\nu(\text{C-H})$ sym. and asy. stretching of methyl and methylene groups respectively. The band at (1467 cm⁻¹) assigned to $\nu(\text{C=C})$ stretching of triazole ring, the band at (1548 cm⁻¹) assigned to $\nu(\text{C=N})$ stretching of thiadiazole ring. While the bands at (1381 cm⁻¹), (1242 cm⁻¹) and (1058 cm⁻¹) attributed to $\nu(\text{N=N})$, $\nu(\text{C-N})$, $\nu(\text{N-N})$ stretching of triazole ring respectively. The absence of bands at (2096, 2111 cm⁻¹) which are assigned to $\nu(\text{N}_3)$ and $\nu(\text{C}\equiv\text{C})$ stretching in the precursors, and appeared the new bands of triazoles ring consider a good evidence to the reaction that occurs and the compound 1,2,3-triazole ring was obtained. While the bands at (879 cm⁻¹), (831cm⁻¹) assigned to bending of $\delta(\text{C-H})$ in plane and out of plane in aromatic ring. The bands at (771cm⁻¹), (723cm⁻¹) attributed to $\nu(\text{C-S-C})$ asym. & sym. stretching of thiadiazole ring, and the band at (640cm⁻¹) assigned to $\nu(\text{C-S})$ stretching of dithaiol group^(55, 56).

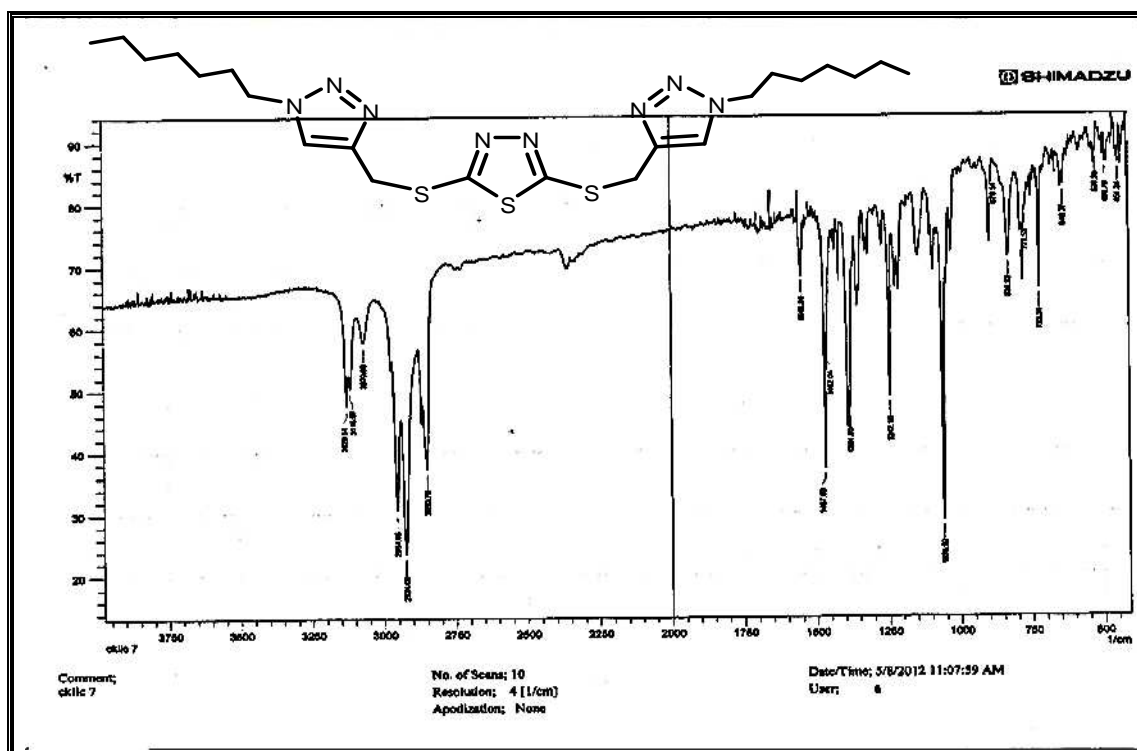


Fig. (3-8) FT-IR spectrum of [L¹] ligand

(3.3.3.2) FT-IR spectral data for 2,5-bis[1-octyl-1H-1,2,3-triazol-4-yl]methylthio]-1,3,4-thiadiazole:

The FT-IR spectrum of 2,5-bis[1-octyl-1H-1,2,3-triazol-4-yl]methylthio]-1,3,4-thiadiazole [L²] ligand **Fig.(3-9)** shows bands at (3128 cm⁻¹), (3116 cm⁻¹) assigned to $\nu(\text{C-H})$ stretching of aromatic ring of triazole group. While the bands at (2958 cm⁻¹), (2922 cm⁻¹) and (2850 cm⁻¹) assigned to $\nu(\text{C-H})$ sym. and asym. stretching of methyl and methylene groups. The bands at (1465 cm⁻¹) and (1548cm⁻¹) assigned to $\nu(\text{C=C})$, $\nu(\text{C=N})$ stretching of thiadiazole ring respectively. The bands at (1386 cm⁻¹), (1238 cm⁻¹) and (1058 cm⁻¹) due to $\nu(\text{N=N})$, $\nu(\text{C-N})$, $\nu(\text{N-N})$ stretching of triazole ring respectively, the absence of bands at (2096, 2111 cm⁻¹) which is assigned to $\nu(\text{N}_3)$ and $\nu(\text{C}\equiv\text{C})$ stretching in the precursors, and shows the new bands of triazole rings considered a good evidence to the reaction occurs and the compound 1,2,3-triazole ring was

obtained. While the bands at (894 cm^{-1}) and (829 cm^{-1}) assigned to $\delta(\text{C-H})$ bending in plane and out of plane of aromatic ring. While the bands at (781 cm^{-1}) and (723 cm^{-1}) due to $\nu(\text{C-S-C})$ asym. & sym. stretching of thiadiazole ring. The band appeared at (646 cm^{-1}) assigned to $\nu(\text{C-S})$ stretching of dithaiol substituted on thiadiazole ring^(55, 56).

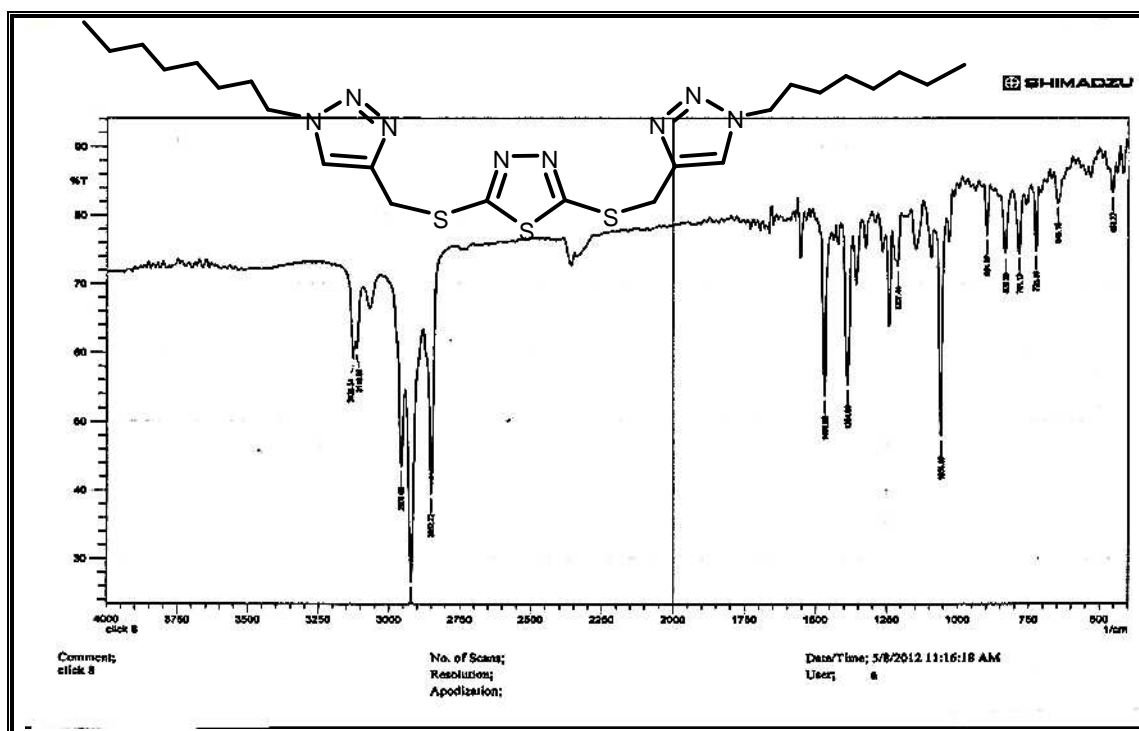


Fig.(3- 9) FT-IR spectrum of $[L^2]$ ligand

(3.3.3.3) FT-IR spectral data for 2,5-bis[1-decyl-1H-1,2,3-triazol-4-yl]methylthio]-1,3,4-thiadiazole:

The FT-IR spectrum of 2,5-bis[1-decyl-1H-1,2,3-triazol-4-yl]methylthio]-1,3,4-thiadiazole $[L^3]$ ligand **Fig.(3-10)** shows bands at (3128 cm^{-1}), (3115 cm^{-1}) assigned to $\nu(\text{C-H})$ asym. and sym. stretching of aromatic ring. The bands appeared at (2958 cm^{-1}), (2901 cm^{-1}) and (2854 cm^{-1}) attributed to $\nu(\text{C-H})$ asym. and sym. stretching of methyl and methylene groups. While the band which appeared at (1467 cm^{-1}) attributed to $\nu(\text{C=C})$ stretching of triazole ring. The band at (1548 cm^{-1})

assigned to $\nu(\text{C}=\text{N})$ stretching of thiadiazole ring. While the bands appeared at (1386 cm^{-1}), (1246 cm^{-1}) and (1056 cm^{-1}) assigned to $\nu(\text{N}=\text{N})$, $\nu(\text{C}-\text{N})$, $\nu(\text{N}-\text{N})$ stretching of triazole ring respectively. The absence of bands at ($2096, 2111 \text{ cm}^{-1}$) which is assigned to $\nu(\text{N}_3)$ and $\nu(\text{C}\equiv\text{C})$ stretching in the precursors, and appearance the new bands of triazoles ring consider good evidence to the reaction was occur and the compound 1,2,3-triazole ring was obtained. While the bands at (890 cm^{-1}), (829 cm^{-1}) assigned to $\delta(\text{C}-\text{H})$ bending in plane and out of plane of aromatic ring. The bands at (781 cm^{-1}) and (721 cm^{-1}) attributed to $\nu(\text{C}-\text{S}-\text{C})$ asym. and sym. stretching of thiadiazole ring, and the band at (648 cm^{-1}) assigned to $\nu(\text{C}-\text{S})$ stretching of dithaiol group substituted on thaiadiazole ring.

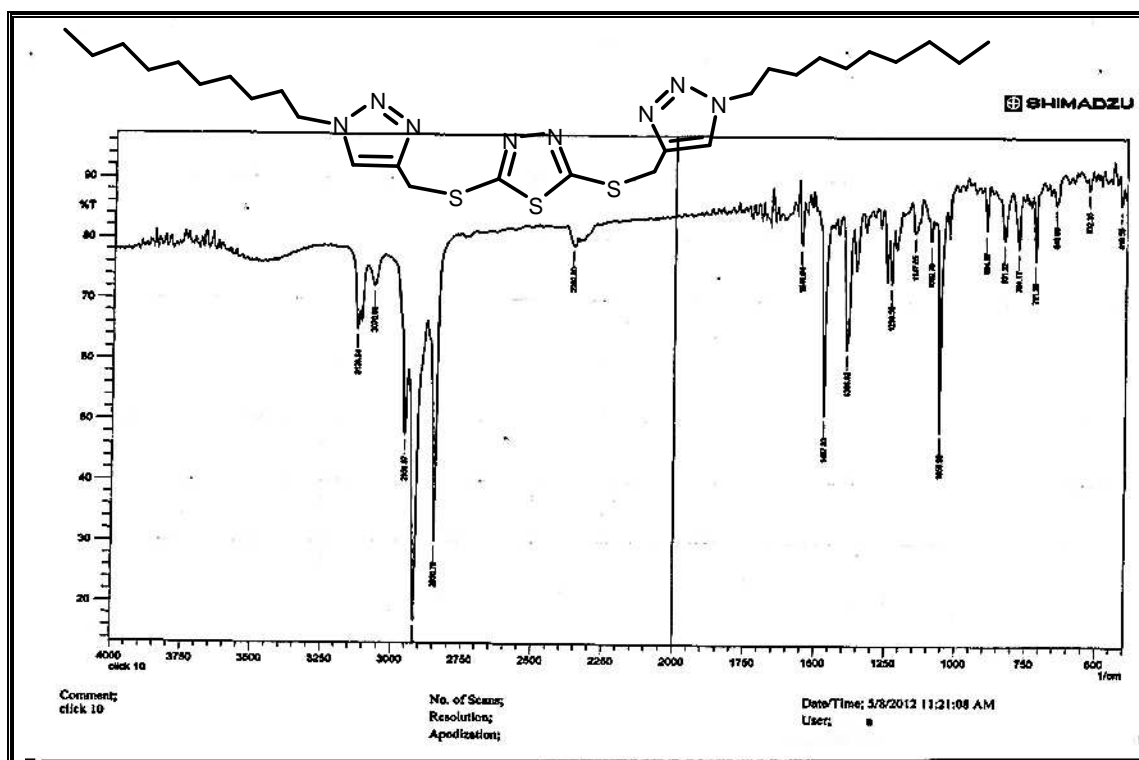


Fig.(3-10) FT-IR spectrum of $[\text{L}^3]$ ligand

The FT-IR spectral data of 2,5-bis[1-alkyl-1H-1,2,3-triazol-4-yl)methylthio]-1,3,4-thiadiazole were summarized in **Table(3-3)**

Table (3-3) FT-IR spectrum of 2,5-bis[1-alkyl-1H-1,2,3-triazol-4-yl) methylthio]-1,3,4-thiadiazole

Compound	$\nu(\text{C-H})$ aromatic	$\nu(\text{C-H})$ aliphatic	$\nu(\text{C=N})$	$\nu(\text{C=C})$	$\nu(\text{N=N})$	$\nu(\text{C-N})$	$\nu(\text{N-N})$	$\delta(\text{C-H})$	$\nu(\text{C-S-C})$	$\nu(\text{C-S})$
L¹	3116w	2954s 2924s	1548 m	1467 m	1381 m	1242 m	1058s	879m 831m	771w 723m	640w
L²	3116w	2958s 2922s	1548 m	1465 m	1386 m	1238 m	1058s	892m 829m	781w 723m	646w
L³	3115w	2958s 2901s	1548 m	1467 m	1386 m	1246 m	1056s	890m 829m	781w 721m	648w

s = strong, m = medium, w = weak

(3.4) (UV-Vis) Spectra of the ligands:

(3.4.1) (UV-Vis) Spectrum of [L¹] ligand:

The (UV-Vis) spectrum of [L¹] **Fig.(3-11)** exhibits a broad absorption peak between (239 - 295 nm) (41841- 38610 cm⁻¹) ($\mathcal{E}_{\max} = 3660$) assigned to ($\pi \rightarrow \pi^*$) and ($n \rightarrow \pi^*$) transitions⁽⁵⁷⁾.

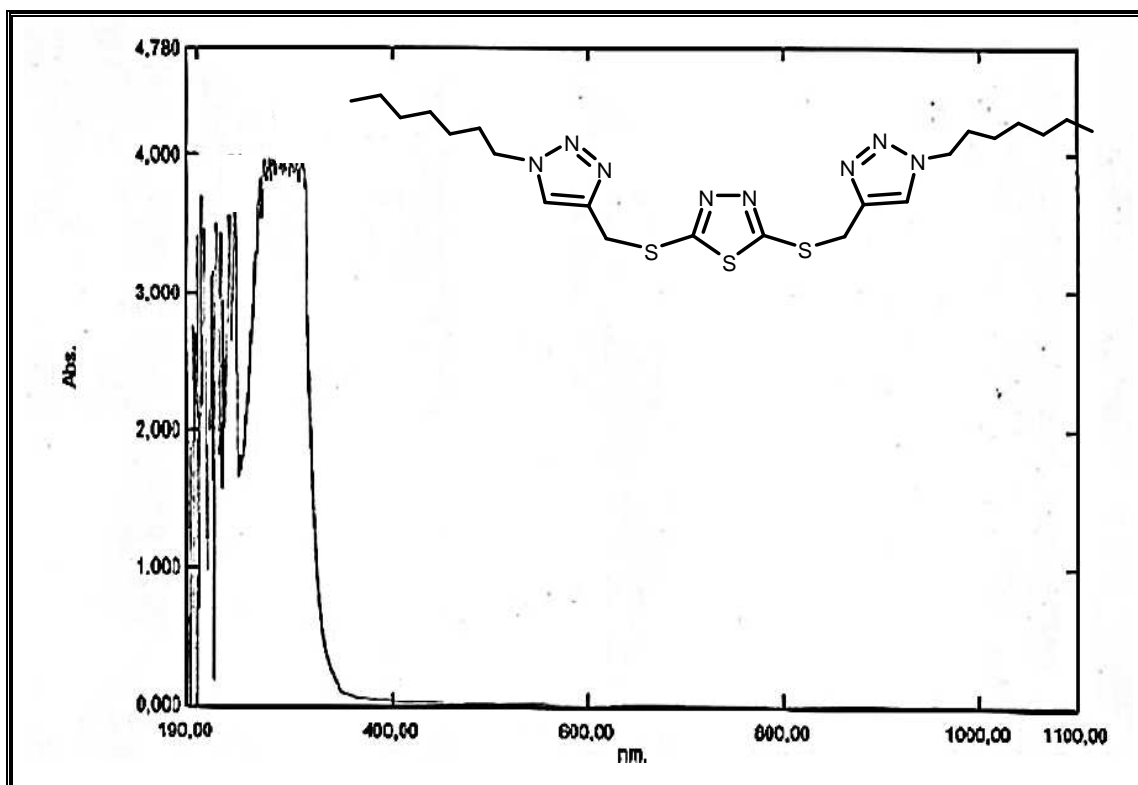


Fig.(3-11) UV-Vis spectrum of [L¹] ligand

(3.4.2) (UV-Vis) Spectrum of [L²] ligand:

The (UV-Vis) spectrum of [L²] **Fig.(3-12)** exhibits a broad absorption peak between (231- 293 nm) (43290 - 34129 cm⁻¹) ($\mathcal{E}_{\max} = 3976$) assigned to ($\pi \rightarrow \pi^*$) and ($n \rightarrow \pi^*$) transitions⁽⁵⁷⁾.

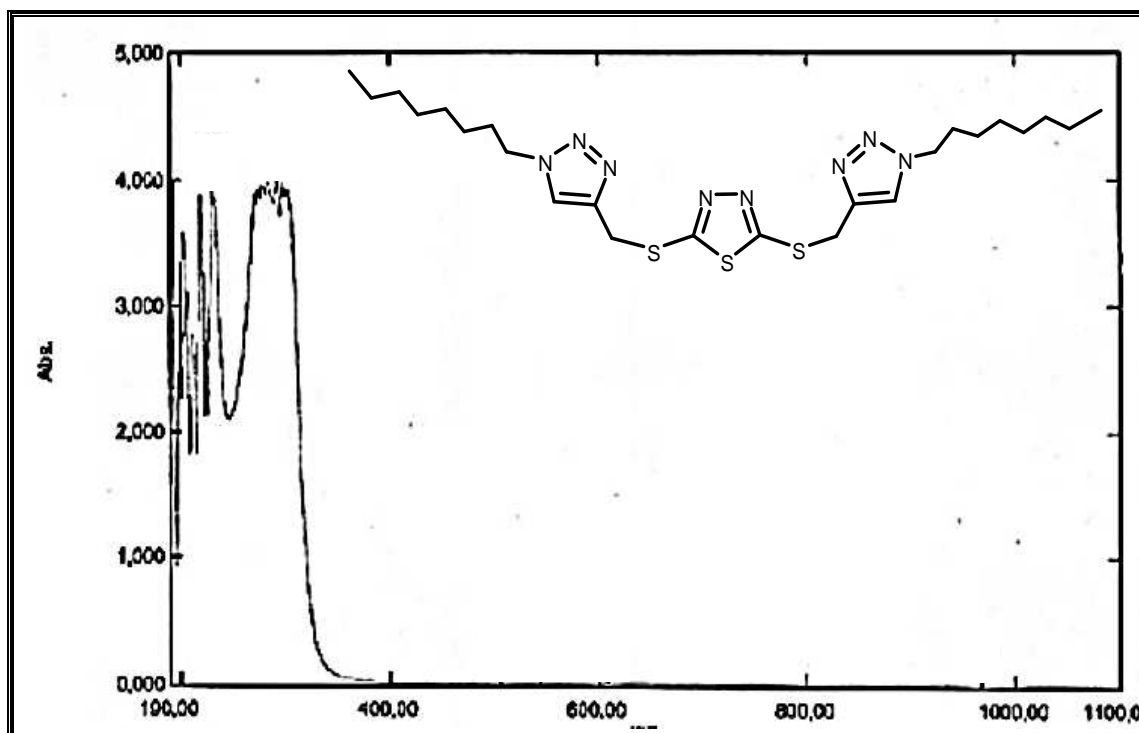


Fig.(3-12) UV-Vis spectrum of [L²] ligand

(3.4.3) (UV-Vis) Spectrum of [L³] ligand:

The (UV-Vis) spectrum of [L³] Fig.(3-13) exhibits a broad absorption peak between (251- 296 nm) ($39840 - 33783 \text{ cm}^{-1}$) ($\epsilon_{\text{max}} = 3974$) assigned to ($\pi \rightarrow \pi^*$) and ($n \rightarrow \pi^*$) transitions⁽⁵⁷⁾.

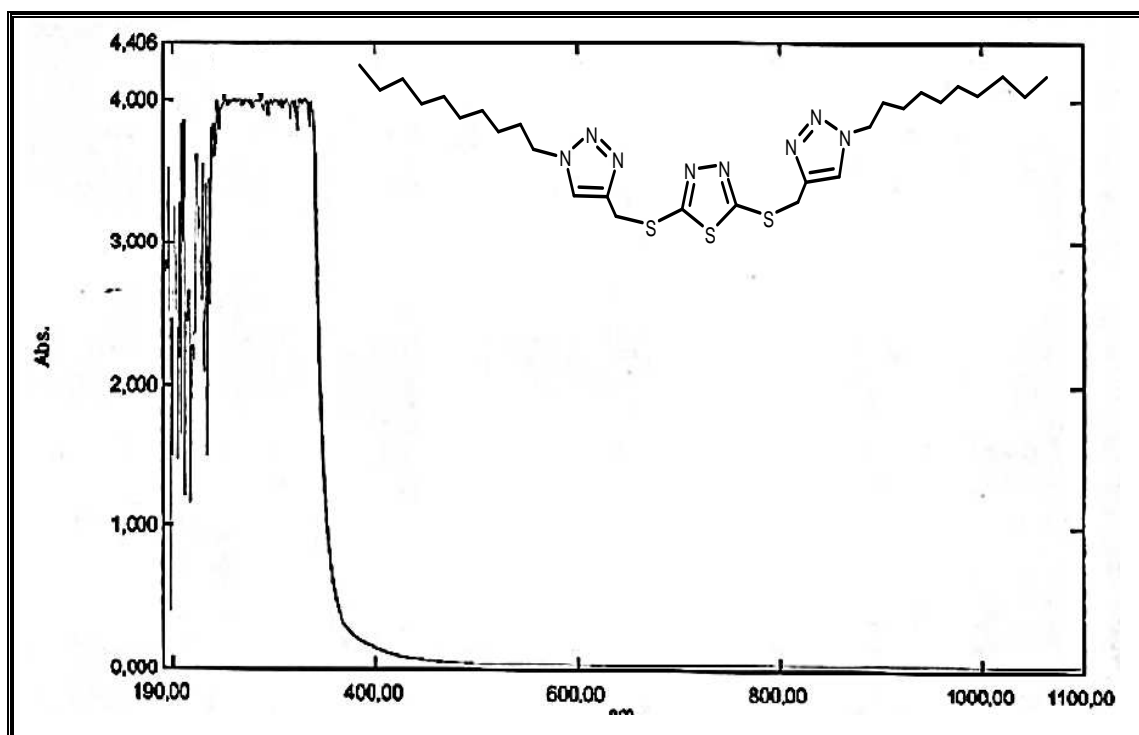
Fig.(3-13) UV-Vis spectrum of [L³] ligand

Table (3-4) Electronic spectral data for the ligands

No.	Compound	λ nm	ν wave number cm^{-1}	ϵ_{max} $\text{molar}^{-1}\text{cm}^{-1}$	assignment
1.	[L ¹]	239	41841	3660	$\pi \rightarrow \pi^*$
		295	38610		$n \rightarrow \pi^*$
2.	[L ²]	231	43290	3976	$\pi \rightarrow \pi^*$
		293	34129		$n \rightarrow \pi^*$
3.	[L ³]	251	39840	3974	$\pi \rightarrow \pi^*$
		296	33783		$n \rightarrow \pi^*$

(3.5) Nuclear magnetic resonance (NMR) spectra:**(3.5.1) ^1H , ^{13}C NMR spectra for the ligand $[\text{L}^1]$:****(3.5.1.1) ^1H NMR spectrum for the ligand $[\text{L}^1]$:**

The ^1H NMR spectrum of $[\text{L}^1]$ Fig.(3-14) in DMSO-d_6 display the signal at ($\delta = 0.98$ ppm, 6H) due to $\text{C}_{7''}$ of methyl groups, the chemical shifts at ($\delta = 1.10, 1.21, 1.39$ ppm, 10H) assigned to $\text{C}_{6''}$, $\text{C}_{r'',4'',5''}$, and $\text{C}_{2''}$ respectively. The signal at ($\delta = 3.45$ ppm, 4H) attributed to the protons attached to carbon $\text{C}_{1''}$ atoms, the chemical shift was affecting by the neighboring group of triazole ring.

The protons of methylene groups which lie between the sulphur atom and triazole ring were appeared at ($\delta = 4.25$ ppm, 4H), the signal at ($\delta = 7.55, 7.60$ ppm, 2H) attributed to the protons on $\text{C}_{4'}$ carbon atoms.

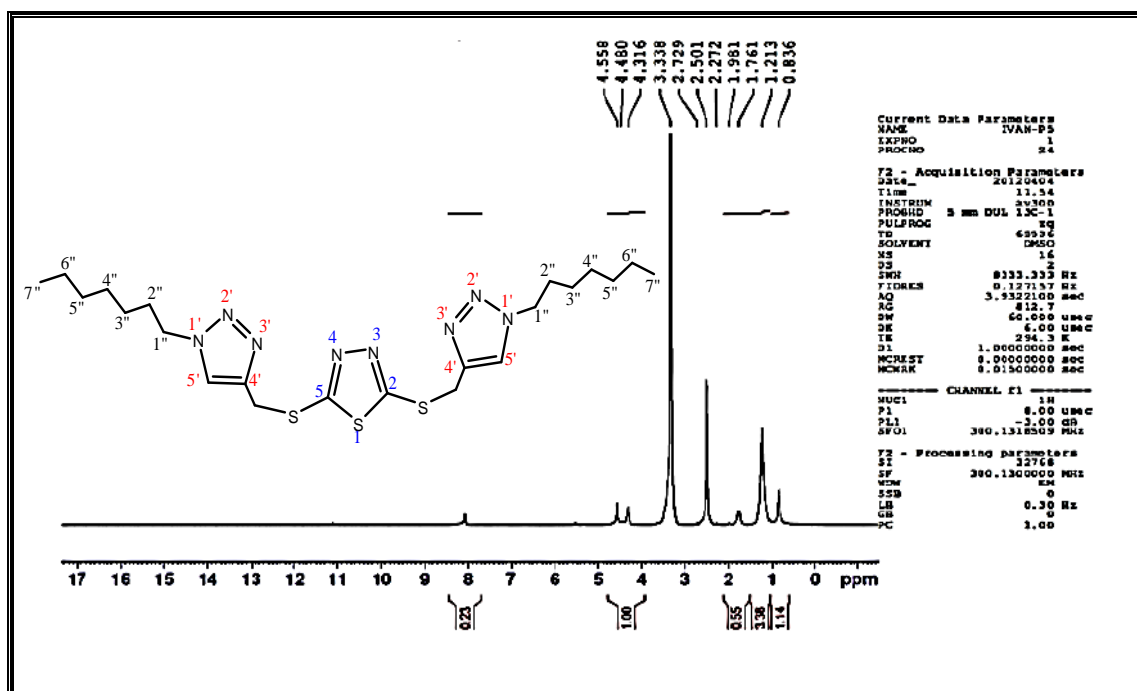


Fig.(3-14) ^1H NMR spectrum of ligand $[\text{L}^1]$

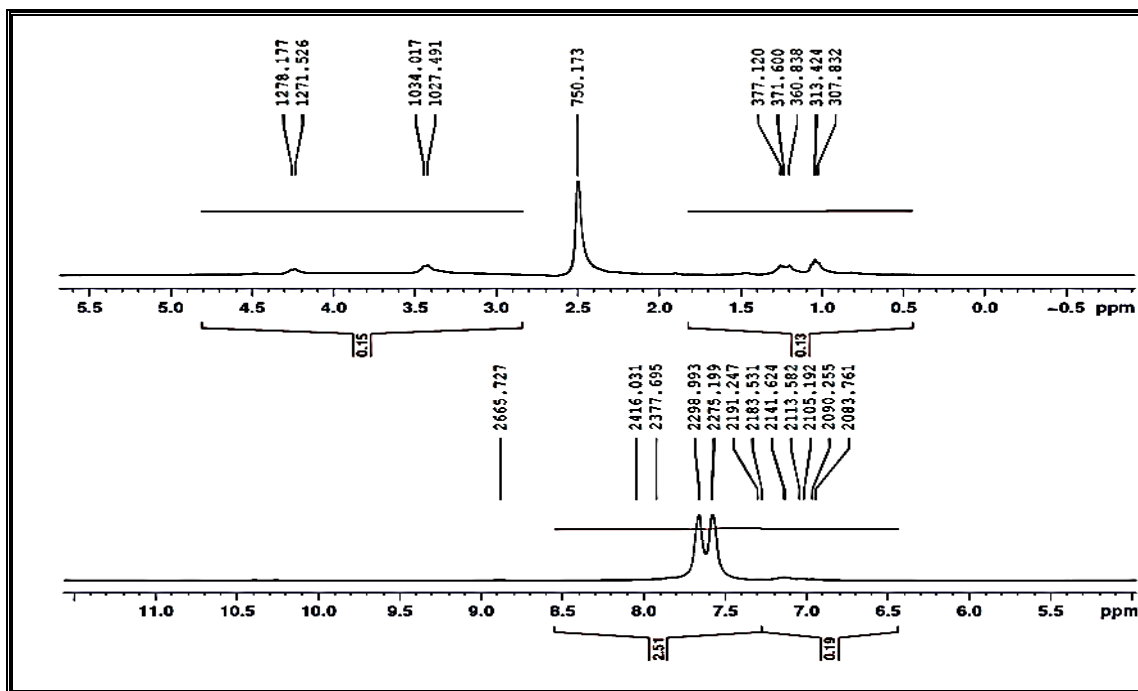


Fig.(3-14) ^1H NMR spectrum of ligand $[\text{L}^1]$

(3.5.1.2) ^{13}C NMR spectrum for the ligand $[\text{L}^1]$:

The ^{13}C NMR spectrum of $[\text{L}^1]$ Fig.(3-15) in DMSO-d_6 shows the signal at ($\delta = 17\text{ppm}$) assigned to C_7'' for terminal methyl group of aliphatic chains, the signals at ($\delta = 22, 23, 24, 33, 35, 37\text{ ppm}$) due to the carbon atoms C_6'' , C_5'' , C_4'' , C_3'' , C_2'' and C-S respectively, while the C_1'' appeared signal at ($\delta = 50\text{ppm}$), the carbon atoms C_4' and C_5' of triazole rings shows the signals at ($\delta = 125, 134\text{ ppm}$), the signal at ($\delta = 153\text{ ppm}$) assigned to carbon atoms C_2 & C_3 of thiadiazole ring.

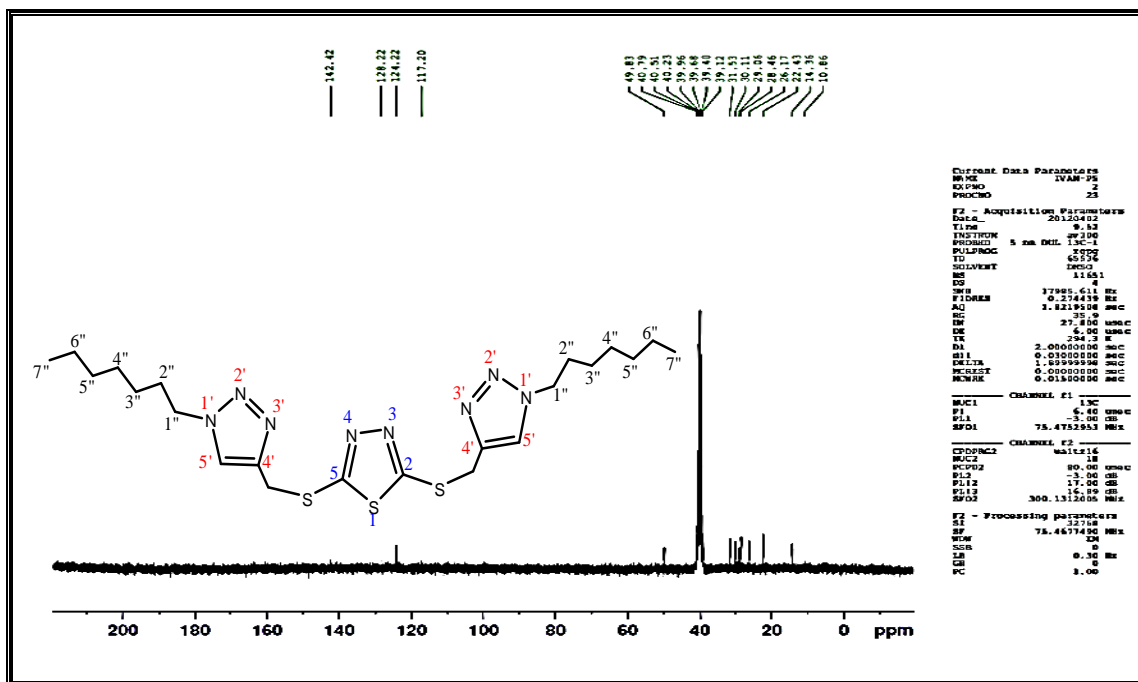


Fig.(3-15) ¹³C NMR of ligand [L¹]

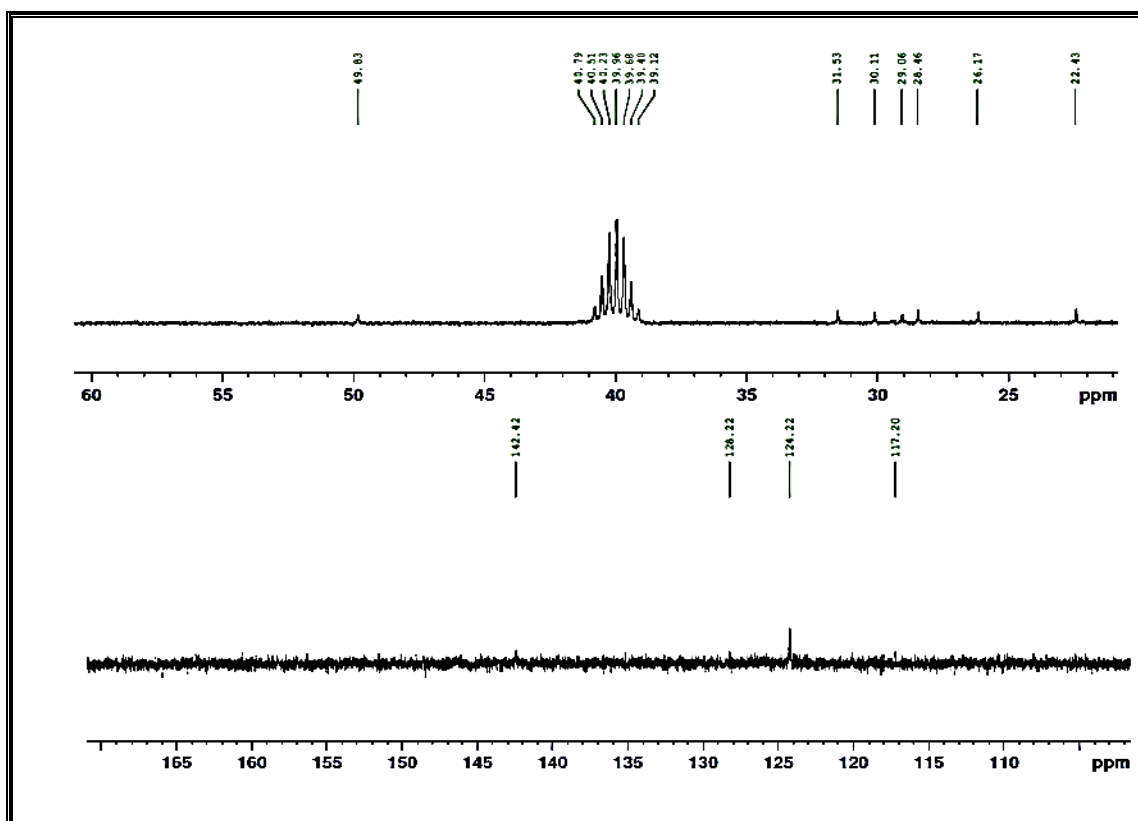
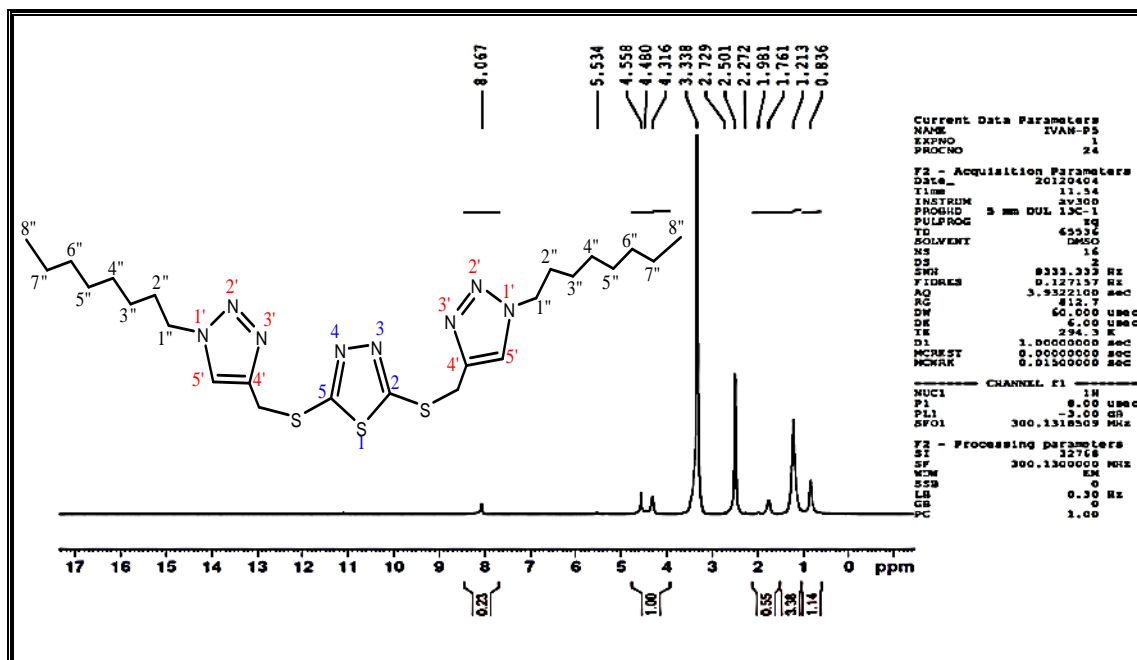


Fig.(3-15) ¹³C NMR of ligand [L¹]

(3.5.2) ^1H , ^{13}C NMR spectra for the ligand $[\text{L}^2]$:**(3.5.2.1) ^1H NMR spectrum for the ligand $[\text{L}^2]$:**

^1H -NMR in DMSO-d_6 of the ligand $[\text{L}^2]$ **Fig.(3-16)** appeared signal at ($\delta=0.836\text{ppm}$, 6H) due to the protons attached to carbon C_8'' , the chemical shift at ($\delta = 1.15, 1.21, 1.23\text{ ppm}$, 20H) assigned to the protons attached to carbon $\text{C}_3'', \text{C}_4'', 5'', 6'',$ and C_7'' of methylene groups of the aliphatic chains respectively. The signal at ($\delta=1.761\text{ppm}$, 4H) assigned to protons of C_2'' methylene group of aliphatic chains, the chemical shift was affecting by the neighboring group of triazole ring. The signal at ($\delta=4.316\text{ ppm}$, 4H) assign to the protons of C_1'' of the aliphatic chains.

The protons of methylene groups which lie between the sulphur atom and triazole ring were appeared at ($\delta = 4.55\text{ ppm}$, 4H), the signal at ($\delta = 8.06, 7.90\text{ ppm}$, 2H) attributed to the protons of C_4' in triazole rings.

**Fig.(3-16) ^1H NMR of ligand $[\text{L}^2]$**

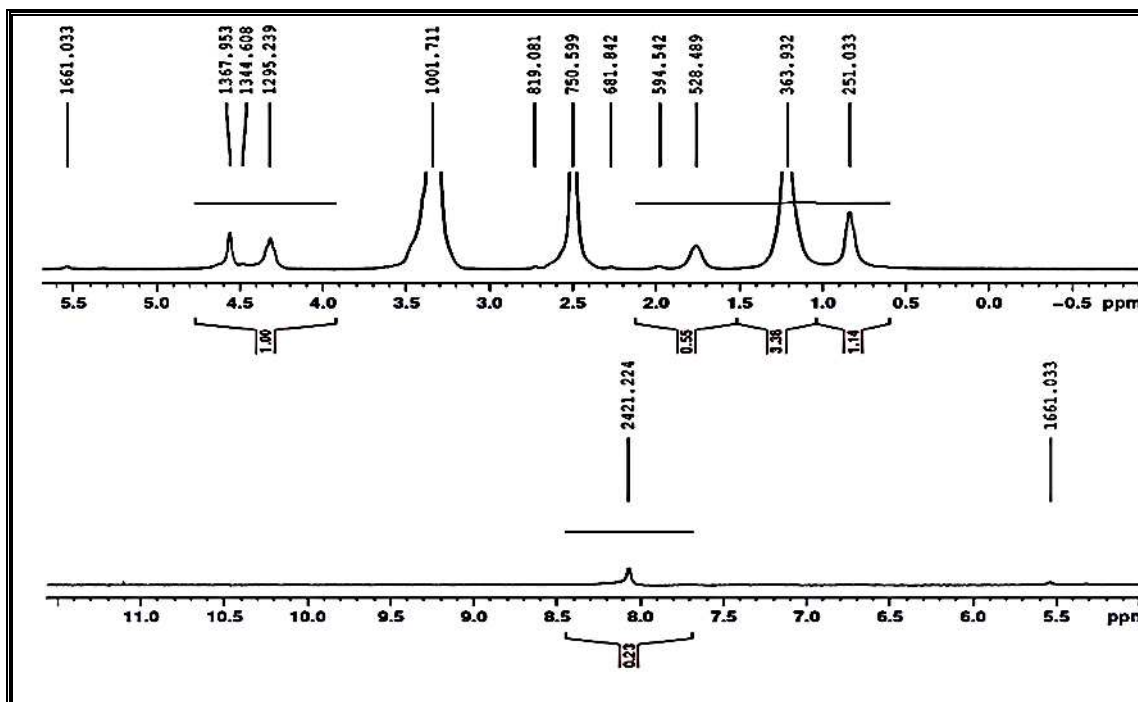
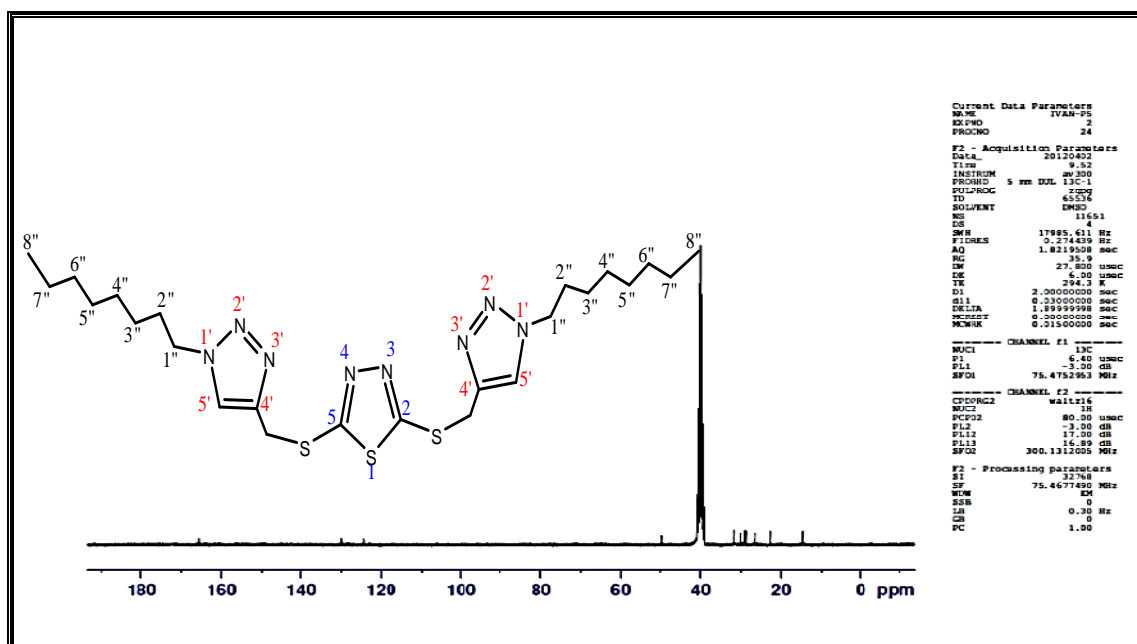
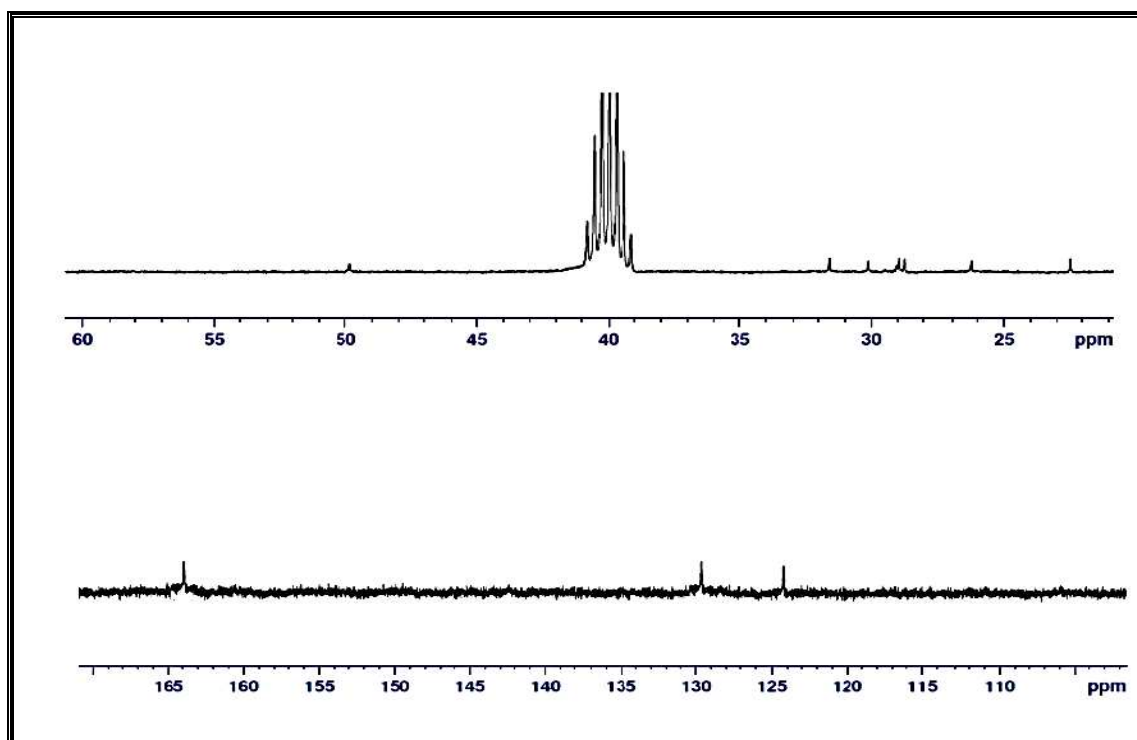


Fig.(3-16) ¹H NMR of ligand [L²]

(3.5.2.2) ¹³C NMR spectrum for the ligand [L²]:

The ¹³C NMR spectrum of [L¹] Fig.(3-17) in DMSO-d⁶ shows the signal at (δ = 22 ppm) assigned to C₈"for terminal methyl group of aliphatic chains, the signals at (δ = 26, 27, 28, 29, 30, 32 ppm) due to the carbon atoms C₃", C₂", C₄", C₅", C₆"and C₇"respectively, while the C₁" appeared signal at (δ = 49 ppm), the carbon atoms C₄' & C₅' of triazole rings shows the signals at (δ = 124, 129 ppm), the signal at (δ = 164 ppm) assigned to carbon atoms C₂ & C₅ of thiadiazole ring.

Fig.(3-17)¹³C NMR of ligand [L²]Fig.(3-17)¹³C NMR of ligand [L²]

(3.5.3) ^1H , ^{13}C NMR spectra for the ligand [L^3]:**(3.5.3.1) ^1H NMR spectrum for the ligand [L^3]:**

The ^1H NMR spectrum of [L^3] Fig.(3-18) in DMSO- d_6 display the signal at ($\delta = 0.84$ ppm, 6H) due to the protons attached to $\text{C}_{10''}$ of methyl groups, the chemical shifts at ($\delta = 1.10, 1.39, 1.877$ ppm, 24H) assigned to $\text{C}_{8''}, \text{C}_{4''}, 5'', 6'', 7''$ and $\text{C}_{3''}$ respectively. The signal at ($\delta = 3.08$ ppm, 4H) attributed to the protons attached to carbon $\text{C}_{2''}$ of the aliphatic chains. The signal at ($\delta = 4.31$ ppm, 4H) assigned to the protons of carbon $\text{C}_{1''}$, the chemical shift was affecting by the neighboring group of triazole ring.

The protons of methylene groups which lie between the sulphur atom and triazole ring were appeared at ($\delta = 4.55$ ppm, 4H), the signal at ($\delta = 8.10 - 7.95$ ppm, 2H) attributed to the protons $\text{C}_{4'}$ of triazole rings.

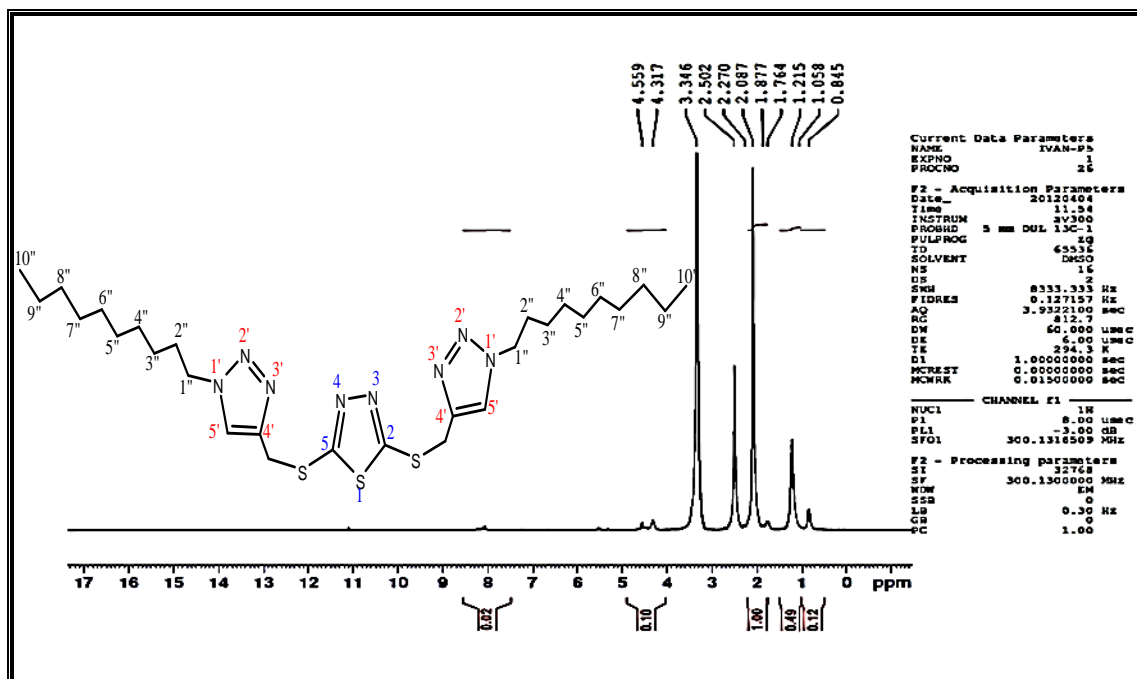


Fig.(3-18) ^1H NMR of the ligand [L^3]

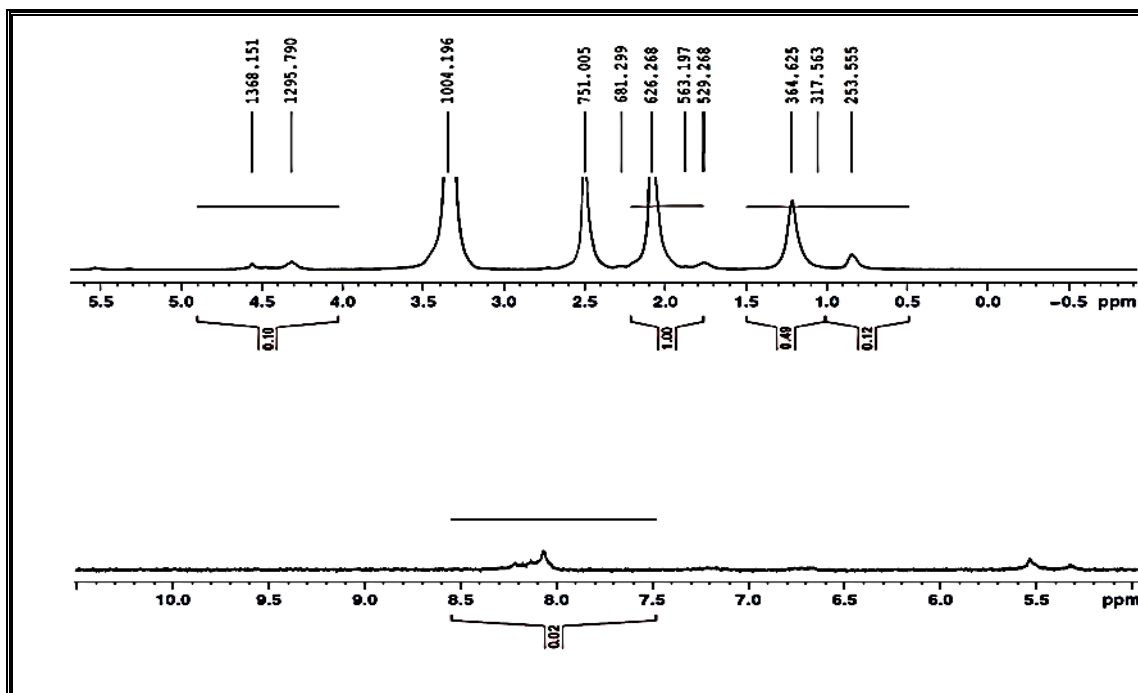
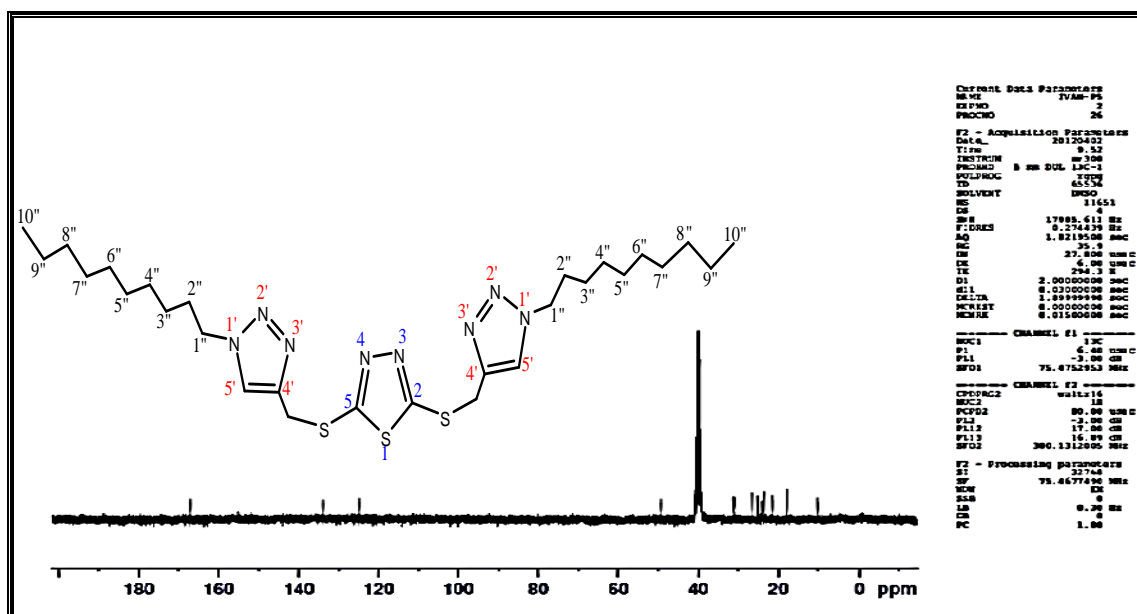
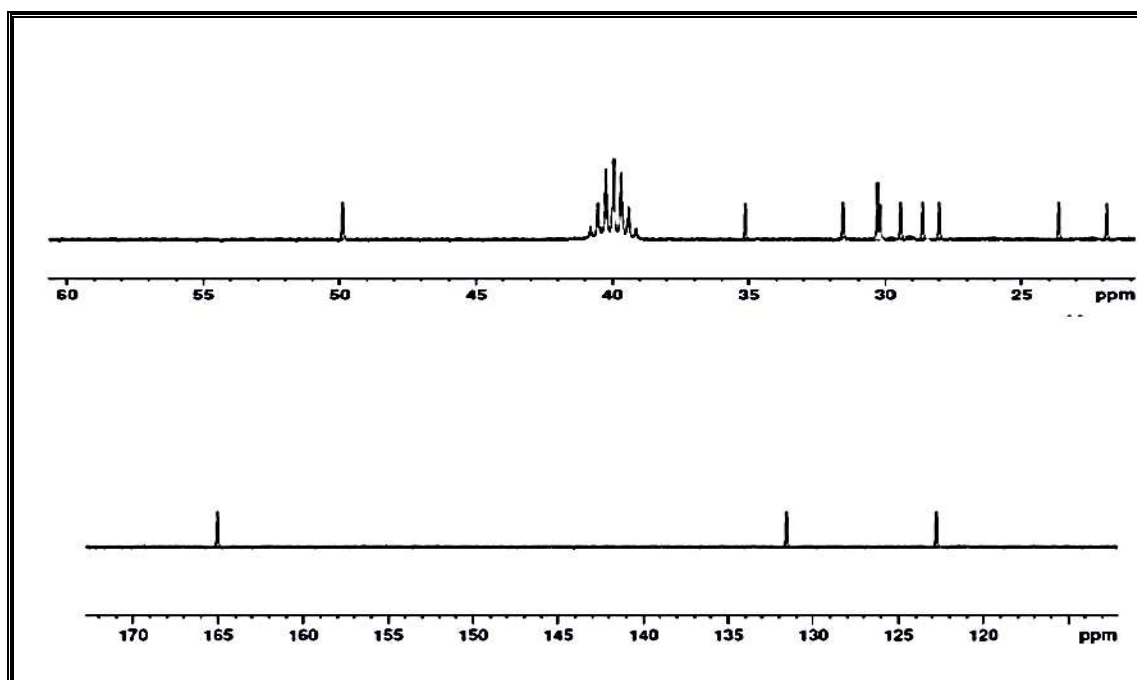


Fig.(3-18)¹H NMR of the ligand [L³]

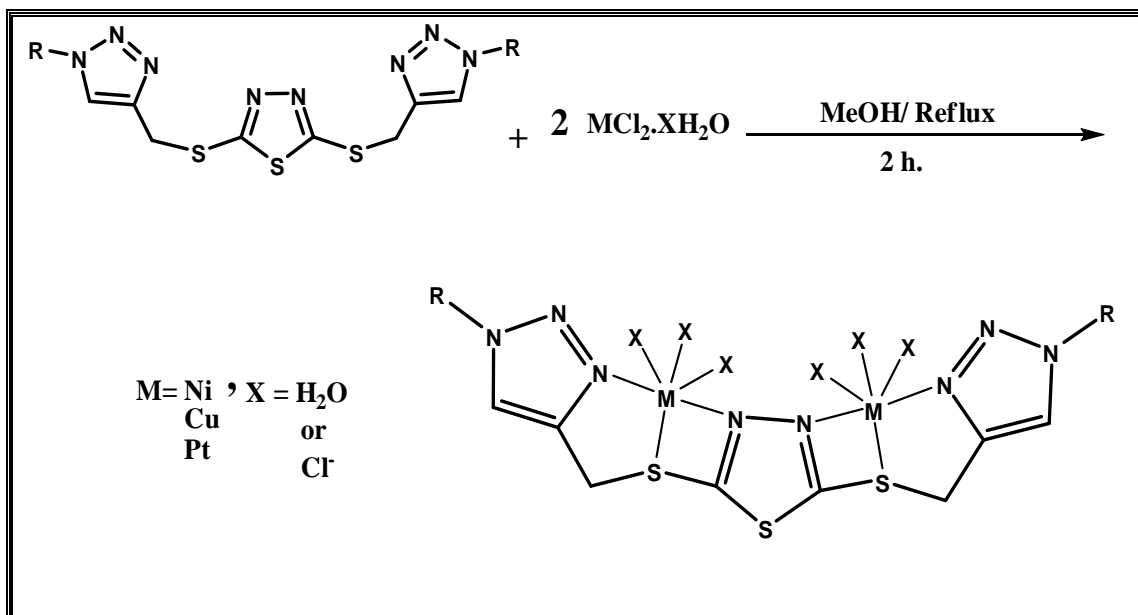
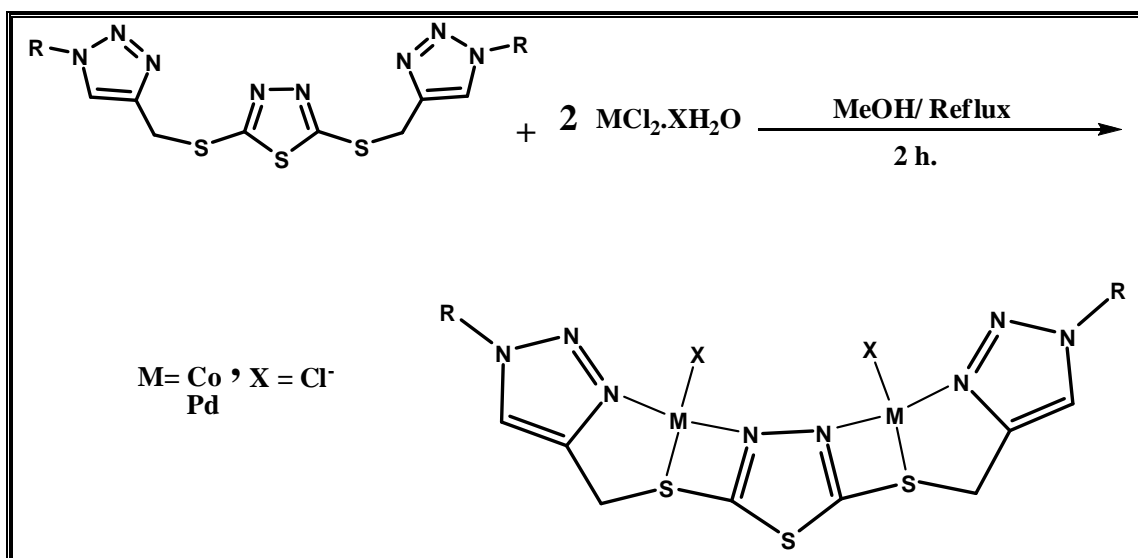
(3.5.3.2)¹³C NMR spectrum for the ligand [L³]:

The ¹³C NMR spectrum of [L³] **Fig.(3-19)** in DMSO-d⁶ shows the signal at ($\delta = 21$ ppm) assigned to C_{10''} for terminal methyl group of aliphatic chains, the signals at ($\delta = 23, 27, 28, 31, 32$ ppm) due to the carbon atoms C_{9''}, C_{3''}, C_{2''}, C_{4''}, 5'', 6'', 7'', and C_{8''} respectively, while the C_{1''} appeared signal at ($\delta = 50$ ppm), the carbon atoms C_{4'} & C_{5'} of triazole rings shows the signals at ($\delta = 123, 131$ ppm), the signal at ($\delta = 165$ ppm) assigned to carbon atoms C₂ & C₅ of thiadiazole ring.

Fig.(3-19) ^{13}C NMR of the ligand $[\text{L}^3]$ Fig.(3-19) ^{13}C NMR of the ligand $[\text{L}^3]$

(3.6) Synthesis and characterization of the complexes

All complexes were prepared by a similar method, shown in **Scheme (3-4)** and **(3-5)**. The complexes were prepared from the reaction of the ligands with metal chloride salt at reflux in methanol, recrystallized with acetonitrile.

**Scheme (3-4): preparation of (Oh) complexes****Scheme (3-5): preparation of (Td or Sp) complexes**

(3.6.1) Synthesis and characterization of [L¹] complexes:

All complexes were prepared by a similar method; the solubility of the complexes in different solvents was summarized in **Table (3-4)**. Spectroscopic methods [FT-IR, UV-Vis], along with molar conductivity, magnetic susceptibility and melting point were used to characterize the complexes.

Table (3-5) solubility of [L¹] complexes in different solvents

Complex	DCM	CH ₃ CN	Et ₂ O	Acetone	C ₆ H ₁₄	MeOH	CHCl ₃	DMSO	DMF
[Co ₂ (L ¹)Cl ₂]Cl ₂	+	+	-	+	-	+	+	+	+
[Ni ₂ (L ¹)(H ₂ O) ₄ Cl ₂]Cl ₂	-	-	-	÷	-	-	-	+	+
[Cu ₂ (L ¹)(H ₂ O) ₆]Cl ₄	+	+	-	+	-	+	+	+	+
[Pd ₂ (L ¹)Cl ₂]Cl ₂	÷	÷	-	÷	-	-	-	+	+
[Pt ₂ (L ¹)(H ₂ O) ₂ Cl ₄]Cl ₄	-	-	-	-	-	-	-	+	+

(+) Soluble

(-) Insoluble

(÷) Sparingly

(3.6.2) Synthesis and characterization of the [L²] complexes

All complexes were prepared by a similar method. **Table (3-5)** summarized the solubility of the complexes in different solvents. Spectroscopic methods [(FT-IR), (U.V-Vis)] along with molar conductivity, magnetic susceptibility measurements and melting point were used to characterize the complexes.

Table (3-6) solubility of $[L^2]$ complexes in different solvents

Complex	DCM	CH ₃ CN	Et ₂ O	Acetone	C ₆ H ₁₄	MeOH	CHCl ₃	DMSO	DMF
$[Co_2(L^2)Cl_2]Cl_2$	+	+	-	+	-	+	+	+	+
$[Ni_2(L^2)(H_2O)_4Cl_2]Cl_2$	-	-	-	÷	-	-	-	+	+
$[Cu_2(L^2)(H_2O)_6]Cl_4$	+	+	-	+	-	+	+	+	+
$[Pd_2(L^2)Cl_2]Cl_2$	÷	÷	-	÷	-	-	-	+	+
$[Pt_2(L^2)(H_2O)_2Cl_4]Cl_4$	-	-	-	-	-	-	-	+	+

(+) Soluble (-) Insoluble (÷) Sparingly

(3.6.3) Synthesis and characterization of the $[L^3]$ complexes:

All complexes were prepared by a similar method **Table (3-6)** summarized the solubility of the complexes in different solvents. Spectroscopic methods [(FT-IR), (U.V-Vis)] along with molar conductivity, magnetic susceptibility measurements and melting point were used to characterize the complexes.

Table (3-7) solubility of $[L^3]$ complexes in different solvents

Complex	DCM	CH ₃ CN	Et ₂ O	Acetone	C ₆ H ₁₄	MeOH	CHCl ₃	DMSO	DMF
$[Co_2(L^3)Cl_2]Cl_2$	+	+	-	+	-	+	+	+	+
$[Ni_2(L^3)(H_2O)_4Cl_2]Cl_2$	-	-	-	÷	-	-	-	+	+
$[Cu_2(L^3)(H_2O)_6]Cl_4$	+	+	-	+	-	+	+	+	+
$[Pd_2(L^3)Cl_2]Cl_2$	÷	÷	-	÷	-	-	-	+	+
$[Pt_2(L^3)(H_2O)_2Cl_4]Cl_4$	-	-	-	-	-	-	-	+	+

(+) Soluble (-) Insoluble (÷) Sparingly

(3.7) FT-IR spectra of synthesis complexes:

(3.7.1) FT-IR spectra of [L¹] metal complexes:

(3.7.1.1) FT-IR spectrum of [Co₂(L¹)Cl₂]Cl₂ :

The FT-IR spectrum of [Co₂(L¹)Cl₂]Cl₂ complex **Fig.(3-20)** appeared the bands at (3132 cm⁻¹), (2956 cm⁻¹), (2922 cm⁻¹) and (2856 cm⁻¹) attributed to $\nu(\text{C-H})$ stretching of aromatic, $\nu(\text{C-H})$ asym. and sym. stretching of aliphatic chain respectively, the bands at (1547cm⁻¹), (1465 cm⁻¹), (1378 cm⁻¹) , (1226 cm⁻¹) and (1047 cm⁻¹) due to stretching of $\nu(\text{C=N})$, $\nu(\text{C=C})$, $\nu(\text{N=N})$, $\nu(\text{C-N})$ and $\nu(\text{N-N})$ respectively. The bands were shifting to the lower frequency compared with the values which that appeared in the free ligand, can be attributed to the delocalization of the electronic density in the π system (HOMO→LUMO) indicating to the donor atoms were coordinate with metal ion [where HOMO= Highest Occupied Molecular Orbital; LUMO= Lowest Unoccupied Molecular Orbital]. While the bands at (785 cm⁻¹), (731 cm⁻¹) and (667 cm⁻¹) assigned to stretching of $\nu(\text{C-S-C})$ asym. and sym. respectively, and $\nu(\text{C-S})$ in thiadiazole ring and dithiol groups respectively, these values appeared shifting (about 8 to 27 cm⁻¹) higher than the base values of these bands in the free ligand, that is mean there was coordinate obtained between S atoms in dithaiol group with metal ion^(55, 56).

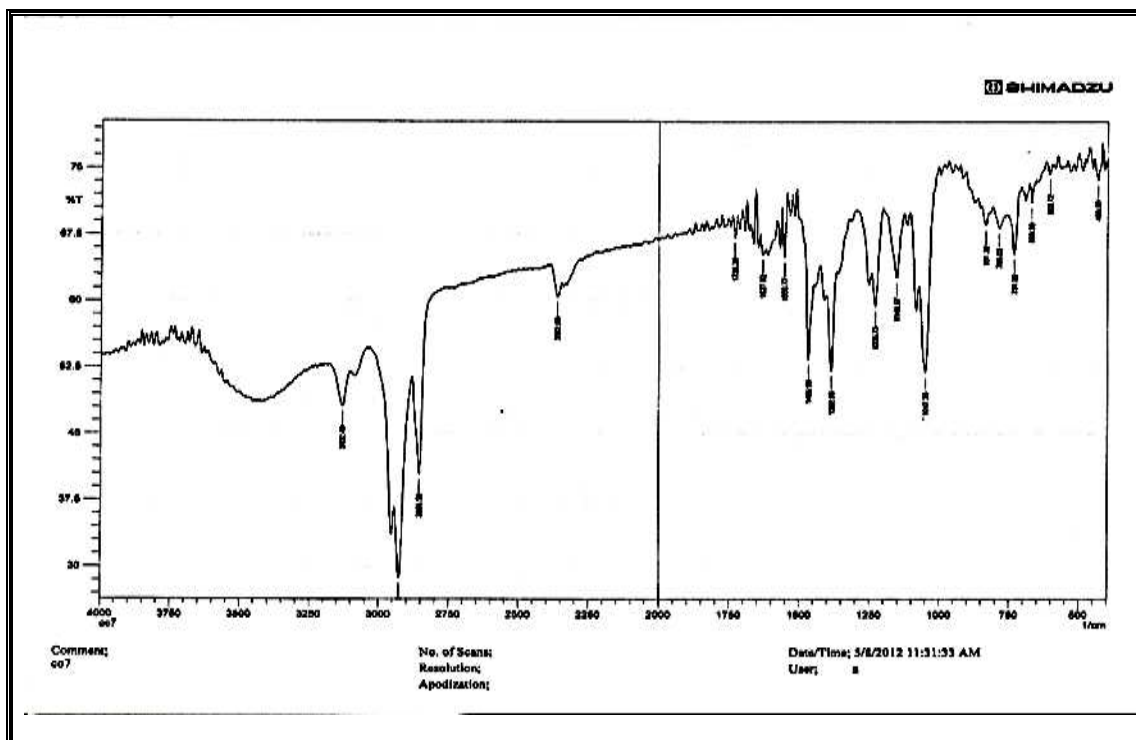


Fig.(3-20) FT-IR spectrum of $[\text{Co}_2(\text{L}^1)\text{Cl}_2]\text{Cl}_2$ complex

(3.7.1.2) FT-IR spectrum of $[\text{Ni}_2(\text{L}^1)(\text{H}_2\text{O})_4\text{Cl}_2]\text{Cl}_2$:

The FT-IR spectrum of $[\text{Ni}_2(\text{L}^1)(\text{H}_2\text{O})_4\text{Cl}_2]\text{Cl}_2$ complex **Fig.(3-21)** appear broad band at (3400cm^{-1}) assigned to stretching of $\nu(\text{O-H})$, in water molecule, the bands at (3130cm^{-1}) , (2955cm^{-1}) , (2927cm^{-1}) and (2856cm^{-1}) attributed to $\nu(\text{C-H})$ stretching of aromatic, $\nu(\text{C-H})$ asym. and sym. stretching of aliphatic respectively. While the bands at (1541cm^{-1}) , (1465cm^{-1}) , (1379cm^{-1}) , (1241cm^{-1}) and (1056cm^{-1}) assigned to $\nu(\text{C=N})$, $\nu(\text{C=C})$, $\nu(\text{N=N})$, $\nu(\text{C-N})$ and $\nu(\text{N-N})$ stretching respectively. The bands were shifting to the lower frequency compared with the values which that appeared in the free ligand, can be attributed to the delocalization of the electronic density in the π system (HOMO \rightarrow LUMO) indicating to the donor atoms were coordinate with metal ion. While the bands at (784cm^{-1}) (729cm^{-1}) and (667cm^{-1}) assigned to $\nu(\text{C-S-C})$ asym. and sym. stretching and $\nu(\text{C-S})$ stretching of

thiadiazole ring and dithiol groups respectively, these values appeared higher shifting compared with base values of these bands in the free ligand before chelating, that is mean the coordinate obtained with thiol groups^(55, 56).

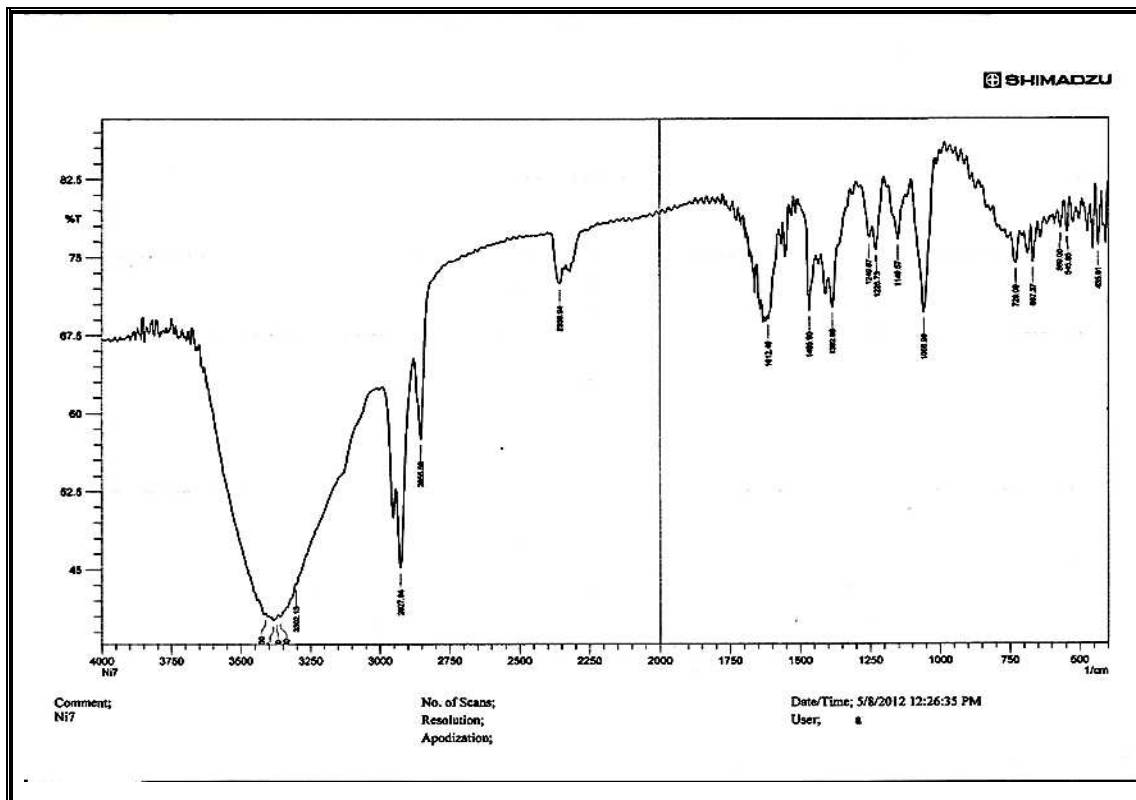


Fig.(3-21) FT-IR spectrum of $[\text{Ni}_2(\text{L}^1)(\text{H}_2\text{O})_4\text{Cl}_2]\text{Cl}_2$ complex

(3.7.1.3) FT-IR spectrum of $[\text{Cu}_2(\text{L}^1)(\text{H}_2\text{O})_6]\text{Cl}_4$:

The FT-IR spectrum of $[\text{Cu}_2(\text{L}^1)(\text{H}_2\text{O})_6]\text{Cl}_4$ complex **Fig.(3-22)** appeared broad band at (3566 cm^{-1}) assigned to stretching of $\nu(\text{O-H})$ in water molecules, the bands at (3130 cm^{-1}) , (2956 cm^{-1}) , (2924 cm^{-1}) and (2856 cm^{-1}) assigned to asym. and sym. stretching of $\nu(\text{C-H})$ aromatic and $\nu(\text{C-H})$ aliphatic respectively. While the bands at (1546 cm^{-1}) , (1456 cm^{-1}) , (1380 cm^{-1}) , (1224 cm^{-1}) and (1047 cm^{-1}) attributed to stretching of $\nu(\text{C=N})$, $\nu(\text{C=C})$, $\nu(\text{N=N})$, $\nu(\text{C-N})$ and $\nu(\text{N-N})$ respectively. The bands were shifting to the lower frequency compared with the values which that

appeared in the free ligand, can be attributed to the delocalization of the electronic density in the π system (HOMO \rightarrow LUMO) indicating to the donor atoms were coordinate with metal ion. While the bands at (772 cm^{-1}) (723 cm^{-1}) and (669 cm^{-1}) attributed to asym. and sym. stretching of $\nu(\text{C-S-C})$ and $\nu(\text{C-S})$ in thiadiazole ring and dithiol groups respectively, these values appeared higher shifting compared with base values of these bands in the free ligand before chelating, that is mean there was coordinate obtained with thiol groups^(55, 56).

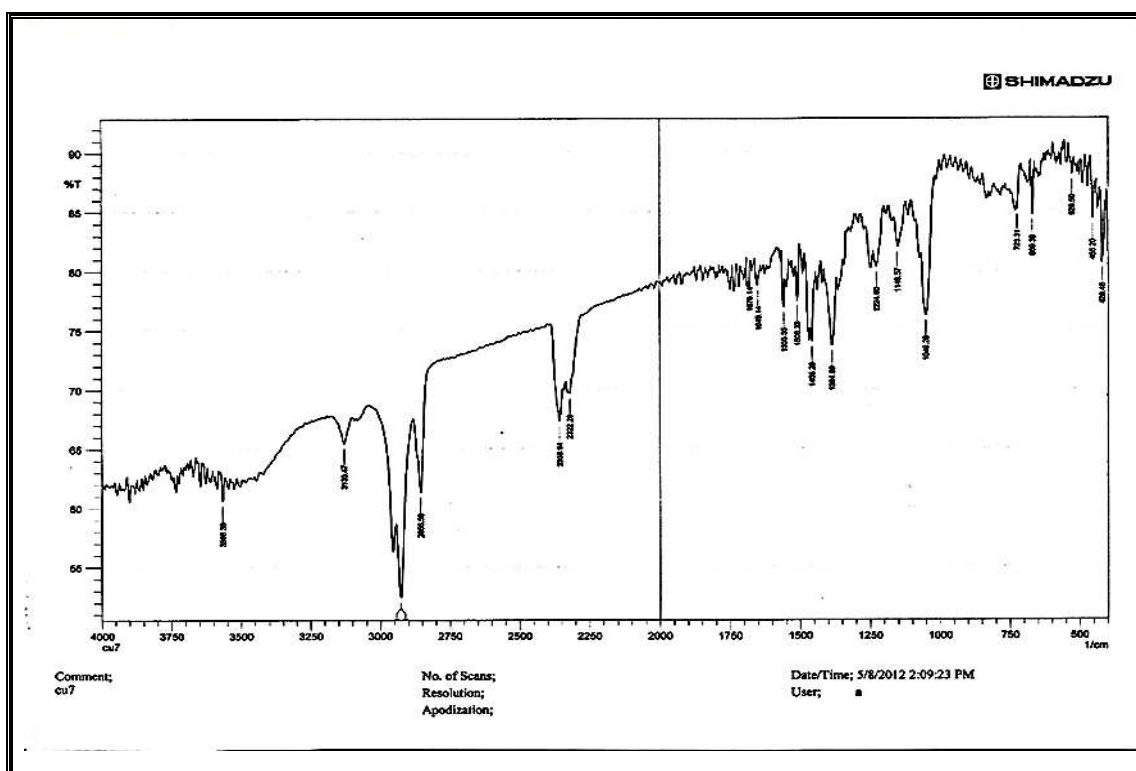


Fig.(3-22) FT-IR spectrum of $[\text{Cu}_2(\text{L}^1)(\text{H}_2\text{O})_6]\text{Cl}_4$ complex

(3.7.1.4) FT-IR-Spectrum of $[\text{Pd}_2(\text{L}^1)\text{Cl}_2]\text{Cl}_2$:

The FT-IR spectrum of $[\text{Pd}_2(\text{L}^1)\text{Cl}_2]\text{Cl}_2$ complex **Fig.(3-23)** appeared the bands at (3134 cm^{-1}), (2955 cm^{-1}), (2928 cm^{-1}) and (2854 cm^{-1}) assigned to $\nu(\text{C-H})$ stretching of aromatic, $\nu(\text{C-H})$ sym. and asym.stretching of aliphatic respectively. While the bands appeared at

(1547 cm^{-1}), (1463 cm^{-1}), (1377 cm^{-1}), (1241 cm^{-1}) and (1049 cm^{-1}) attributed to $\nu(\text{C}=\text{N})$, $\nu(\text{C}=\text{C})$, $\nu(\text{N}=\text{N})$, $\nu(\text{C}-\text{N})$ and $\nu(\text{N}-\text{N})$ stretching respectively. The bands were shifting to the lower frequency compared with the values which that appeared in the free ligand, can be attributed to the delocalization of the electronic density in the π system (HOMO \rightarrow LUMO) indicating to the donor atoms were coordinate with metal ion. While the bands at (792 cm^{-1}), (727 cm^{-1}) and (667 cm^{-1}) assigned to $\nu(\text{C}-\text{S}-\text{C})$ sym. and asym. stretching, and $\nu(\text{C}-\text{S})$ stretching of thiadiazole ring and dithiol groups respectively, these values appeared higher shifting compared with base values of these bonds in the free ligand, that is mean there was coordinate obtained with thiol groups^(55, 56).

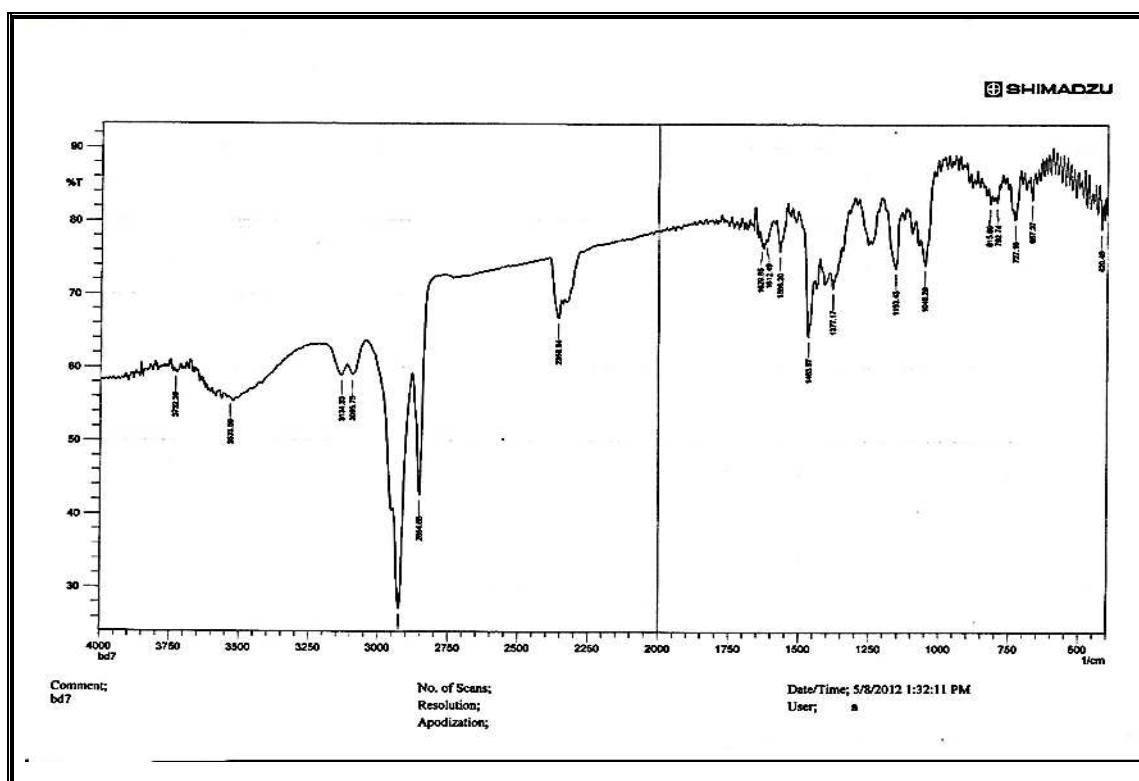


Fig.(3-23) FT-IR spectrum of $[\text{Pd}_2(\text{L}^1)\text{Cl}_2]\text{Cl}_2$ complex

(3.7.1.5) FT-IR-Spectrum of $[\text{Pt}_2(\text{L}^1)(\text{H}_2\text{O})_2\text{Cl}_4]\text{Cl}_4$:

The FT-IR spectrum of $[\text{Pt}_2(\text{L}^1)(\text{H}_2\text{O})_2\text{Cl}_4]\text{Cl}_4$ complex **Fig.(3-24)** appeared broad band at (3508 cm^{-1}) assigned to stretching of $\nu(\text{O-H})$ in water molecules coordinated with platinum ion, it referred to existence of (H_2O) in complex coordinate with platinum ion. While bands appeared at (3138 cm^{-1}) , (2955 cm^{-1}) , (2924 cm^{-1}) and (2858 cm^{-1}) assigned to $\nu(\text{C-H})$ stretching of aromatic, $\nu(\text{C-H})$ sym. and asym. stretching of aliphatic respectively. The bands exhibit at (1546 cm^{-1}) , (1463 cm^{-1}) , (1374 cm^{-1}) , (1230 cm^{-1}) and (1051 cm^{-1}) assigned to $\nu(\text{C=N})$, $\nu(\text{C=C})$, $\nu(\text{N=N})$, $\nu(\text{C-N})$ and $\nu(\text{N-N})$ stretching respectively. The bands were shifting to the lower frequency compared with the values which that appeared in the free ligand, can be attributed to the delocalization of the electronic density in the π system (HOMO \rightarrow LUMO) indicating to the donor atoms were coordinate with metal ion. While the bands appeared at (773 cm^{-1}) (736 cm^{-1}) and (667 cm^{-1}) attributed to $\nu(\text{C-S-C})$ sym. and asym. stretching, and $\nu(\text{C-S})$ stretching of thiadiazole ring and dithiol groups respectively, these values appeared higher shifting compared with base values of these bands in the free ligand, that is mean there was coordinate obtained with thiol groups^(55, 56).

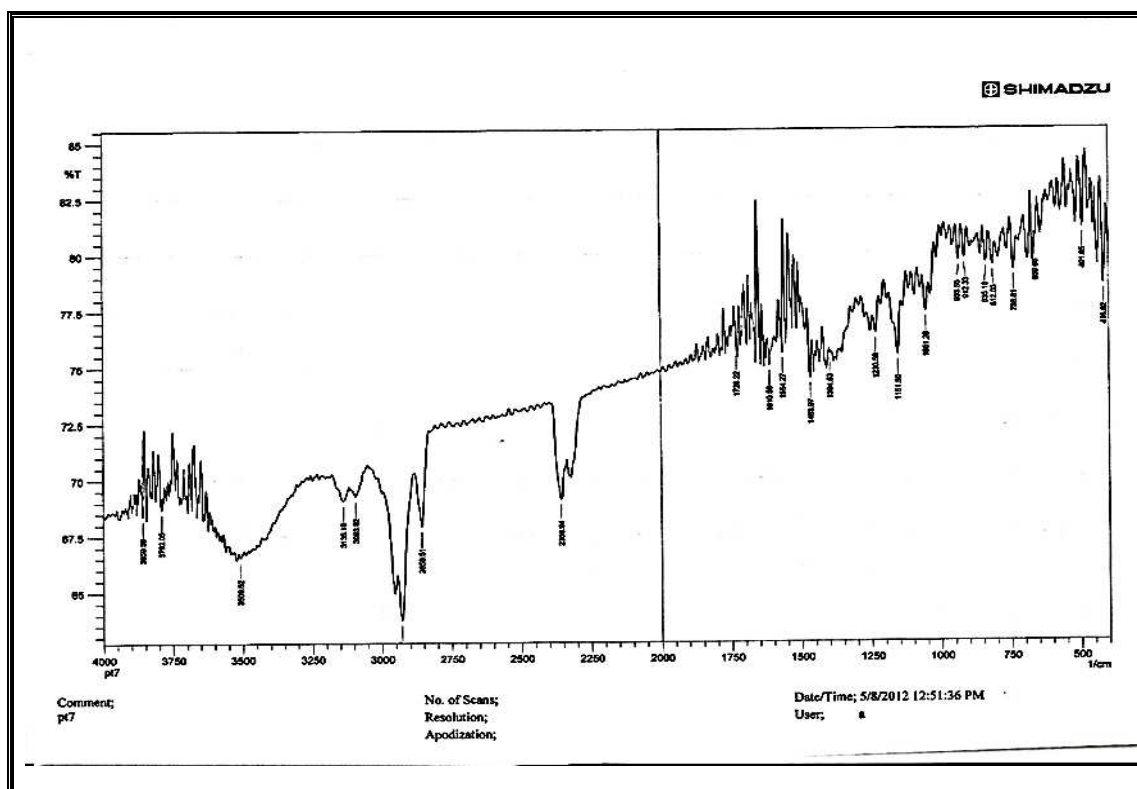


Fig.(3-24) FT-IR spectrum of $[\text{Pt}_2(\text{L}^1)(\text{H}_2\text{O})_2\text{Cl}_4]\text{Cl}_4$ complex

The FT-IR bands of $[\text{L}^1]$ ligand and Co(II), Ni(II), Cu(II), Pd(II) and Pt(IV) complexes were summarized in **Table. (3-8)**

Table. (3-8) The FT-IR bands of [L¹] ligand and Co(II), Ni(II),

Compound	v(O-H)	v(C-H) aromatic	v(C-H) aliphatic	v(C=N)	v(C=C)	v(N=N)	v(C-N)	v(N-N)	v(C-S-C)	v(C-S)
L ¹	—	3128s 3116s	2954s 2924s 2850s	1548m	1467m	1381m	1242m	1058s	771w 723m	640w
[Co ₂ (L ¹)Cl ₂]Cl ₂	—	3132s	2956s 2922s 2856s	1547m	1465m	1378m	1226w	1047m	785w 731m	667w
[Ni ₂ (L ¹)(H ₂ O) ₄ (Cl) ₂]Cl ₂	3400br	3130s	2955s 2927s 2856s	1541m	1465m	1379m	1241w	1056m	784w 729m	667w
[Cu ₂ (L ¹)(H ₂ O) ₆]Cl ₄	3566br	3130s	2956s 2924s 2854s	1546m	1456m	1380m	1224w	1047m	772w 723m	669w
[Pd ₂ (L ¹)Cl ₂]Cl ₂	—	3134s	2955s 2928s 2854s	1547m	1463m	1377m	1241w	1049m	792w 722m	667w
[Pt ₂ (L ¹)(H ₂ O) ₂ (Cl) ₄]Cl ₄	3508br	3138s	2955s 2924s 2858s	1564m	1463m	1374m	1230w	1051m	773w 736m	667w

Cu(II), Pd(II) and Pt(IV) complexes

br = broad, s = strong, m = medium, w = weak

(3.7.2) FT-IR spectra of [L²] metal complexes:**(3.7.2.1) FT-IR spectrum of [Co₂(L²)Cl₂]Cl₂ :**

The FT-IR spectrum of [Co₂(L²)Cl₂]Cl₂ complex **Fig.(3-25)** appeared the bands at (3132 cm⁻¹), (2956 cm⁻¹), (2922 cm⁻¹) and (2852 cm⁻¹) assigned to $\nu(\text{C-H})$ aromatic stretching and $\nu(\text{C-H})$ sym. and asym. stretching of aliphatic respectively. While the bands at (1546 cm⁻¹), (1465 cm⁻¹), (1377 cm⁻¹) , (1224 cm⁻¹) and (1047 cm⁻¹) assigned to $\nu(\text{C=N})$, $\nu(\text{C=C})$, $\nu(\text{N=N})$, $\nu(\text{C-N})$ and $\nu(\text{N-N})$ stretching respectively. The bands were shifting to the lower frequency compared with the values which that appeared in the free ligand, can be attributed to the delocalization of the electronic density in the π system (HOMO→LUMO) indicating to the donor atoms were coordinate with metal ion [where HOMO= Highest Occupied Molecular Orbital; LUMO= Lowest Unoccupied Molecular Orbital]. While the bands at (781 cm⁻¹), (732 cm⁻¹) and (669 cm⁻¹) assigned to $\nu(\text{C-S-C})$ sym. and asym. stretching $\nu(\text{C-S})$ stretching of thiadiazole ring and dithiol group respectively, these values appeared higher shifting compared with the base values of these bands in the free ligand before chelating , that is mean there was coordinate obtained with thiol groups^(55, 56).

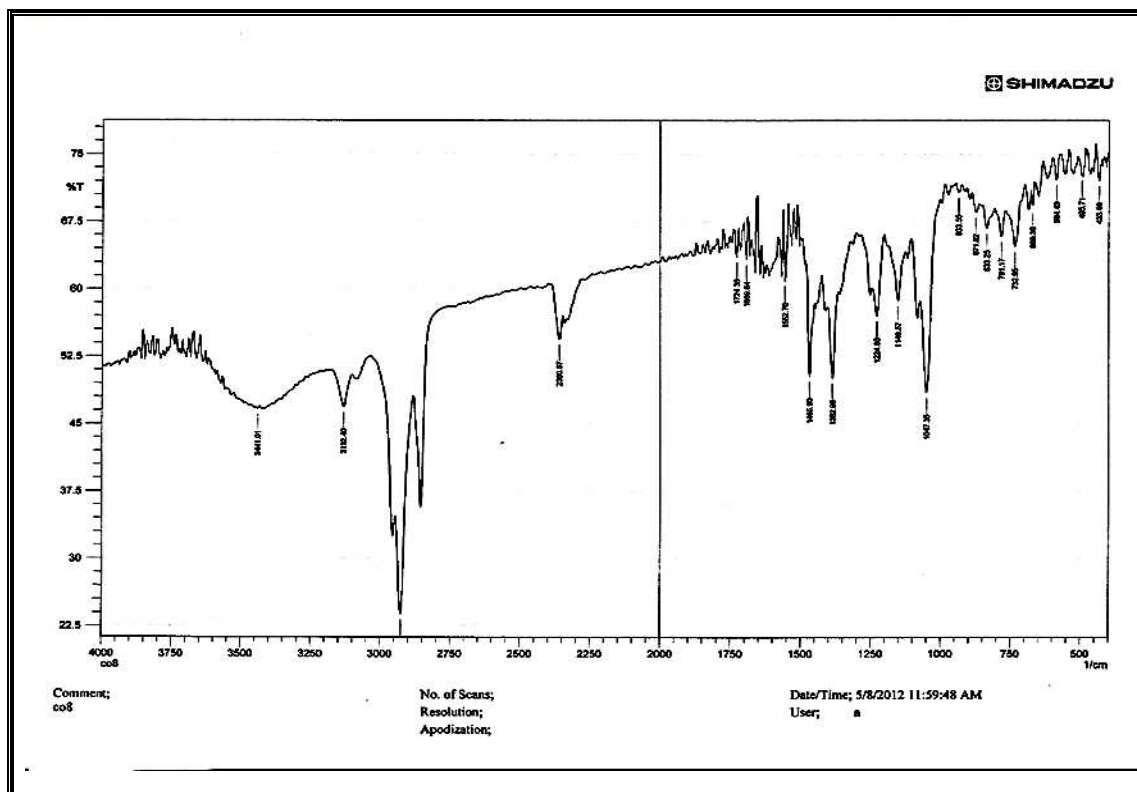


Fig.(3-25) FT-IR spectrum of $[\text{Co}_2(\text{L}^2)\text{Cl}_2]\text{Cl}_2$ complex

(3.7.2.2) FT-IR spectrum of $[\text{Ni}_2(\text{L}^2)(\text{H}_2\text{O})_4\text{Cl}_2]\text{Cl}_2$:

The FT-IR spectrum of $[\text{Ni}_2(\text{L}^2)(\text{H}_2\text{O})_4\text{Cl}_2]\text{Cl}_2$ complex **Fig. (3-26)** appeared broad bands at (3381 cm^{-1}) , (3361 cm^{-1}) assigned to $\nu(\text{O-H})$ stretchin of water molecules, this band is an evidence to existence of (H_2O) in the complex. While the bands appeared at (3131 cm^{-1}) , (2956 cm^{-1}) , (2921 cm^{-1}) and (2854 cm^{-1}) due to $\nu(\text{C-H})$ aromatic stretching, sy $\nu(\text{C-H})$ sym. and asym. stretching of aliphatic respectively. The bands at (1548 cm^{-1}) , (1465 cm^{-1}) , (1381 cm^{-1}) , (1226 cm^{-1}) and (1056 cm^{-1}) attributed to $\nu(\text{C=N})$, $\nu(\text{C=C})$, $\nu(\text{N=N})$, $\nu(\text{C-N})$ and $\nu(\text{N-N})$ stretching respectively. The bands were shifting to the lower frequency compared with the values which that appeared in the free ligand, can be attributed to the delocalization of the electronic density in the π system

(HOMO→LUMO) indicating to the donor atoms were coordinate with metal ion. While the bands appeared at (781 cm^{-1}), (724 cm^{-1}) and (669 cm^{-1}) due to $\nu(\text{C-S-C})$ and $\nu(\text{C-S})$ stretching of thiadiazole ring and dithiol groups respectively, these values appeared higher shifting compared with base value of these bands in the free ligand before chelating, that is mean the coordinate obtained between metal ion with thiol groups^(55, 56).

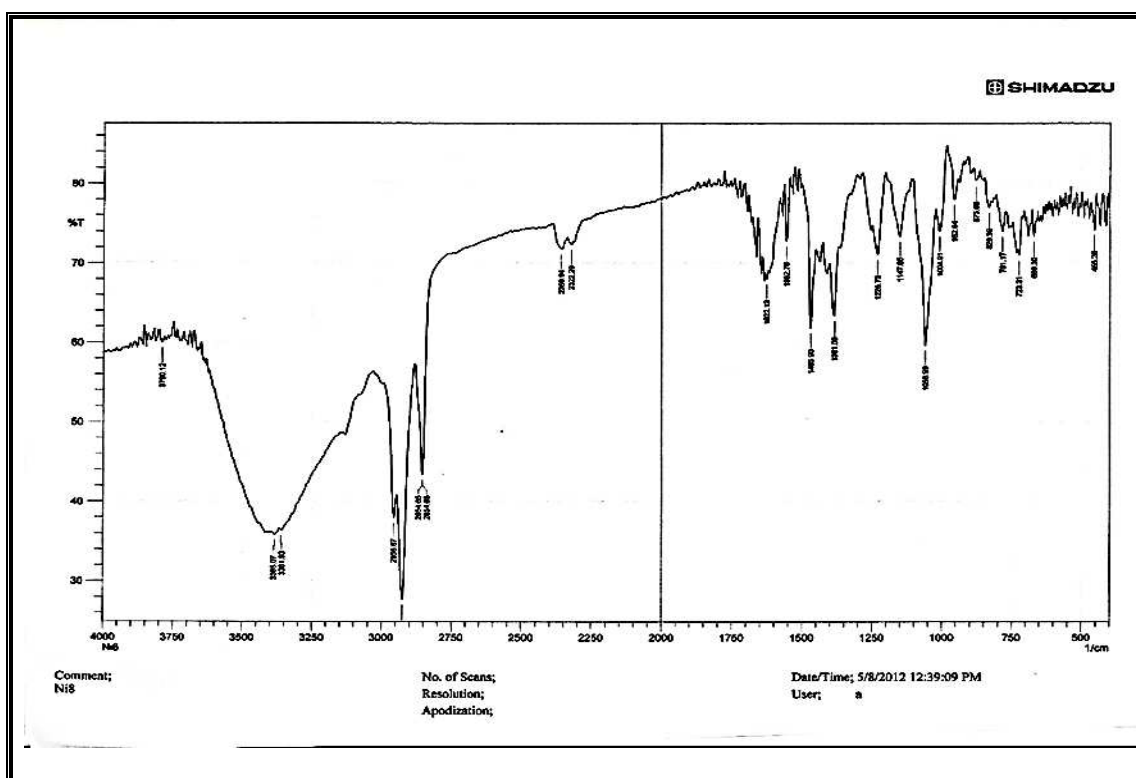


Fig.(3-26) FT-IR spectrum of $[\text{Ni}_2(\text{L}^2)(\text{H}_2\text{O})_4\text{Cl}_2]\text{Cl}_2$ complex

(3.7.2.3) FT-IR spectrum of $[\text{Cu}_2(\text{L}^2)(\text{H}_2\text{O})_6]\text{Cl}_4$:

The FT-IR spectrum of $[\text{Cu}_2(\text{L}^2)(\text{H}_2\text{O})_6]\text{Cl}_4$ complex **Fig.(3-27)** appeared broad band at (3444 cm^{-1}) assigned to stretching of $\nu(\text{O-H})$ of water molecules. While the bands at (3132 cm^{-1}), (2922 cm^{-1}) and (2850 cm^{-1}) assigned to $\nu(\text{C-H})$ stretching of aromatic, $\nu(\text{C-H})$ sym. and asym. stretching of aliphatic respectively. While the bands at (1546 cm^{-1}),

(1456 cm^{-1}), (1384 cm^{-1}), (1226 cm^{-1}) and (1049 cm^{-1}) attributed to $\nu(\text{C}=\text{N})$, $\nu(\text{C}=\text{C})$, $\nu(\text{N}=\text{N})$, $\nu(\text{C}-\text{N})$ and $\nu(\text{N}-\text{N})$ stretching respectively. The bands were shifting to the lower frequency compared with the values which that appeared in the free ligand, can be attributed to the delocalization of the electronic density in the π system (HOMO \rightarrow LUMO) indicating to the donor atoms were coordinate with metal ion. While the bands appeared at (782 cm^{-1}), (732 cm^{-1}) and (669 cm^{-1}) assigned to $\nu(\text{C}-\text{S}-\text{C})$ sym. and asym. stretching and $\nu(\text{C}-\text{S})$ stretching of thiadiazole ring and dithiol groups respectively, these values appeared higher shifting compared with base values of these bands in the free ligand before chelating , that is mean coordinate obtained between metal ion with thiol groups^(55, 56).

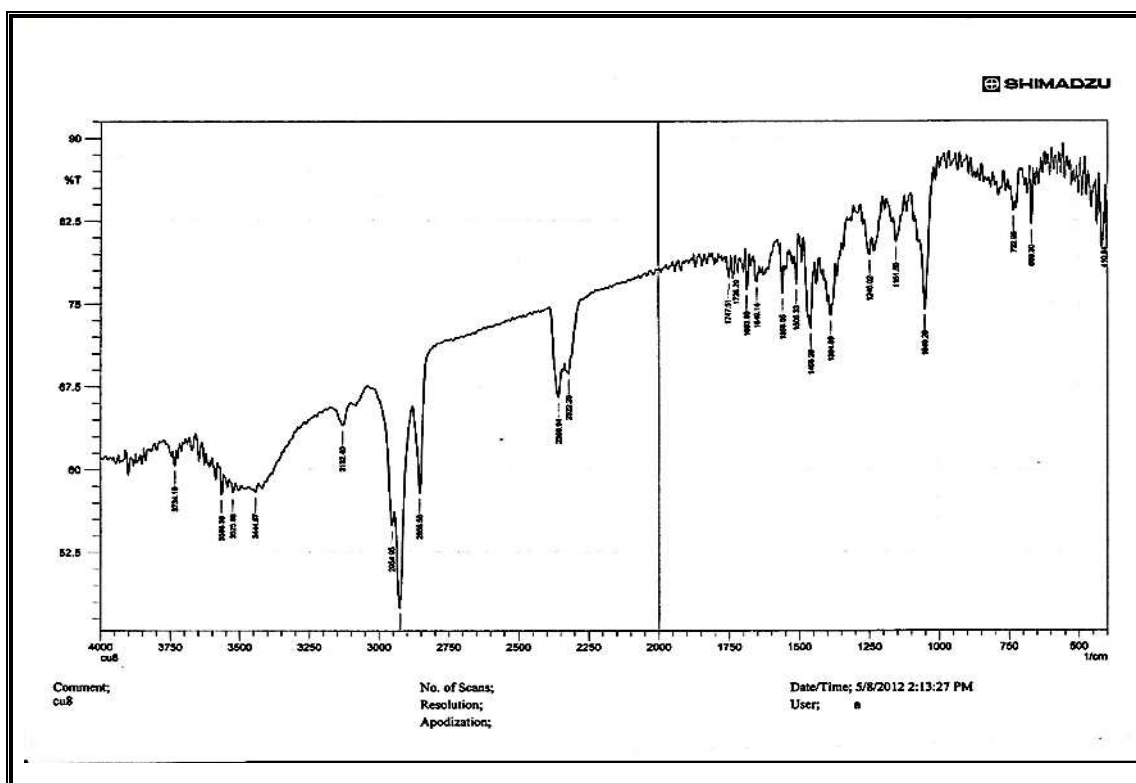
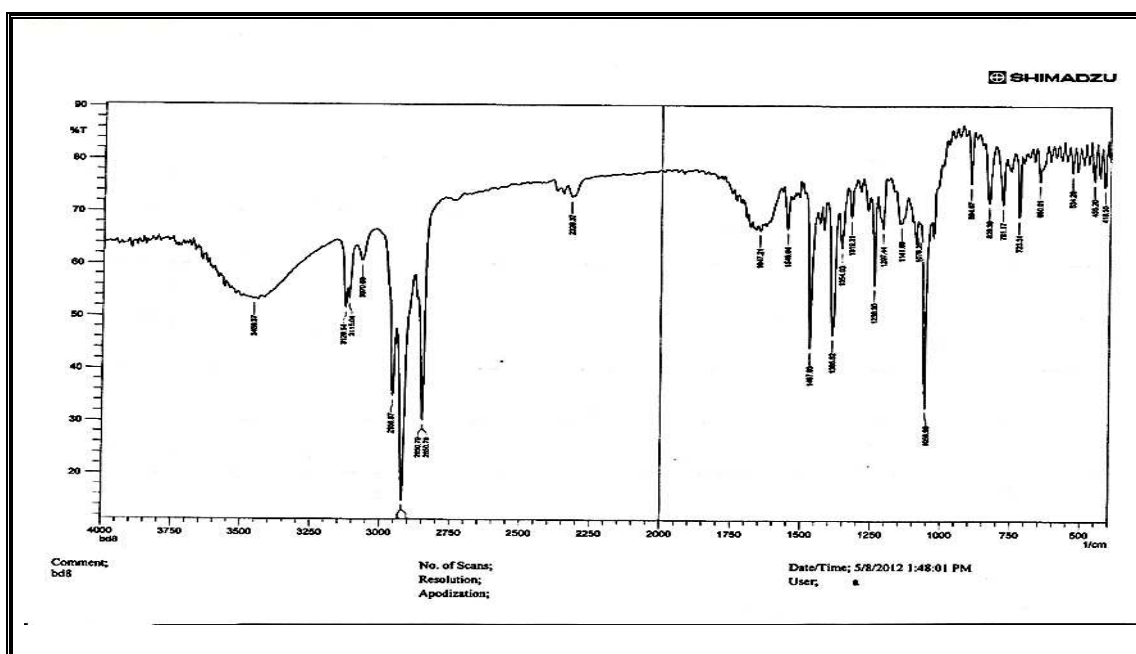


Fig.(3-27) FT-IR spectrum of [Cu₂(L²)(H₂O)₆]Cl₄ complex

(3.7.2.4) FT-IR spectrum of $[\text{Pd}_2(\text{L}^2)\text{Cl}_2]\text{Cl}_2$:

The FT-IR spectrum of $[\text{Pd}_2(\text{L}^2)\text{Cl}_2]\text{Cl}_2$ complex **Fig.(3-28)** appeared the bands at (3128 cm^{-1}), (2956 cm^{-1}), (2923 cm^{-1}) and (2850 cm^{-1}) attributed to $\nu(\text{C-H})$ stretching of aromatic, sym. and asym. stretching of aliphatic respectively. The bands at (1548 cm^{-1}), (1464 cm^{-1}), (1385 cm^{-1}), (1234 cm^{-1}) and (1056 cm^{-1}) assigned to $\nu(\text{C=N})$, $\nu(\text{C=C})$, $\nu(\text{N=N})$, $\nu(\text{C-N})$ and $\nu(\text{N-N})$ stretching respectively. The bands were shifting to the lower frequency compared with the values which that appeared in the free ligand, can be attributed to the delocalization of the electronic density in the π system ($\text{HOMO} \rightarrow \text{LUMO}$) indicating to the donor atoms were coordinate with metal ion. While the bands exhibit at (781 cm^{-1}), (724 cm^{-1}) and (650 cm^{-1}) assigned to $\nu(\text{C-S-C})$ sym. and asym. stretching, and $\nu(\text{C-S})$ stretching of thiadiazole ring and dithiol groups respectively, these values appeared higher shifting compared with the base value of these bands in the free ligand, that is mean coordinate obtained between metal ion with thiol groups^(55, 56).

**Fig.(3-28) FT-IR spectrum of $[\text{Pd}_2(\text{L}^2)\text{Cl}_2]\text{Cl}_2$ complex**

(3.7.2.5) FT-IR spectrum of $[\text{Pt}_2(\text{L}^2)(\text{H}_2\text{O})_2\text{Cl}_4]\text{Cl}_4$:

The FT-IR spectrum of $[\text{Pt}_2(\text{L}^2)(\text{H}_2\text{O})_2\text{Cl}_4]\text{Cl}_4$ complex **Fig.(3-29)** appeared broad band at (3508 cm^{-1}) attributed to $\nu(\text{O-H})$ stretching of water molecules, it assigned to existence of (H_2O) molecules in the complex. The bands at (3138 cm^{-1}) , (2955 cm^{-1}) , (2924 cm^{-1}) and (2858 cm^{-1}) assigned to $\nu(\text{C-H})$ stretching of aromatic, $\nu(\text{C-H})$ sym. and asym. stretching of aliphatic respectively. The bands appeared at (1546 cm^{-1}) , (1463 cm^{-1}) , (1374 cm^{-1}) , (1230 cm^{-1}) and (1051 cm^{-1}) due to of $\nu(\text{C=N})$, $\nu(\text{C=C})$, $\nu(\text{N=N})$, $\nu(\text{C-N})$ and $\nu(\text{N-N})$ stretching respectively The bands were shifting to the lower frequency compared with the values which that appeared in the free ligand, can be attributed to the delocalization of the electronic density in the π system (HOMO \rightarrow LUMO) indicating to the donor atoms were coordinate with metal ion. While the bands appeared at (782 cm^{-1}) , (736 cm^{-1}) and (667 cm^{-1}) assigned to $\nu(\text{C-S-C})$ sym. and asym. stretching, $\nu(\text{C-S})$ stretching of thiadiazole ring and dithiol groups respectively, these values appeared higher shifting compared with the base value of these bands in free ligand, that is mean coordinate was obtained between metal ion with thiol groups^(55, 56).

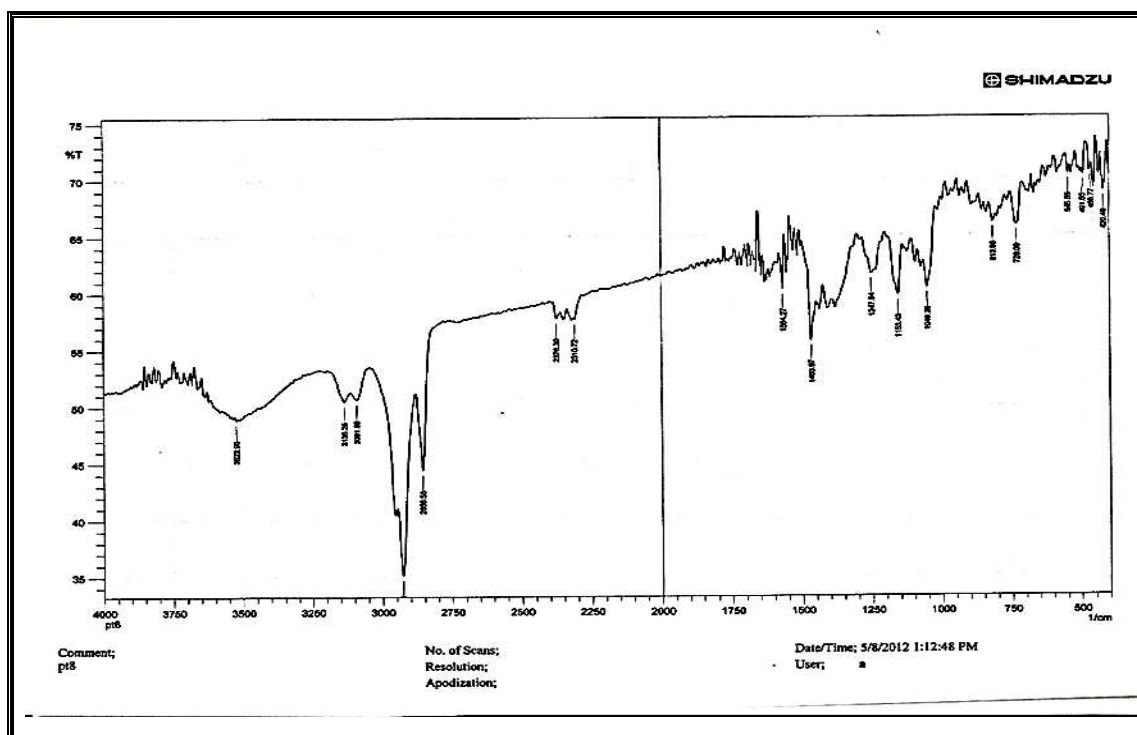


Fig.(3-29) FT-IR spectrum of $[\text{Pt}_2(\text{L}^2)(\text{H}_2\text{O})_2\text{Cl}_4]\text{Cl}_4$ complex

Table.(3-9) FT-IR of (L^2) ligand and its Co(II), Ni(II), Cu(II), Pd(II) and Pt(IV) complexes

Compound	$\nu(\text{O-H})$	$\nu(\text{C-H})$ aromatic	$\nu(\text{C-H})$ aliphatic	$\nu(\text{C=N})$	$\nu(\text{C=C})$	$\nu(\text{N=N})$	$\nu(\text{C-N})$	$\nu(\text{N-N})$	$\nu(\text{C-S-C})$	$\nu(\text{C-S})$
L^2	–	3128s 3116s	2958s 2922s 2850s	1548m	1465m	1386m	1238m	1058s	781w 723m	646w
$[\text{Co}_2(L^2)\text{Cl}_2]\text{Cl}_2$	–	3132s	2956s 2922s 2852s	1546m	1465m	1377m	1224w	1047m	781w 732m	669w
$[\text{Ni}_2(L^2)(\text{H}_2\text{O})_4\text{Cl}_2]\text{Cl}_2$	3381br	3131s	2956s 2921s 2854s	1548m	1465m	1381m	1226w	1056m	781w 724m	669w
$[\text{Cu}_2(L^2)(\text{H}_2\text{O})_6]\text{Cl}_4$	3444br	3130s	2956s 2924s 2854s	1546m	1456m	1384m	1226w	1049m	782w 732m	669w
$[\text{Pd}_2(L^2)\text{Cl}_2]\text{Cl}_2$	–	3128s	2956s 2923s 2850s	1548m	1464m	1385m	1234w	1056m	781w 724m	650w
$[\text{Pt}_2(L^2)(\text{H}_2\text{O})_2\text{Cl}_4]\text{Cl}_4$	3508br	3138s	2955s 2924s 2858s	1546m	1463m	1374m	1230w	1051m	782w 736m	667w

br = broad, s = strong, m = medium, w = weak

(3.7.3) FT-IR spectra of [L³] metal complexes:**(3.7.3.1) FT-IR spectrum of [Co₂(L³)Cl₂]Cl₂:**

The FT-IR spectrum of [Co₂(L³)Cl₂]Cl₂ **Fig(3-30)** appeared the bands at (3140 cm⁻¹), (2956 cm⁻¹), (2918 cm⁻¹) and (2854 cm⁻¹) assigned to $\nu(\text{C-H})$ stretching of aromatic, $\nu(\text{C-H})$ sym. and asym. stretching of aliphatic respectively. The bands appeared at (1545 cm⁻¹), (1465 cm⁻¹), (1381 cm⁻¹), (1228 cm⁻¹) and (1056 cm⁻¹) attributed to $\nu(\text{C=N})$, $\nu(\text{C=C})$, $\nu(\text{N=N})$, $\nu(\text{C-N})$ and $\nu(\text{N-N})$ stretching respectively. The bands were shifting to the lower frequency compared with the values which that appeared in the free ligand, can be attributed to the delocalization of the electronic density in the π system (HOMO→LUMO) indicating to the donor atoms were coordinate with metal ion[where HOMO= Highest Occupied Molecular Orbital; LUMO= Lowest Unoccupied Molecular Orbital]. While the bands appeared at (779 cm⁻¹), (732 cm⁻¹) and (667 cm⁻¹) assigned to $\nu(\text{C-S-C})$ sym. and asym. stretching, $\nu(\text{C-S})$ stretching of thiadiazole ring and dithiol groups respectively, these values shown higher shifting compared with base values of these bands in free ligand before chelating , that is referred the coordinate obtained between metal ion with thiol groups^(55, 56).

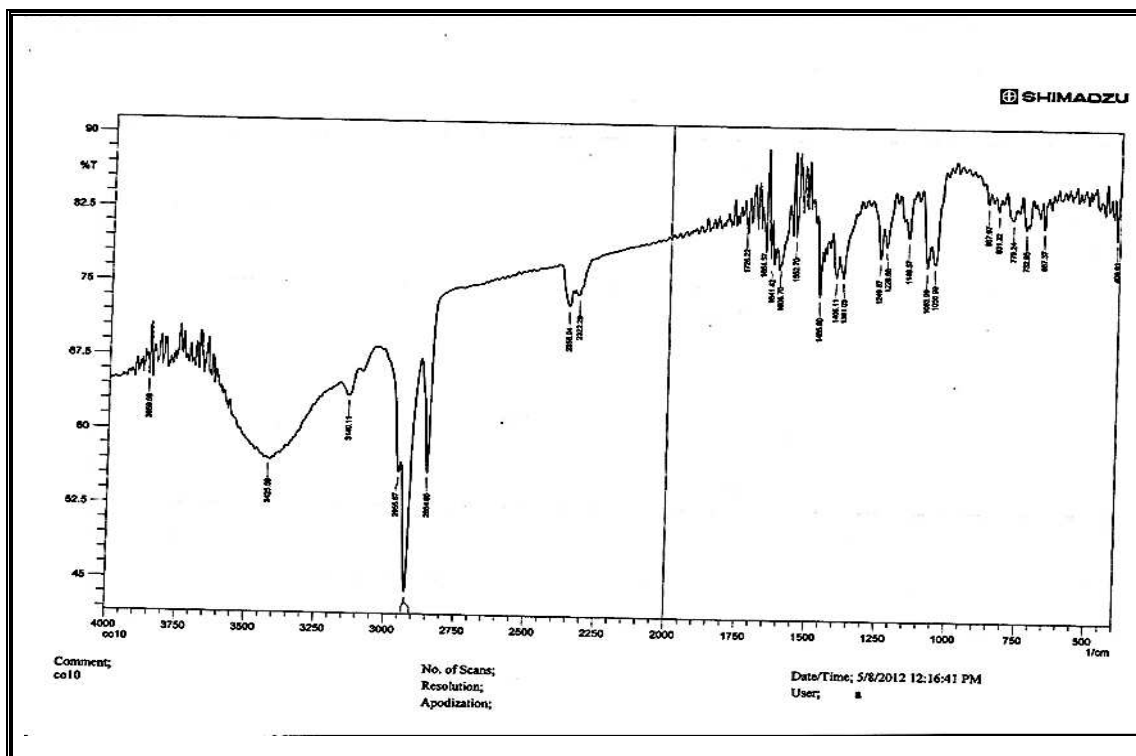


Fig.(3-30) FT-IR spectrum of $[\text{Co}_2(\text{L}^3)\text{Cl}_2]\text{Cl}_2$ complex

(3.7.3.2) FT-IR spectrum of $[\text{Ni}_2(\text{L}^3)(\text{H}_2\text{O})_4\text{Cl}_2]\text{Cl}_2$:

The FT-IR spectrum of $[\text{Ni}_2(\text{L}^3)(\text{H}_2\text{O})_4\text{Cl}_2]\text{Cl}_2$ complex **Fig.(3-31)** appeared a broad band at (3406 cm^{-1}) assigned to $\nu(\text{O-H})$ stretching of water molecules. While the bands exhibit at (3130 cm^{-1}) , (2956 cm^{-1}) , (2922 cm^{-1}) and (2852 cm^{-1}) assigned to $\nu(\text{C-H})$ stretching of aromatic, $\nu(\text{C-H})$ sym. and asym. stretching of aliphatic respectively. The bands at (1547 cm^{-1}) , (1467 cm^{-1}) , (1381 cm^{-1}) , (1230 cm^{-1}) and (1056 cm^{-1}) attributed to $\nu(\text{C=N})$, $\nu(\text{C=C})$, $\nu(\text{N=N})$, $\nu(\text{C-N})$ and $\nu(\text{N-N})$ stretching respectively. The bands were shifting to the lower frequency compared with the values which that appeared in the free ligand, can be attributed to the delocalization of the electronic density in the π system (HOMO \rightarrow LUMO) indicating to the donor atoms were coordinate with metal ion. The bands at (784 cm^{-1}) , (721 cm^{-1}) and (667 cm^{-1}) assigned to $\nu(\text{C-S-C})$ sym. and asym. stretching, $\nu(\text{C-S})$ stretching of thiadiazole ring

and dithiol groups respectively, these values appeared higher shifting compared with the base value of these bands in free ligand before chelating, that is mean coordinate obtained between metal ion with thiol groups^(55, 56).

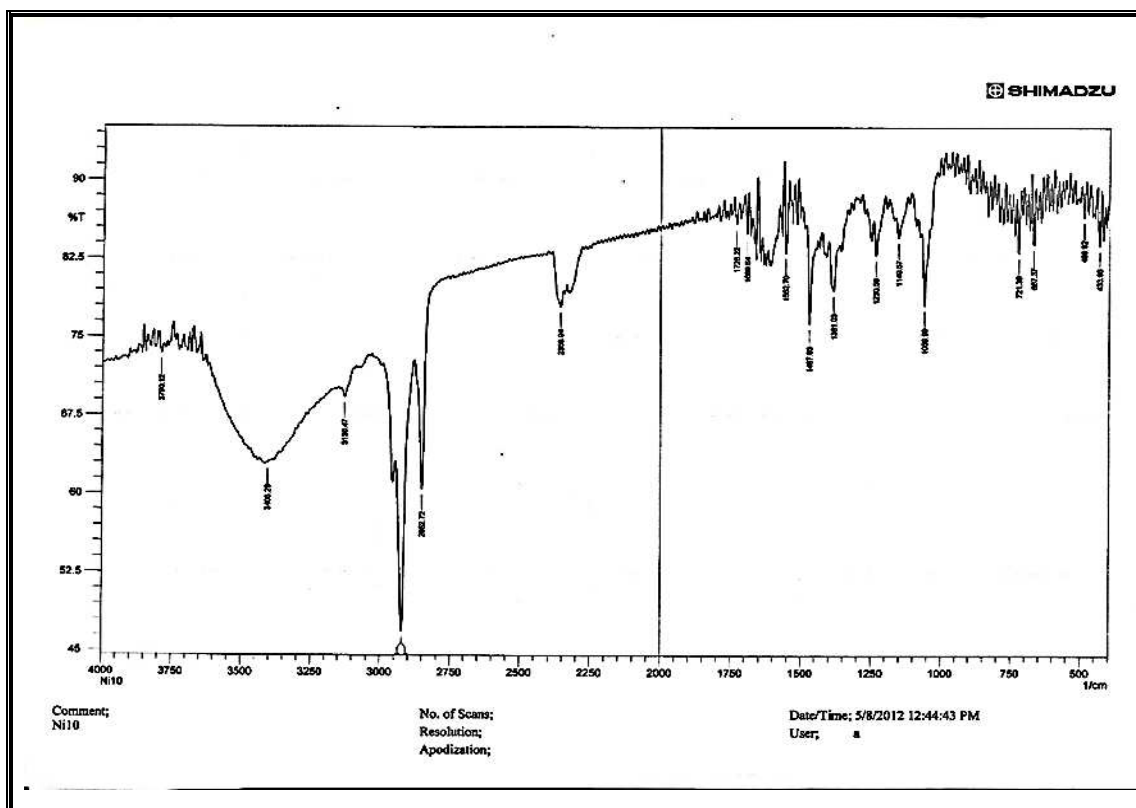


Fig.(3-31) FT-IR spectrum of $[\text{Ni}_2(\text{L}^3)(\text{H}_2\text{O})_4\text{Cl}_2]\text{Cl}_2$ complex

(3.7.3.3) FT-IR spectrum of $[\text{Cu}_2(\text{L}^3)(\text{H}_2\text{O})_6]\text{Cl}_4$:

The FT-IR spectrum of $[\text{Cu}_2(\text{L}_3)(\text{H}_2\text{O})_6]\text{Cl}_4$ **Fig.(3-32)** appeared a broad band at (3533 cm^{-1}) assigned to $\nu(\text{O-H})$ stretching of water molecules, this band assigned to existence of (H_2O) in complex of copper ion. While the bands appeared at (3101 cm^{-1}) , (2952 cm^{-1}) , (2922 cm^{-1}) and (2850 cm^{-1}) assigned to $\nu(\text{C-H})$ stretching of aromatic, $\nu(\text{C-H})$ sym. and asym. stretching of aliphatic respectively. The bands at (1541 cm^{-1}) , (1456 cm^{-1}) , (1361 cm^{-1}) , (1238 cm^{-1}) and (1051 cm^{-1}) attributed to $\nu(\text{C=N})$, $\nu(\text{C=C})$, $\nu(\text{N=N})$, $\nu(\text{C-N})$ and $\nu(\text{N-N})$ stretching respectively.

The bands were shifting to the lower frequency compared with the values which that appeared in the free ligand, can be attributed to the delocalization of the electronic density in the π system (HOMO \rightarrow LUMO) indicating to the donor atoms were coordinate with metal ion. While the bands appeared at (780 cm^{-1}), (723 cm^{-1}) and (667 cm^{-1}) due to $\nu(\text{C-S-C})$ asym. and sym. stretching, $\nu(\text{C-S})$ stretching of thiadiazole ring and dithiol groups respectively, these values shown higher shifting compared with the base value of these bands in free ligand before chelating, that is mean coordinate obtained between metal ion with thiol groups^(55, 56).

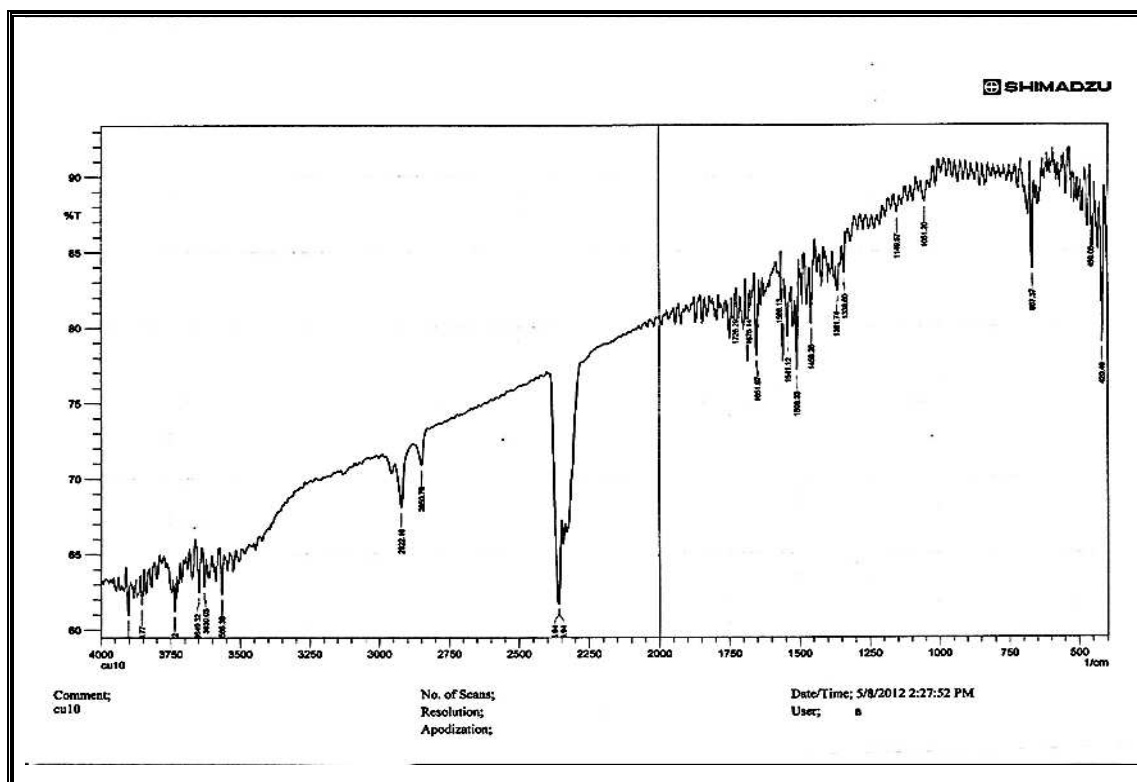
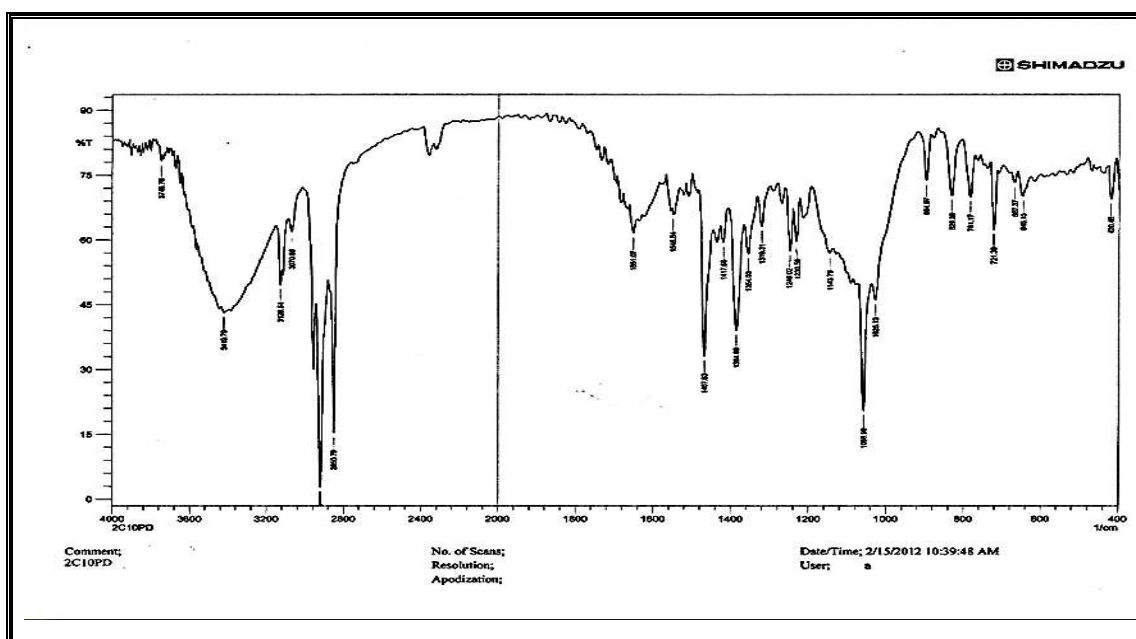


Fig.(3-32) FT-IR spectrum of $[\text{Cu}_2(\text{L}^3)(\text{H}_2\text{O})_6]\text{Cl}_4$ complex

(3.7.3.4) FT-IR spectrum of $[\text{Pd}_2(\text{L}^3)\text{Cl}_2]\text{Cl}_2$:

The FT-IR spectrum of $[\text{Pd}_2(\text{L}^3)\text{Cl}_2]\text{Cl}_2$ complex **Fig.(3-33)** appeared the bands at (3128 cm^{-1}), (2957 cm^{-1}), (2922 cm^{-1}) and (2850 cm^{-1}) assigned to $\nu(\text{C-H})$ stretching of aromatic, $\nu(\text{C-H})$ sym. and asym. stretching of aliphatic respectively. The bands at (1546 cm^{-1}), (1463 cm^{-1}), (1384 cm^{-1}), (1242 cm^{-1}) and (1055 cm^{-1}) attributed to $\nu(\text{C=N})$, $\nu(\text{C=C})$, $\nu(\text{N=N})$, $\nu(\text{C-N})$ and $\nu(\text{N-N})$ stretching respectively. The bands were shifting to the lower frequency compared with the values which that appeared in the free ligand, can be attributed to the delocalization of the electronic density in the π system ($\text{HOMO} \rightarrow \text{LUMO}$) indicating to the donor atoms were coordinate with metal ion. While the bands appeared at (783 cm^{-1}), (724 cm^{-1}) and (667 cm^{-1}) attributed to $\nu(\text{C-S-C})$ sym. and asym. stretching, $\nu(\text{C-S})$ stretching of thiadiazole ring and dithiol groups respectively, these values shown higher shifting compared with the base value of these bands in free ligand, that is mean coordinate obtained between metal ion with thiol groups^(55, 56).

**Fig.(3-33) FT-IR spectrum of $[\text{Pd}_2(\text{L}^3)\text{Cl}_2]\text{Cl}_2$ complex**

(3.7.3.5) FT-IR spectrum of $[\text{Pt}_2(\text{L}^3)(\text{H}_2\text{O})_2\text{Cl}_4]\text{Cl}_4$:

The FT-IR spectrum of $[\text{Pt}_2(\text{L}^3)(\text{H}_2\text{O})_2\text{Cl}_4]\text{Cl}_4$ complex **Fig.(3-34)** appeared a broad band at (3510 cm^{-1}) assigned to $\nu(\text{O-H})$ stretching of water molecules, it assigned to existence of (H_2O) in complex of platinum ion. The bands appeared at (3138 cm^{-1}) , (2954 cm^{-1}) , (2921 cm^{-1}) and (2856 cm^{-1}) assigned to $\nu(\text{C-H})$ stretching of aromatic, $\nu(\text{C-H})$ sym. and asym. stretching of aliphatic respectively. While the bands at (1546 cm^{-1}) , (1463 cm^{-1}) , (1377 cm^{-1}) , (1237 cm^{-1}) and (1049 cm^{-1}) assigned to $\nu(\text{C=N})$, $\nu(\text{C=C})$, $\nu(\text{N=N})$, $\nu(\text{C-N})$ and $\nu(\text{N-N})$ stretching respectively. The bands were shifting to the lower frequency compared with the values which that appeared in the free ligand, can be attributed to the delocalization of the electronic density in the π system (HOMO→LUMO) indicating to the donor atoms were coordinate with metal ion. While the bands at (782cm^{-1}) , (731cm^{-1}) and (667cm^{-1}) attributed to sym. and asym. stretching of $\nu(\text{C-S-C})$,and $\nu(\text{C-S})$ in thiadiazole ring and dithiol groups respectively, these values shown shifting (about 1 to 19 cm^{-1}) compared with base values of these bands in free ligand, that is mean coordinate obtained between metal ion with thiol groups^(55, 56).

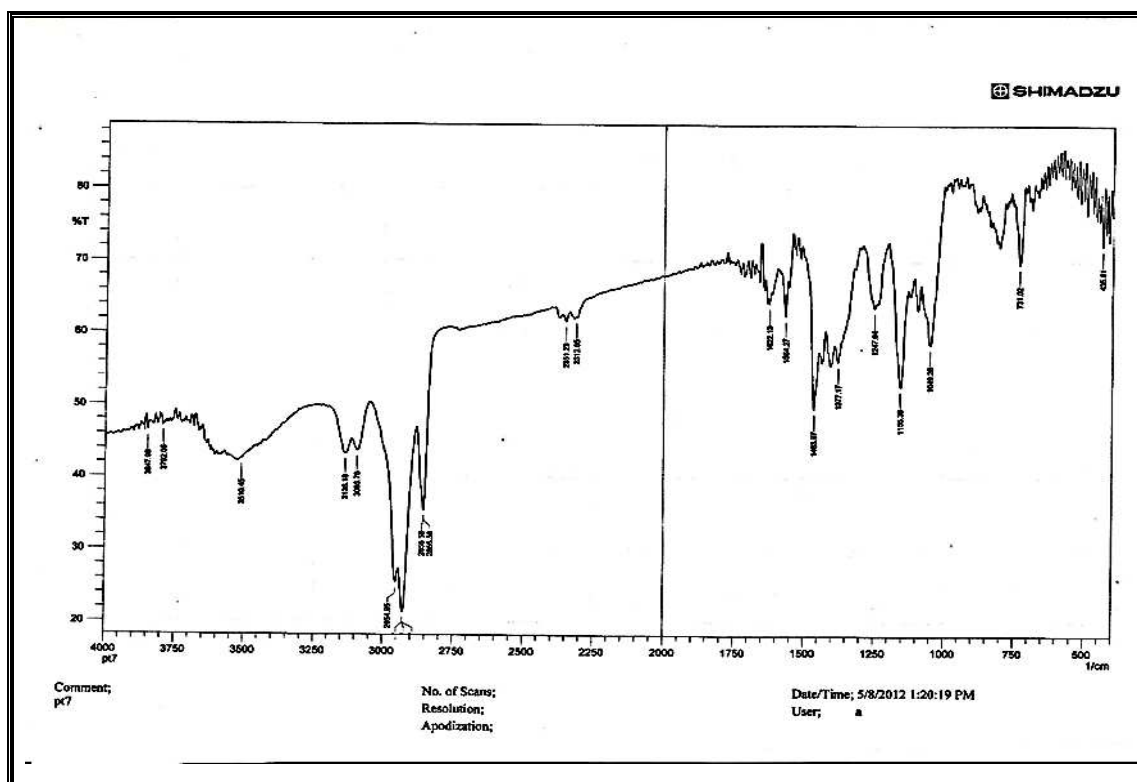


Fig.(3-34) FT-IR spectrum of $[\text{Pt}_2(\text{L}^3)(\text{H}_2\text{O})_2\text{Cl}_4]\text{Cl}_4$ complex

Table.(3-10) FT-IR spectrum of [L³] and its Co(II), Ni(II), Cu(II), Pd(II) and Pt(IV) complexes

Compound	v(O-H)	v(C-H) aromatic	v(C-H) aliphatic	v(C=N)	v(C=C)	v(N=N)	v(C-N)	v(N-N)	v(C-S-C)	v(C-S)
L ³	–	3128s 3115s	2958s 2901s 2850s	1548m	1467m	1386m	1246m	1056s	781w 721m	648w
[Co ₂ (L ³)Cl ₂]Cl ₂	–	3140s	2956s 2918s 2854s	1545m	1465m	1381m	1228w	1056m	779w 732m	667w
[Ni ₂ (L ³)(H ₂ O) ₄ Cl ₂]Cl ₂	3406br	3130s	2956s 2922s 2852s	1547m	1467m	1381m	1230w	1056m	784w 721m	667w
[Cu ₂ (L ³)(H ₂ O) ₆]Cl ₄	3533br	3101s	2952s 2922s 2850s	1541m	1456m	1361m	1238w	1051m	780w 723m	667w
[Pd ₂ (L ³)Cl ₂]Cl ₂	–	3128s	2957s 2922s 2850s	1546m	1463m	1384m	1242w	1055m	783w 724m	667w
[Pt ₂ (L ³)(H ₂ O) ₂ Cl ₄]Cl ₄	3510br	3138s	2954s 2921s 2856s	1546m	1463m	1377m	1237w	1049m	782w 731m	667w

br = broad, s = strong, m = medium, w = weak

(3.8) UV-Vis spectral data of synthesized complexes:**(3.8.1) UV-Vis spectral data of [L¹] complexes:****(3.8.1.1) UV-Vis spectrum of [Co₂(L¹)Cl₂]Cl₂ complex:**

The electronic spectra of the complex [Co₂(L¹)Cl₂]Cl₂ **Fig.(3-35)** exhibits four absorption peaks, a broad peak at (306 nm) (32679 cm⁻¹) (ϵ_{\max} = 3990 molar⁻¹cm⁻¹) assigned to ligand field and charge transfer, the other three peaks at (572 nm) (17482 cm⁻¹) (ϵ_{\max} = 1008 molar⁻¹cm⁻¹), (610 nm) (16393 cm⁻¹) (ϵ_{\max} = 1112 molar⁻¹cm⁻¹) and (637 nm) (15698 cm⁻¹) (ϵ_{\max} = 1130molar⁻¹cm⁻¹) which are assigned d-d transitions type (⁴A₂→⁴T₂), (⁴A₂→⁴T₁^(F)) and (⁴A₂→⁴T₁^(P)), respectively indicating a tetrahedral structure about Co²⁺. This result is in agreement with that reported previously about the electronic spectra of four coordinate (tetrahedral) cobalt(II) complexes^(58, 59, 60).

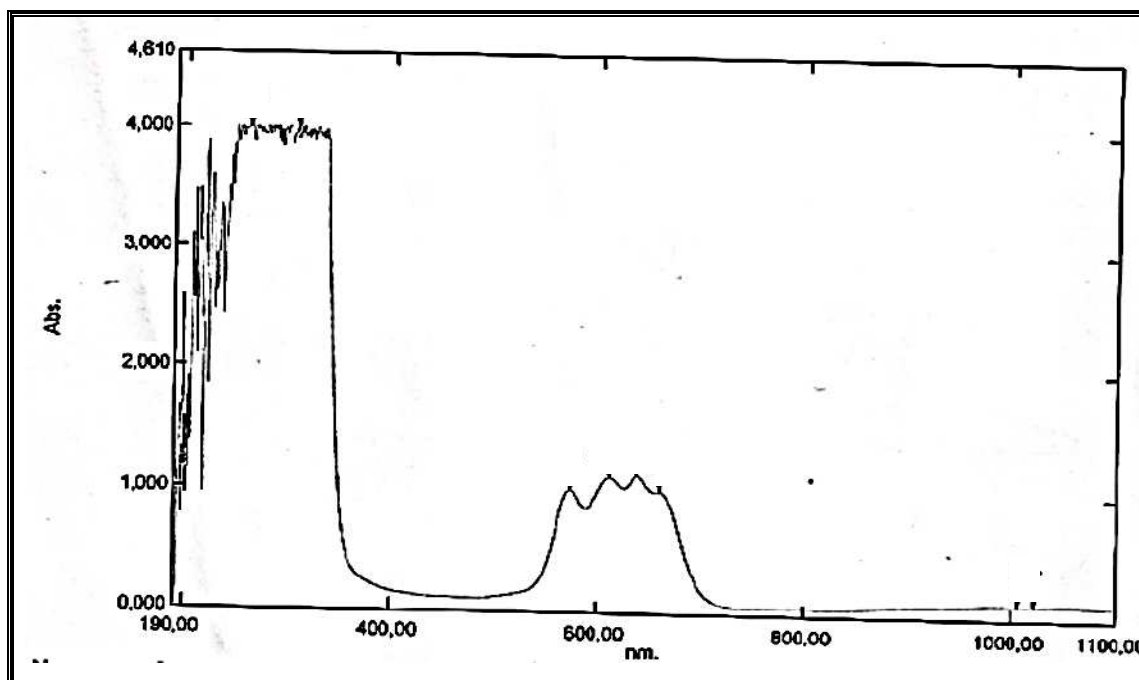
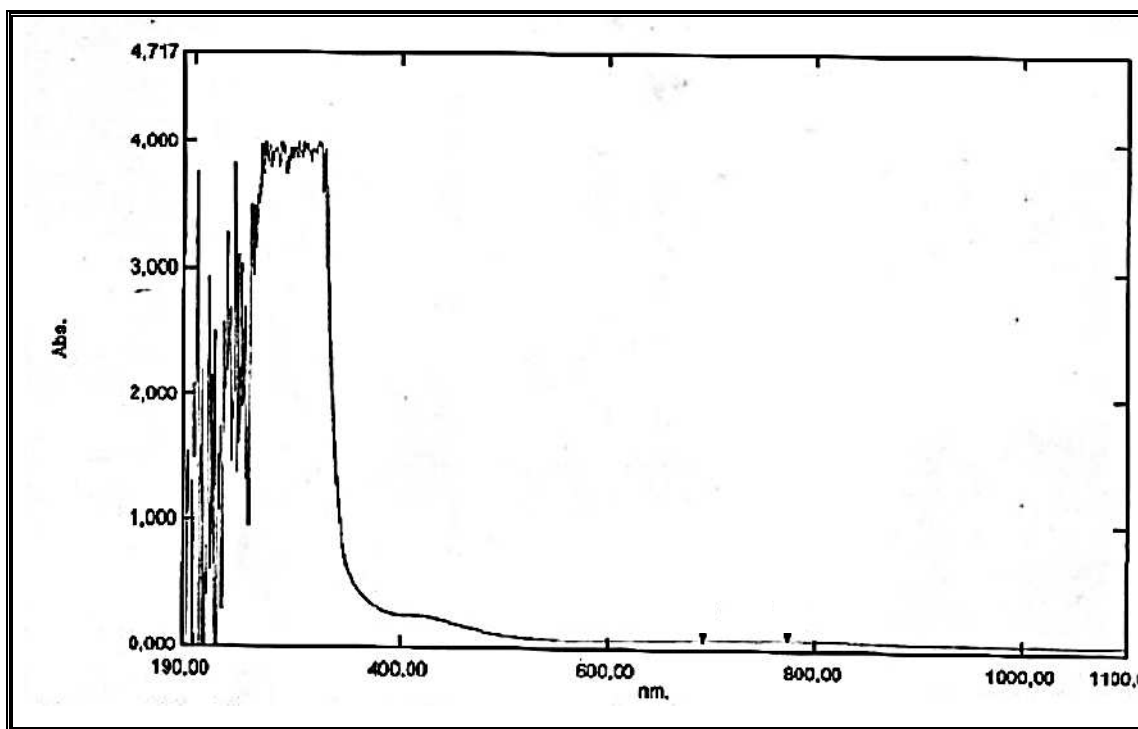


Fig.(3-35) UV-Vis spectrum of [Co₂(L¹)Cl₂]Cl₂complex

(3.8.1.2) UV-Vis spectrum of $[\text{Ni}_2(\text{L}^1)(\text{H}_2\text{O})_4\text{Cl}_2]\text{Cl}_2$ complex:

The electronic spectrum of the complex $[\text{Ni}_2(\text{L}^1)(\text{H}_2\text{O})_4\text{Cl}_2]\text{Cl}_2$ **Fig.(3-36)** exhibits a broad absorption peak at (285 nm) (35087 cm^{-1}) ($\epsilon_{\text{max}} = 3858 \text{ molar}^{-1}\text{cm}^{-1}$), which assigned to ligand field and charge transfer. The peaks appeared at (455 nm) (21978 cm^{-1}) ($\epsilon_{\text{max}} = 258 \text{ molar}^{-1}\text{cm}^{-1}$), (624 nm) (16025 cm^{-1}) ($\epsilon_{\text{max}} = 53 \text{ molar}^{-1}\text{cm}^{-1}$) and (693 nm) (14430 cm^{-1}) ($\epsilon_{\text{max}} = 63 \text{ molar}^{-1}\text{cm}^{-1}$) which are assigned to the d-d transitions type (${}^3\text{A}_{2g} \rightarrow {}^3\text{T}_{2g}$), (${}^3\text{A}_{2g} \rightarrow {}^3\text{T}_{1g}(\text{F})$) and (${}^3\text{A}_{2g} \rightarrow {}^3\text{T}_{1g}(\text{P})$), respectively indicating a distorted octahedral structure about Ni^{2+} . This result is in agreement with that reported previously about the electronic spectra of six coordinate (octahedral) nickel(II) complexes^(59, 61, 62).

**Fig.(3-36) UV-Vis spectrum of $[\text{Ni}_2(\text{L}^1)(\text{H}_2\text{O})_4\text{Cl}_2]\text{Cl}_2$ complex**

(3.8.1.3) UV-Vis spectrum of $[\text{Cu}_2(\text{L}^1)(\text{H}_2\text{O})_6]\text{Cl}_4$ complex:

The electronic spectrum of the complex $[\text{Cu}_2(\text{L}^1)(\text{H}_2\text{O})_6]\text{Cl}_4$ **Fig.(3-37)** exhibits abroad absorption peak at (264 nm) (37878 cm^{-1}) ($\epsilon_{\text{max}} = 3757 \text{ molar}^{-1}\text{cm}^{-1}$) assigned to the ligand field and charge transfer. The absorption peaks appeared at (541 nm) (18484 cm^{-1}) ($\epsilon_{\text{max}} = 53 \text{ molar}^{-1}\text{cm}^{-1}$) (610 nm) (16393 cm^{-1}) ($\epsilon_{\text{max}} = 145 \text{ molar}^{-1}\text{cm}^{-1}$) and (735 nm) (13605 cm^{-1}) ($\epsilon_{\text{max}} = 291 \text{ molar}^{-1}\text{cm}^{-1}$), which are attributed to the d-d transitions type (${}^2\text{B}_{1g} \rightarrow {}^2\text{A}_{1g}$), (${}^2\text{B}_{1g} \rightarrow {}^1\text{B}_{2g}$) and (${}^2\text{B}_{1g} \rightarrow {}^2\text{E}_g$) respectively indicating a distorted octahedral structure about Cu^{2+} . This result is in agreement with that reported previously about the electronic spectra of six coordinate (octahedral) copper(II) complexes^(18, 63).

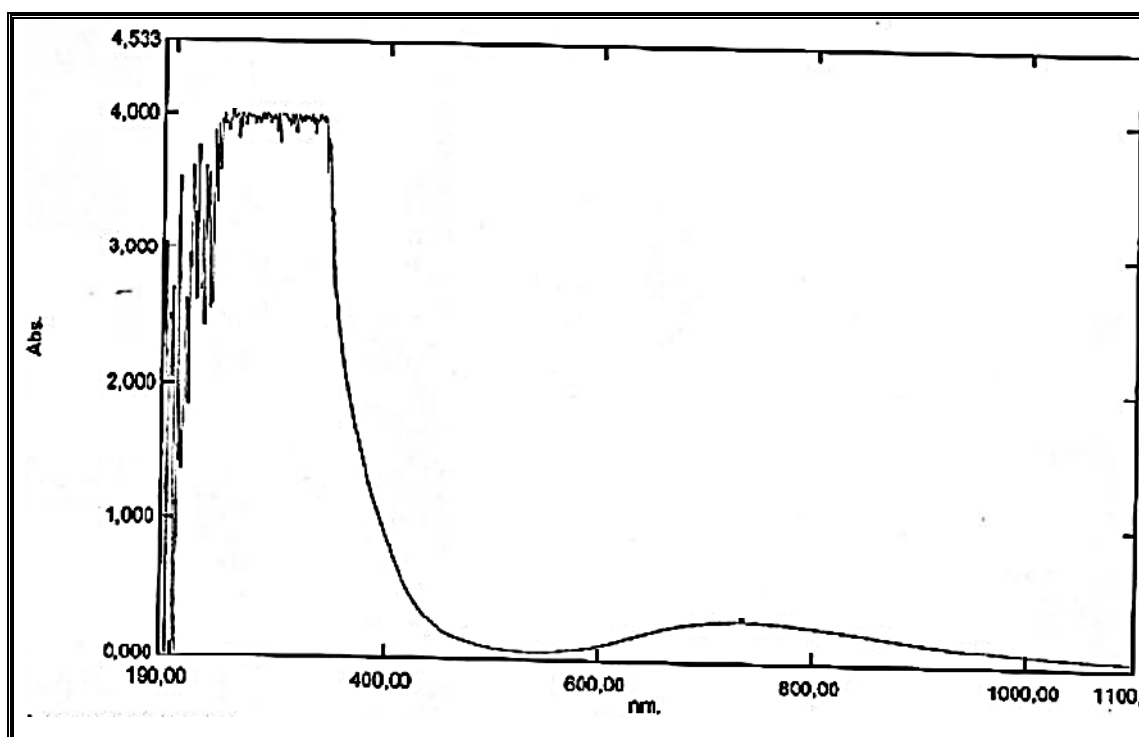


Fig.(3-37) UV-Vis spectrum of $[\text{Cu}_2(\text{L}^1)(\text{H}_2\text{O})_6]\text{Cl}_4$ complex

(3.8.1.4) UV-Vis spectrum of $[\text{Pd}_2(\text{L}^1)\text{Cl}_2]\text{Cl}_2$ complex:

The electronic spectrum of the complex $[\text{Pd}_2(\text{L}^1)\text{Cl}_2]\text{Cl}_2$ **Fig.(3-38)** exhibits abroad absorption peak at (334 nm) (29940 cm^{-1}) ($\epsilon_{\text{max}} = 3257 \text{ molar}^{-1}\text{cm}^{-1}$) assigned to the ligand field and charge transfer. The absorption peak at (590 nm) (16949 cm^{-1}) ($\epsilon_{\text{max}} = 615 \text{ molar}^{-1}\text{cm}^{-1}$) assigned to d-d transition type ($\text{B}_{1g} \rightarrow \text{B}_{2g}$), this result is agreement with that reported previously about the electronic spectra of four coordinate (square planar) palladium(II) complexes⁽⁶⁴⁾.

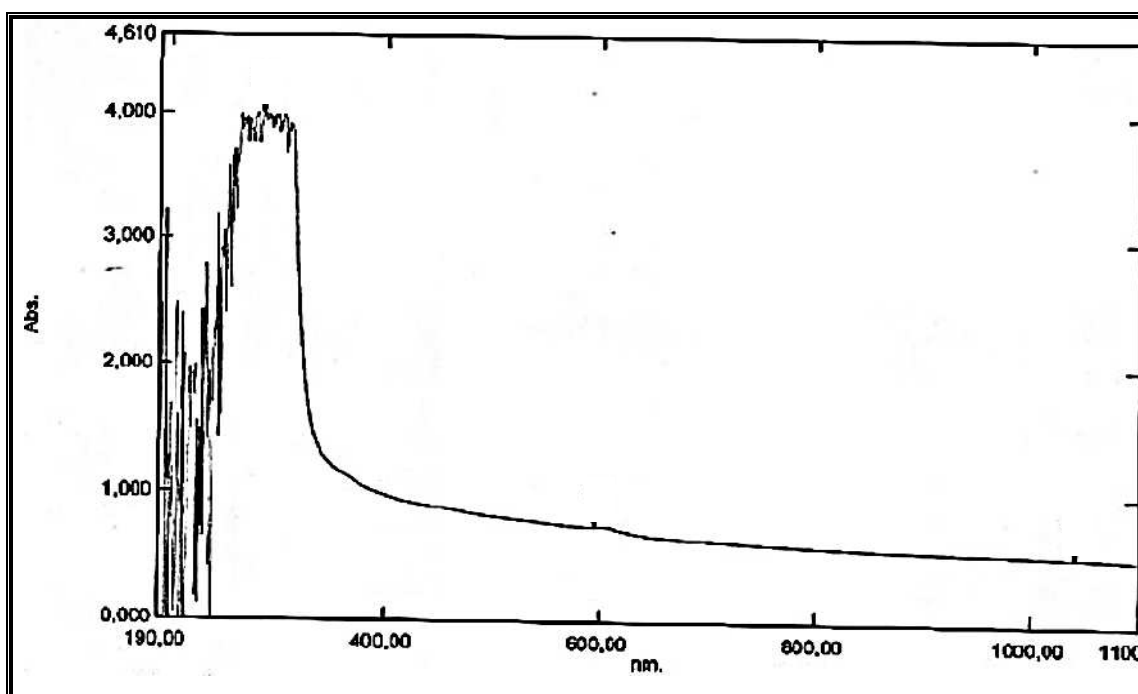


Fig.(3-38) UV-Vis spectrum of $[\text{Pd}_2(\text{L}^1)\text{Cl}_2]\text{Cl}_2$ complex

(3.8.1.5) UV-Vis spectrum of $[\text{Pt}_2(\text{L}^1)(\text{H}_2\text{O})_2\text{Cl}_4]\text{Cl}_4$ complex:

The electronic spectrum of the complex $[\text{Pt}_2(\text{L}^1)(\text{H}_2\text{O})_2\text{Cl}_4]\text{Cl}_4$ **Fig.(3-39)** exhibits three absorption peaks, a broad peak at (218 nm) (45871 cm^{-1}) ($\epsilon_{\text{max}} = 3257 \text{ molar}^{-1}\text{cm}^{-1}$) assigned to the ligand field and charge transfer, the peaks at (455 nm) (21978 cm^{-1}) ($\epsilon_{\text{max}} = 158 \text{ molar}^{-1}\text{cm}^{-1}$) and (580 nm) (17241 cm^{-1}) ($\epsilon_{\text{max}} = 218 \text{ molar}^{-1}\text{cm}^{-1}$) assigned to d-d transitions type (${}^1\text{B}_{2g} \rightarrow {}^1\text{A}_{1g}$) and (${}^1\text{B}_{2g} \rightarrow {}^1\text{B}_{1g}$) respectively, indicated to distorted octahedral structure about Pt^{4+} complex. This result is agreement with that reported previously about the electronic spectra of six coordinate (octahedral) platinum(IV) complexes⁽⁶⁵⁾.

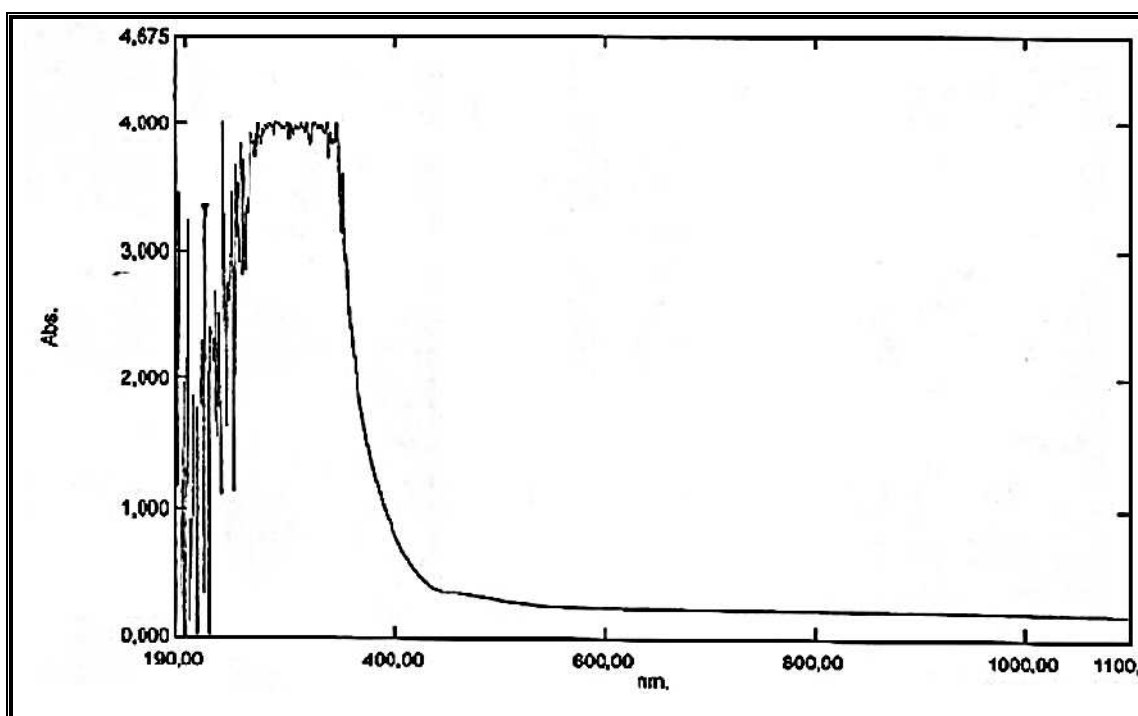


Fig.(3-39) UV-Vis spectrum of $[\text{Pt}_2(\text{L}^1)(\text{H}_2\text{O})_2\text{Cl}_4]\text{Cl}_4$ complex

Table (3-11) summarized the electronic spectral data of $[\text{L}^1]$ and its Co(II), Ni(II), Cu(II), Pd(II) and (Pt(IV) complexes:

Table (3-11) Electronic spectral data of [L¹] and its metal complexes

Compound	λ_{nm}	$\nu_{cm^{-1}}$	ϵ_{max} molar ⁻¹ cm ⁻¹	Assignment
[L ¹]	239	41841	3660	$\pi \rightarrow \pi^*$
	295	38610		$n \rightarrow \pi^*$
[Co ₂ (L ¹)Cl ₂]Cl ₂	306	32679	3990	ligand field
	572	17482	1008	$^4A_2 \rightarrow ^4T_2$
	610	16393	1112	$^4A_2 \rightarrow ^4T_1^{(F)}$
	637	15698	1130	$^4A_2 \rightarrow ^4T_1^{(P)}$
[Ni ₂ (L ¹)(H ₂ O) ₄ Cl ₂]Cl ₂	285	35087	3858	ligand field
	455	21978	258	$^3A_{2g} \rightarrow ^3T_{2g}$
	624	16025	53	$^3A_{2g} \rightarrow ^3T_{1g}^{(F)}$
	693	14430	63	$^3A_{2g} \rightarrow ^3T_{1g}^{(P)}$
[Cu ₂ (L ¹)(H ₂ O) ₆]Cl ₄	264	37878	3757	Ligand field
	541	18484	53	$^2B_{1g} \rightarrow ^2A_{1g}$
	610	16939	145	$^2B_{1g} \rightarrow ^1B_{2g}$
	735	13605	291	$^2B_{1g} \rightarrow ^2E_g$
[Pd ₂ (L ¹)Cl ₂]Cl ₂	334	29940	3257	Ligand field
	590	16949	615	$B_{1g} \rightarrow B_{2g}$
[Pt ₂ (L ¹)(H ₂ O) ₂ Cl ₄]Cl ₄	218	45871	3257	ligand field
	455	21978	158	$^1B_{2g} \rightarrow ^1A_{1g}$
	580	17241	218	$^1B_{2g} \rightarrow ^1B_{1g}$

(3.8.2) UV-Vis spectral data of [L²] complexes:

(3.8.2.1) UV-Vis spectrum of [Co₂(L²)Cl₂]Cl₂ complex:

The electronic spectrum of the complex [Co₂(L²)Cl₂]Cl₂ **Fig.(3-40)** exhibits four absorption peaks, a broad peak at (308 nm) (32467 cm⁻¹) ($\epsilon_{\text{max}} = 3982 \text{ molar}^{-1}\text{cm}^{-1}$) assigned to ligand field and charge transfer. While the peaks at (572 nm) (17482 cm⁻¹) ($\epsilon_{\text{max}} = 741 \text{ molar}^{-1}\text{cm}^{-1}$), (610 nm) (16393 cm⁻¹) ($\epsilon_{\text{max}} = 812 \text{ molar}^{-1}\text{cm}^{-1}$) and (637 nm) (15698 cm⁻¹) ($\epsilon_{\text{max}} = 829 \text{ molar}^{-1}\text{cm}^{-1}$) which are assigned to d-d transitions type (${}^4A_2 \rightarrow {}^4T_2$), (${}^4A_2 \rightarrow {}^4T_1^{(F)}$) and (${}^4A_2 \rightarrow {}^4T_1^{(P)}$) respectively, indicated to tetrahedral structure about Co²⁺ complex. This result is in agreement with that reported previously about the electronic spectra of four coordinate (tetrahedral) cobalt(II) complexes^(58, 59, 60).

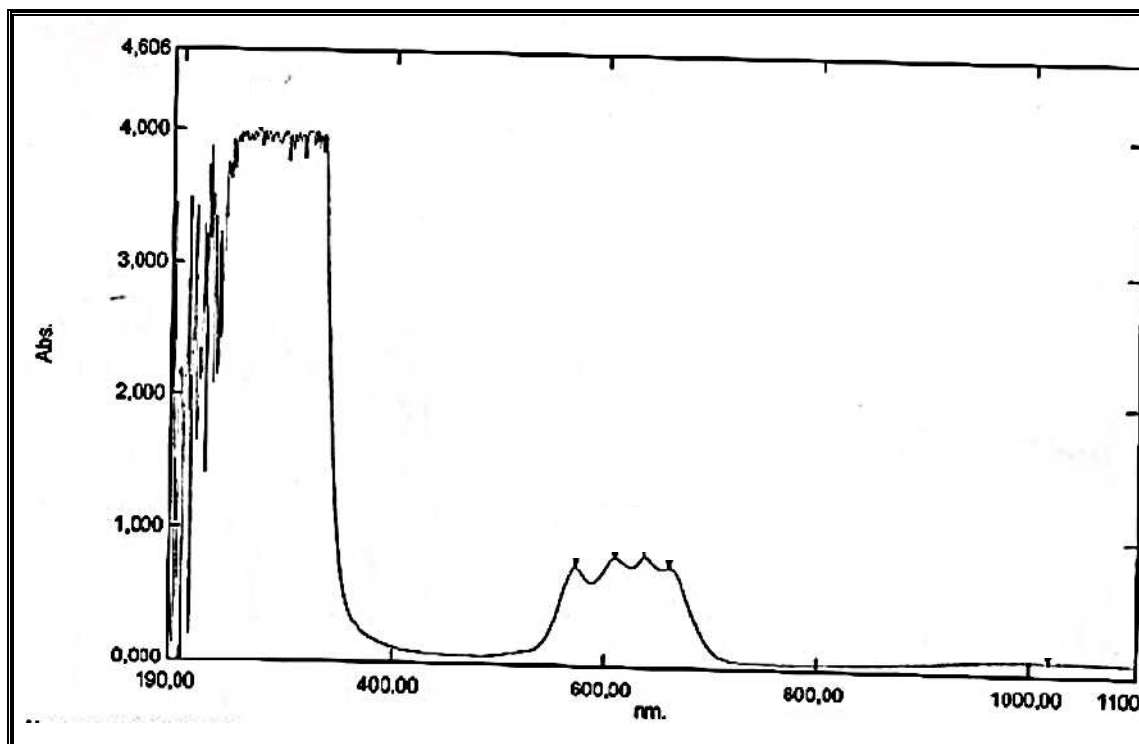


Fig.(3-40) UV-Vis spectrum of [Co₂(L²)Cl₂]Cl₂ complex

(3.8.2.2) UV-Vis spectrum of $[\text{Ni}_2(\text{L}^2)(\text{H}_2\text{O})_4\text{Cl}_2]\text{Cl}_2$ complex:

The electronic spectrum of the complex $[\text{Ni}_2(\text{L}^2)(\text{H}_2\text{O})_4\text{Cl}_2]\text{Cl}_2$ **Fig.(3-41)** exhibits a broad absorption peak at (278 nm) (35971 cm^{-1}) ($\epsilon_{\text{max}} = 3627 \text{ molar}^{-1}\text{cm}^{-1}$) which assigned to the ligand field and charge transfer. The absorption peaks appeared at (410 nm) (24390 cm^{-1}) ($\epsilon_{\text{max}} = 227 \text{ molar}^{-1}\text{cm}^{-1}$), (622 nm) (16077 cm^{-1}) ($\epsilon_{\text{max}} = 43 \text{ molar}^{-1}\text{cm}^{-1}$) and (690 nm) (14492 cm^{-1}) ($\epsilon_{\text{max}} = 61 \text{ molar}^{-1}\text{cm}^{-1}$) are assigned to the ligand field and d-d transitions type (${}^3\text{A}_{2g} \rightarrow {}^3\text{T}_{2g}$), (${}^3\text{A}_{2g} \rightarrow {}^3\text{T}_{1g}(\text{F})$) and (${}^3\text{A}_{2g} \rightarrow {}^3\text{T}_{1g}(\text{P})$) respectively, indicated to distorted octahedral structure about Ni^{2+} complex. This result is in agreement with that reported previously about the electronic spectra of six coordinate (octahedral) nickel(II) complexes^(59, 61, 62).

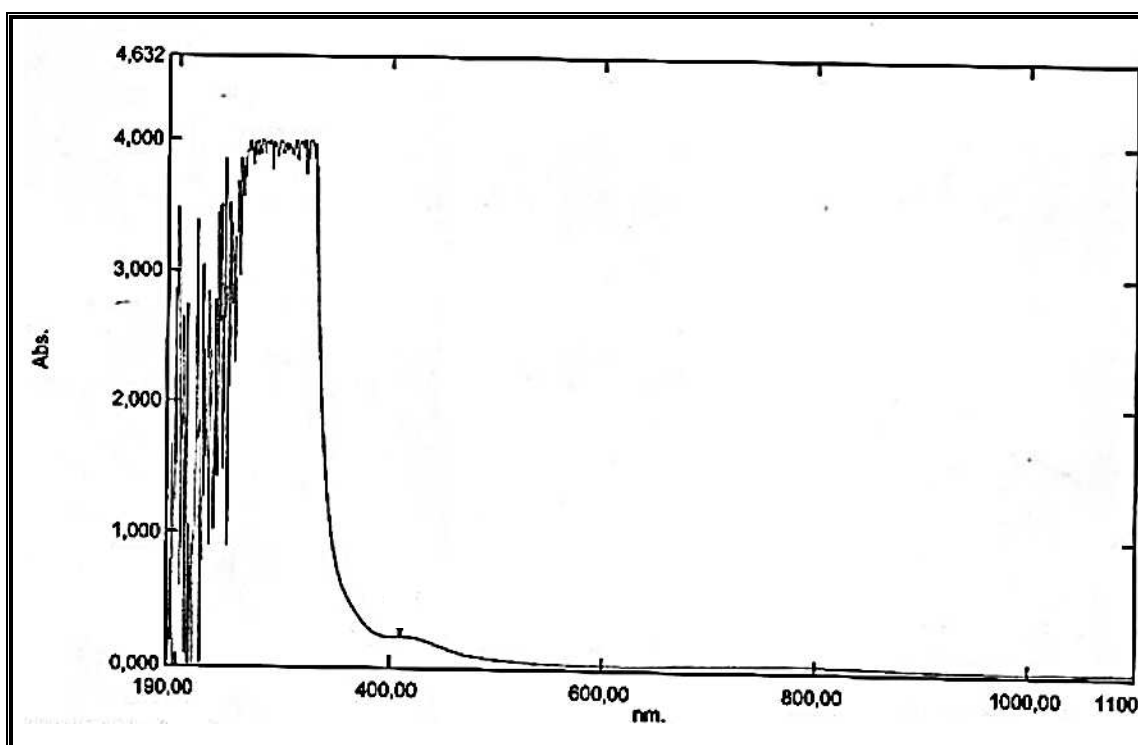


Fig.(3-41) UV-Vis spectrum of $[\text{Ni}_2(\text{L}^2)(\text{H}_2\text{O})_4\text{Cl}_2]\text{Cl}_2$ complex

(3.8.2.3) UV-Vis spectrum of $[\text{Cu}_2(\text{L}^2)(\text{H}_2\text{O})_6]\text{Cl}_4$ complex:

The electronic spectrum of the complex $[\text{Cu}_2(\text{L}^2)(\text{H}_2\text{O})_6]\text{Cl}_4$ **Fig.(3-42)** exhibits a broad absorption peak at (266 nm) (37939 cm^{-1}) ($\epsilon_{\text{max}} = 3657 \text{ molar}^{-1}\text{cm}^{-1}$) attributed to the ligand field and charge transfer. The peaks at (541 nm) (18484 cm^{-1}) ($\epsilon_{\text{max}} = 101 \text{ molar}^{-1}\text{cm}^{-1}$), (608 nm) (16447 cm^{-1}) ($\epsilon_{\text{max}} = 198 \text{ molar}^{-1}\text{cm}^{-1}$) and (736 nm) (13586 cm^{-1}) ($\epsilon_{\text{max}} = 309 \text{ molar}^{-1}\text{cm}^{-1}$) which are assigned to the d-d transitions type (${}^2\text{B}_{1g} \rightarrow {}^2\text{A}_{1g}$), (${}^2\text{B}_{1g} \rightarrow {}^1\text{B}_{2g}$) and (${}^2\text{B}_{1g} \rightarrow {}^2\text{E}_g$) respectively, indicated to distorted octahedral structure about Cu^{2+} complex. This result is in agreement with that reported previously about the electronic spectra of six coordinate (octahedral) copper(II) complexes^(18, 63).

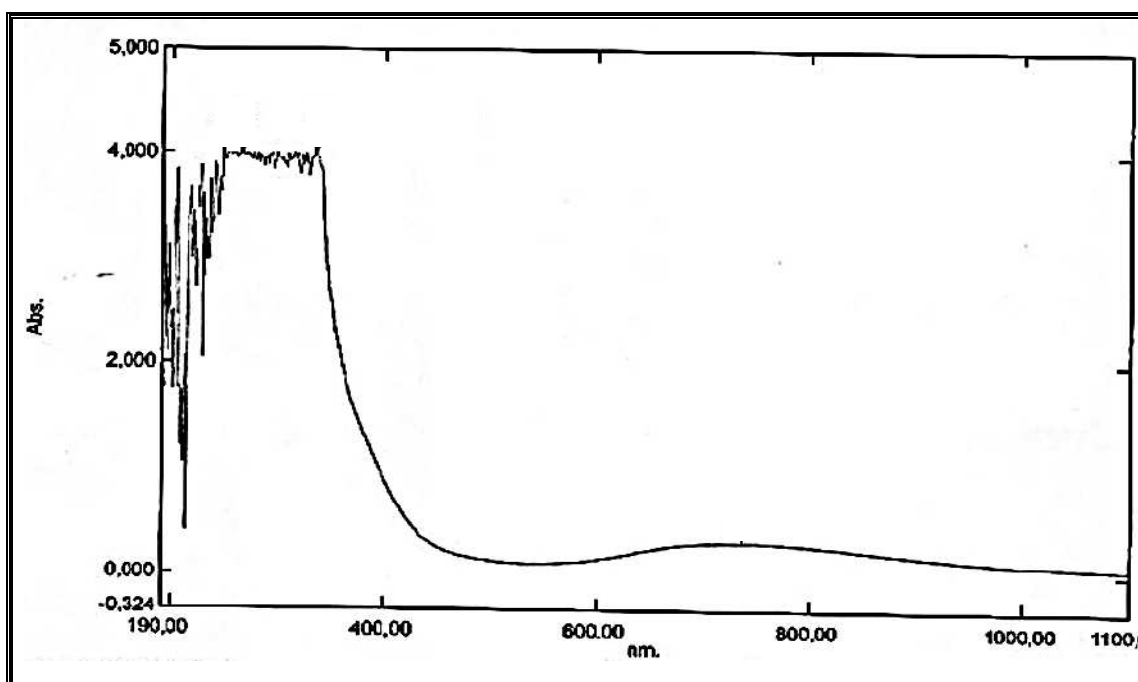


Fig.(3-42) UV-Vis spectrum of $[\text{Cu}_2(\text{L}^2)(\text{H}_2\text{O})_6]\text{Cl}_4$ complex

(3.8.2.4) UV-Vis spectrum of $[\text{Pd}_2(\text{L}^2)\text{Cl}_2]\text{Cl}_2$ complex:

The electronic spectrum of the complex $[\text{Pd}_2(\text{L}^2)\text{Cl}_2]\text{Cl}_2$ **Fig.(3-43)** exhibits a broad absorption peak at (324 nm) (30864 cm^{-1}) ($\epsilon_{\text{max}} = 3548 \text{ molar}^{-1}\text{cm}^{-1}$) assigned to the ligand field and charge transfer. The absorption peak at (597 nm) (16750 cm^{-1}) ($\epsilon_{\text{max}} = 582 \text{ molar}^{-1}\text{cm}^{-1}$) assigned to d-d transition type (${}^1\text{B}_{1g} \rightarrow {}^1\text{B}_{2g}$), this result is agreement with that reported previously about the electronic spectra of four coordinate (square planar) palladium(II) complexes ⁽⁶⁴⁾.

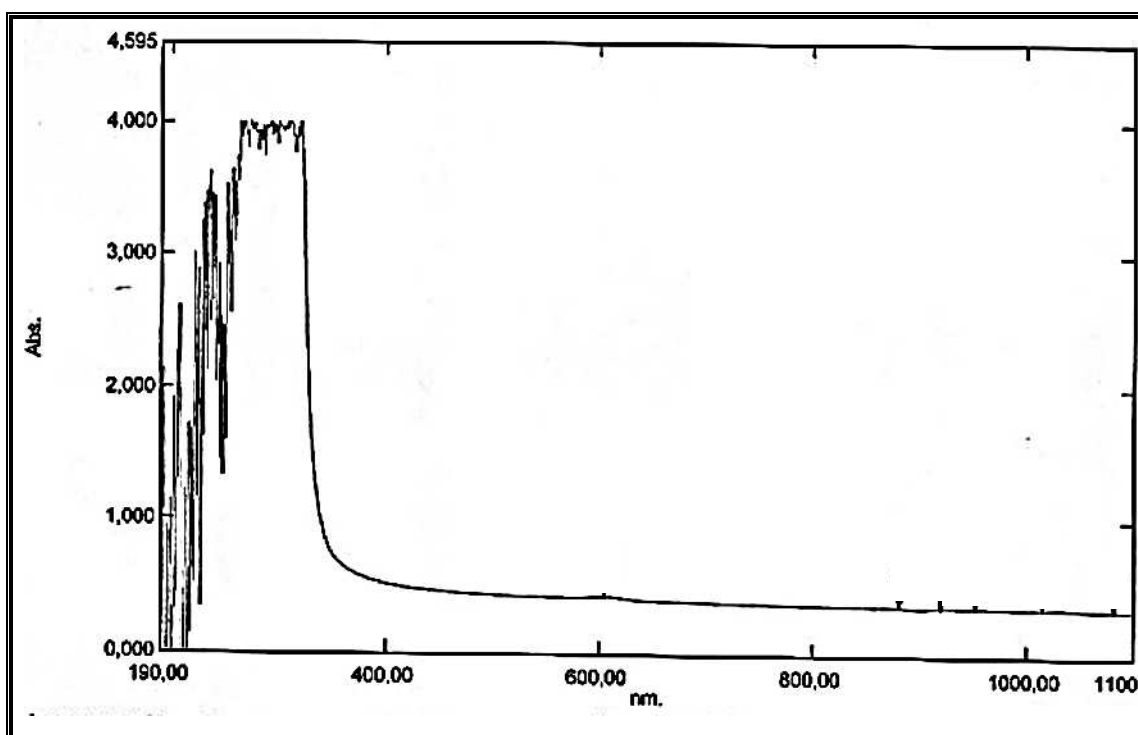


Fig.(3-43) UV-Vis spectrum of $[\text{Pd}_2(\text{L}^2)\text{Cl}_2]\text{Cl}_2$ complex

(3.8.2.5) UV-Vis spectrum of $[\text{Pt}_2(\text{L}^2)(\text{H}_2\text{O})_2\text{Cl}_4]\text{Cl}_4$ complex:

The electronic spectrum of the complex $[\text{Pt}_2(\text{L}^2)(\text{H}_2\text{O})_2\text{Cl}_4]\text{Cl}_4$ **Fig.(3-44)** exhibits a broad absorption peak at (236 nm) (42372 cm^{-1}) ($\epsilon_{\text{max}} = 3214 \text{ molar}^{-1}\text{cm}^{-1}$), which assigned to ligand field and charge transfer. The absorption peaks at (455 nm) (21978 cm^{-1}) ($\epsilon_{\text{max}} = 58 \text{ molar}^{-1}\text{cm}^{-1}$) and (577 nm) (17331 cm^{-1}) ($\epsilon_{\text{max}} = 74 \text{ molar}^{-1}\text{cm}^{-1}$) which d-d transitions type (${}^1\text{B}_{2g} \rightarrow {}^1\text{A}_{1g}$) and (${}^1\text{B}_{2g} \rightarrow {}^1\text{B}_{1g}$) respectively, indicated to distorted octahedral structure about Pt^{4+} complex. This result is in agreement with that reported previously about the electronic spectra of six coordinate (octahedral) platinum(IV) complexes⁽⁶⁵⁾.

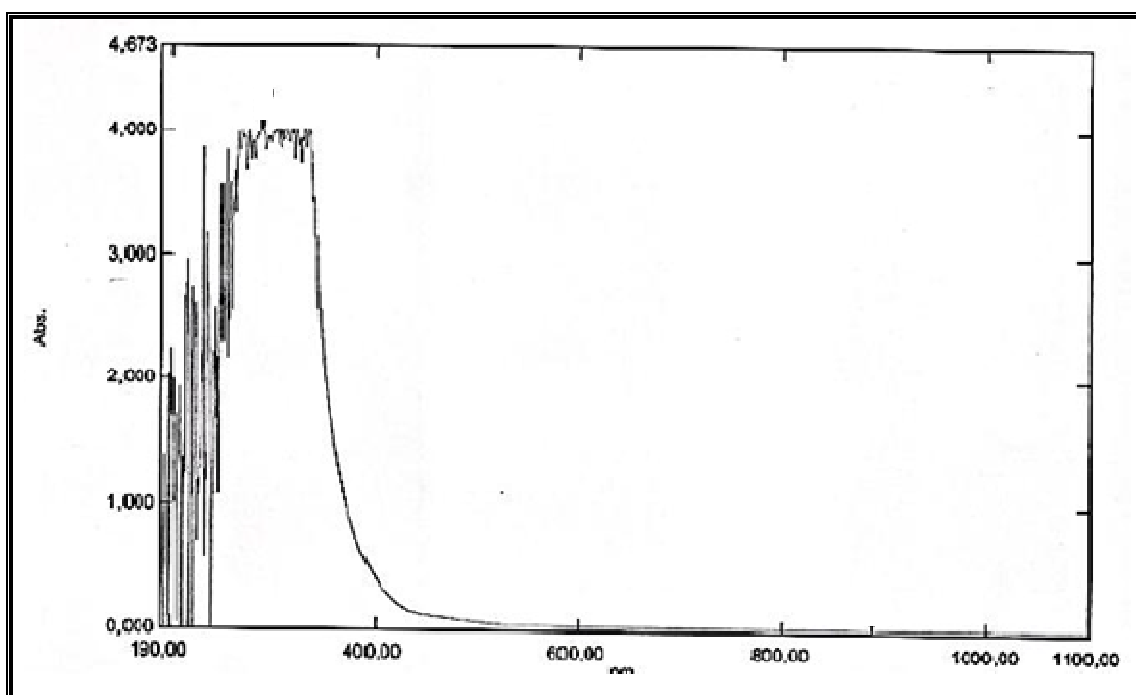


Fig.(3-44) UV-Vis spectrum of $[\text{Pt}_2(\text{L}^2)(\text{H}_2\text{O})_2\text{Cl}_4]\text{Cl}_4$ complex

Table (3-12) summarized the electronic spectral data of $[\text{L}^2]$ and its Co(II), Ni(II), Cu(II), Pd(II) and Pt(IV) complexes:

Table (3-12) Electronic spectral data of $[L^2]$ and its metal complexes

Compound	λ_{nm}	$\nu_{cm^{-1}}$	ϵ_{max} molar ⁻¹ cm ⁻¹	Assignment
$[L^2]$	231	43290	3976	$\pi \rightarrow \pi^*$
	293	34129		$n \rightarrow \pi^*$
$[Co_2(L^2)Cl_2]Cl_2$	308	32467	3982	ligand field
	572	17482	741	$^4A_2 \rightarrow ^4T_2$
	610	16393	812	$^4A_2 \rightarrow ^4T_1^{(F)}$
	637	15698	829	$^4A_2 \rightarrow ^4T_1^{(P)}$
$[Ni_2(L^2)(H_2O)_4Cl_2]Cl_2$	278	35971	3627	ligand field
	410	24390	227	$^3A_2g \rightarrow ^3T_2g$
	622	16077	43	$^3A_2g \rightarrow ^3T_1g^{(F)}$
	690	14492	61	$^3A_2g \rightarrow ^3T_1g^{(P)}$
$[Cu_2(L^2)(H_2O)_6]Cl_4$	266	37939	3657	ligand field
	541	18484	101	$^2B_1g \rightarrow ^2A_1g$
	608	16447	198	$^2B_1g \rightarrow ^1B_2g$
	736	13586	309	$^2B_1g \rightarrow ^2Eg$
$[Pd_2(L^2)Cl_2]Cl_2$	324	30864	3548	ligand field
	597	16750	583	$^1B_1g \rightarrow ^1B_2g$
$[Pt_2(L^2)(H_2O)_2Cl_4]Cl_4$	236	42372	3214	ligand field
	455	21978	58	$^1B_2g \rightarrow ^1A_1g$
	577	17331	74	$^1B_2g \rightarrow ^1B_1g$

(3.8.3) UV-Vis spectral data of [L³] complexes:

(3.8.3.1) UV-Vis spectrum of [Co₂(L³)Cl₂]Cl₂ complex:

The electronic spectrum of the complex [Co₂(L³)Cl₂]Cl₂ **Fig.(3-45)** exhibits four absorption peaks, a broad peak at (310 nm) (32258 cm⁻¹) ($\mathcal{E}_{\text{max}} = 3995 \text{ molar}^{-1}\text{cm}^{-1}$) assigned to ligand field and charge transfer. While the peaks at (571 nm) (17513 cm⁻¹) ($\mathcal{E}_{\text{max}} = 992 \text{ molar}^{-1}\text{cm}^{-1}$), (610 nm) (16393 cm⁻¹) ($\mathcal{E}_{\text{max}} = 1017 \text{ molar}^{-1}\text{cm}^{-1}$) and (637 nm) (15698 cm⁻¹) ($\mathcal{E}_{\text{max}} = 1018 \text{ molar}^{-1}\text{cm}^{-1}$) which are assigned to the d-d transitions type (${}^4A_2 \rightarrow {}^4T_2$), (${}^4A_2 \rightarrow {}^4T_1^{(F)}$) and (${}^4A_2 \rightarrow {}^4T_1^{(P)}$) respectively, indicated to tetrahedral structure about Co²⁺ complex. This result is in agreement with that reported previously about the electronic spectra of four coordinate (tetrahedral) cobalt(II) complexes^(58, 59, 60).

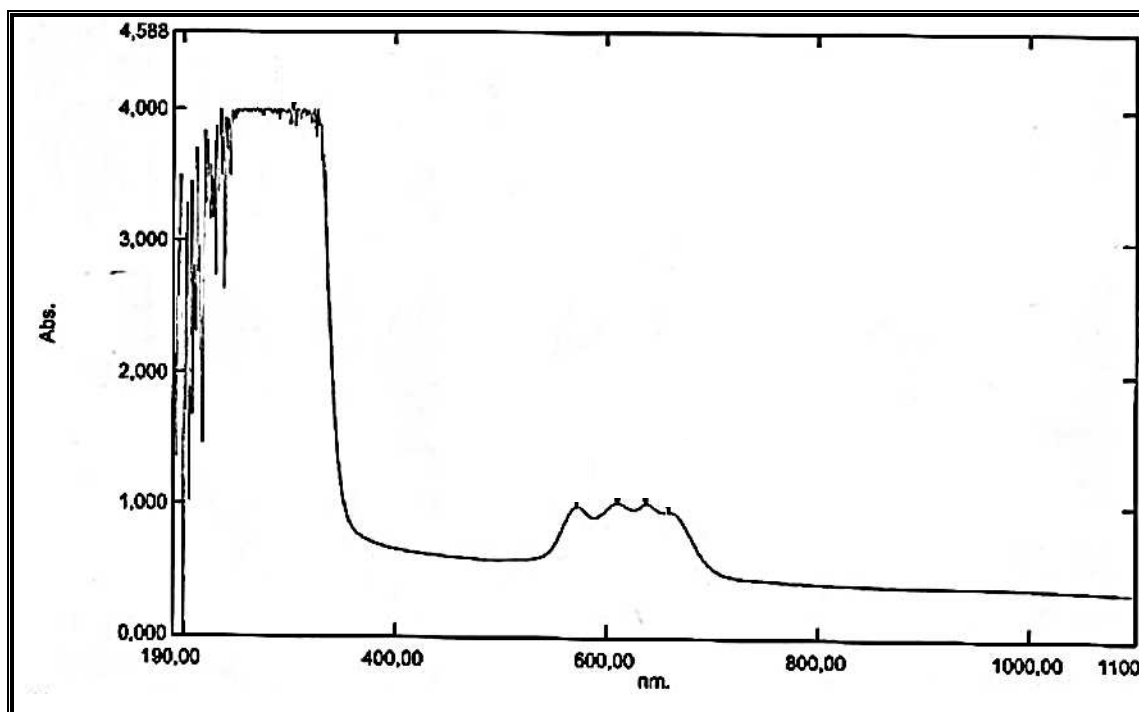
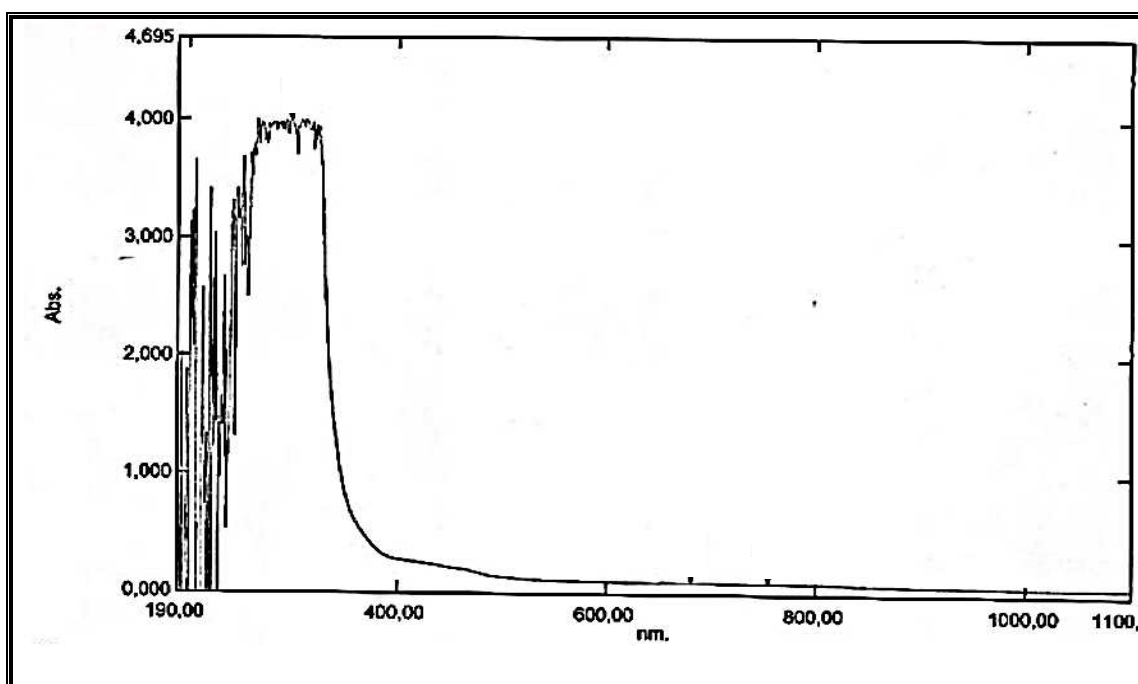


Fig.(3-45) UV-Vis spectrum of [Co₂(L³)Cl₂]Cl₂ complex

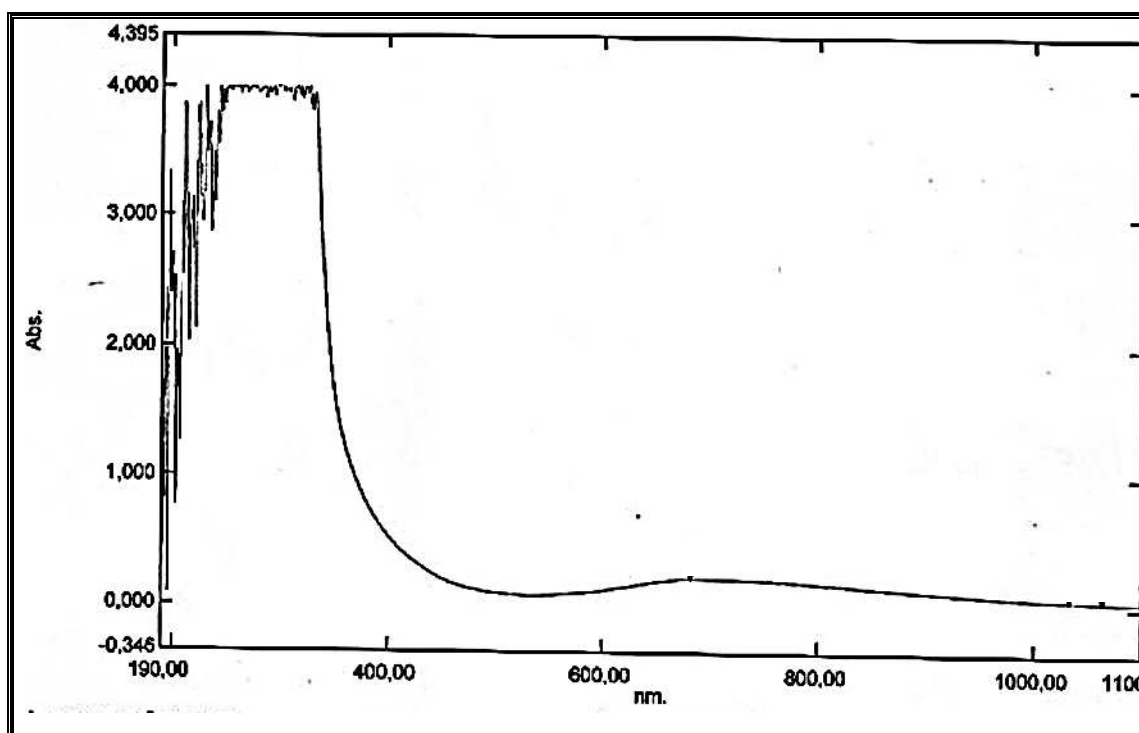
(3.8.3.2) UV-Vis spectrum of $[\text{Ni}_2(\text{L}^3)(\text{H}_2\text{O})_4\text{Cl}_2]\text{Cl}_2$ complex:

The electronic spectrum of the complex $[\text{Ni}_2(\text{L}^3)(\text{H}_2\text{O})_4\text{Cl}_2]\text{Cl}_2$ **Fig.(3-46)** exhibits a broad absorption peak at (283 nm) (35335 cm^{-1}) ($\epsilon_{\text{max}} = 3867 \text{ molar}^{-1} \text{ cm}^{-1}$) attributed to the ligand field and charge transfer. While the absorption peaks at (413 nm) (24213 cm^{-1}) ($\epsilon_{\text{max}} = 229 \text{ molar}^{-1} \text{ cm}^{-1}$), (639 nm) (15649 cm^{-1}) ($\epsilon_{\text{max}} = 88 \text{ molar}^{-1} \text{ cm}^{-1}$) and (681 nm) (14684 cm^{-1}) ($\epsilon_{\text{max}} = 92 \text{ molar}^{-1} \text{ cm}^{-1}$) which assigned to the ligand field and d-d transitions type (${}^3\text{A}_{2g} \rightarrow {}^3\text{T}_{2g}$), (${}^3\text{A}_{2g} \rightarrow {}^3\text{T}_{1g}(\text{F})$) and (${}^3\text{A}_{2g} \rightarrow {}^3\text{T}_{1g}(\text{P})$) respectively, indicated to distorted octahedral structure about Ni^{2+} complex. This result is in agreement with that reported previously about the electronic spectra of six coordinate (octahedral) nickel(II) complexes^(59, 61, 62).

**Fig.(3-46) UV-Vis spectrum of $[\text{Ni}_2(\text{L}^3)(\text{H}_2\text{O})_4\text{Cl}_2]\text{Cl}_2$ complex**

(3.8.3.3) UV-Vis spectrum of $[\text{Cu}_2(\text{L}^3)(\text{H}_2\text{O})_6]\text{Cl}_4$ complex:

The electronic spectrum of the complex $[\text{Cu}_2(\text{L}^3)(\text{H}_2\text{O})_6]\text{Cl}_4$ **Fig.(3-47)** exhibits a broad absorption peak at (299 nm) (33444 cm^{-1}) ($\epsilon_{\text{max}} = 3842 \text{ molar}^{-1}\text{cm}^{-1}$) attributed to the ligand field and charge transfer. While the absorption peaks at (535 nm) (18691 cm^{-1}) ($\epsilon_{\text{max}} = 76 \text{ molar}^{-1}\text{cm}^{-1}$) (623 nm) (16051 cm^{-1}) ($\epsilon_{\text{max}} = 214 \text{ molar}^{-1}\text{cm}^{-1}$) and (722 nm) (13850 cm^{-1}) ($\epsilon_{\text{max}} = 229 \text{ molar}^{-1} \text{ cm}^{-1}$) which are assigned to the d-d transitions type (${}^2\text{B}_{1g} \rightarrow {}^2\text{A}_{1g}$), (${}^2\text{B}_{1g} \rightarrow {}^1\text{B}_{2g}$) and (${}^2\text{B}_{1g} \rightarrow {}^2\text{E}_g$) respectively, indicated to distorted octahedral structure about Cu^{2+} complex. This result is in agreement with that reported previously about the electronic spectra of six coordinate (octahedral) copper(II) complexes^(18, 63).

**Fig.(3-47) UV-Vis spectrum of $[\text{Cu}_2(\text{L}^3)(\text{H}_2\text{O})_6]\text{Cl}_4$ complex**

(3.8.3.4) UV-Vis spectrum of $[\text{Pd}_2(\text{L}^3)\text{Cl}_2]\text{Cl}_2$ complex:

The electronic spectrum of the complex $[\text{Pd}_2(\text{L}^3)\text{Cl}_2]\text{Cl}_2$ **Fig.(3-48)** exhibits a broad absorption peak at (322 nm) (31055 cm^{-1}) ($\epsilon_{\text{max}} = 3764 \text{ molar}^{-1}\text{cm}^{-1}$) assigned to the ligand field and charge transfer. The absorption peak at (599 nm) (16694 cm^{-1}) ($\epsilon_{\text{max}} = 564 \text{ molar}^{-1}\text{cm}^{-1}$) assigned to d-d transition type (${}^1\text{B}_{1g} \rightarrow {}^1\text{B}_{2g}$), this result is agreement with that reported previously about the electronic spectra of four coordinate (square planar) palladium(II) complexes ⁽⁶⁴⁾.

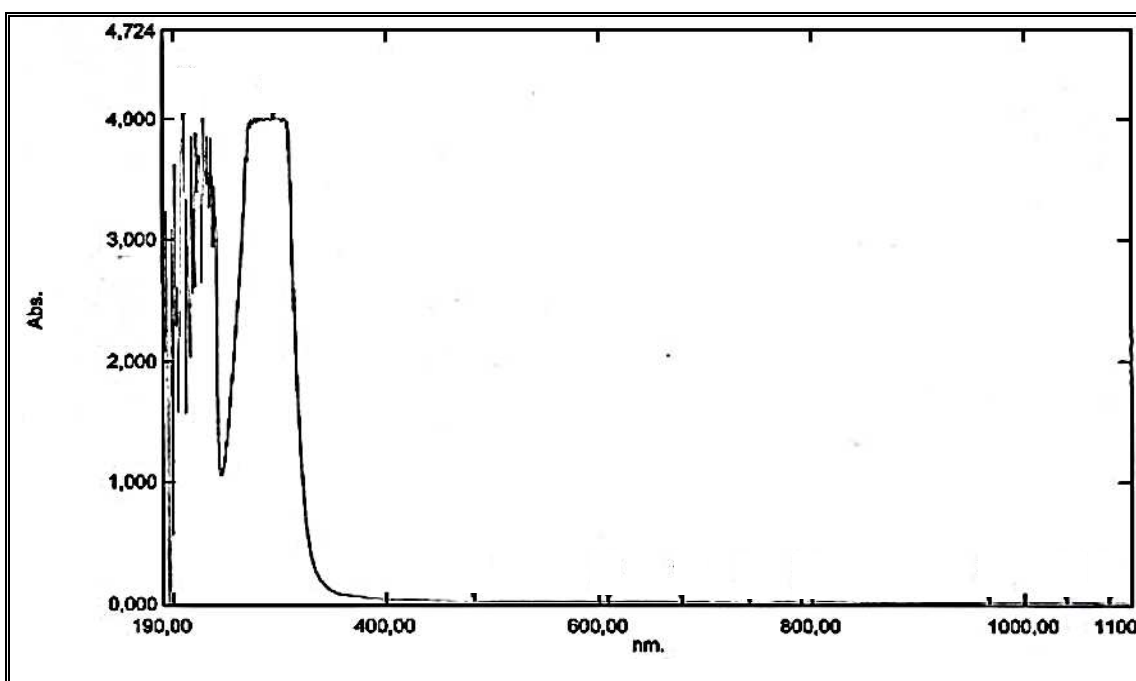


Fig.(3-48) UV-Vis spectrum of $[\text{Pd}_2(\text{L}^3)\text{Cl}_2]\text{Cl}_2$ complex

(3.8.3.5) UV-Vis spectrum of $[\text{Pt}_2(\text{L}^3)(\text{H}_2\text{O})_2\text{Cl}_4]\text{Cl}_4$ complex:

The electronic spectrum of the complex $[\text{Pt}_2(\text{L}^3)(\text{H}_2\text{O})_2\text{Cl}_4]\text{Cl}_4$ **Fig.(3-49)** exhibits a broad absorption peak at (233 nm) (42918 cm^{-1}) ($\epsilon_{\text{max}} = 2214 \text{ molar}^{-1}\text{cm}^{-1}$) attributed to the ligand field and charge transfer. While the absorption peaks at (457 nm) (21881 cm^{-1}) ($\epsilon_{\text{max}} = 78 \text{ molar}^{-1}\text{cm}^{-1}$) and (547 nm) (18281 cm^{-1}) ($\epsilon_{\text{max}} = 86 \text{ molar}^{-1}\text{cm}^{-1}$) which assigned to the d-d transitions type (${}^1\text{B}_{2g} \rightarrow {}^1\text{A}_{1g}$) and (${}^1\text{B}_{2g} \rightarrow {}^1\text{B}_{1g}$) respectively, indicated to distorted octahedral structure about Pt^{4+} complex. This result is in agreement with that reported previously about the electronic spectra of six coordinate (octahedral) platinum(IV) complexes⁽⁶⁵⁾.

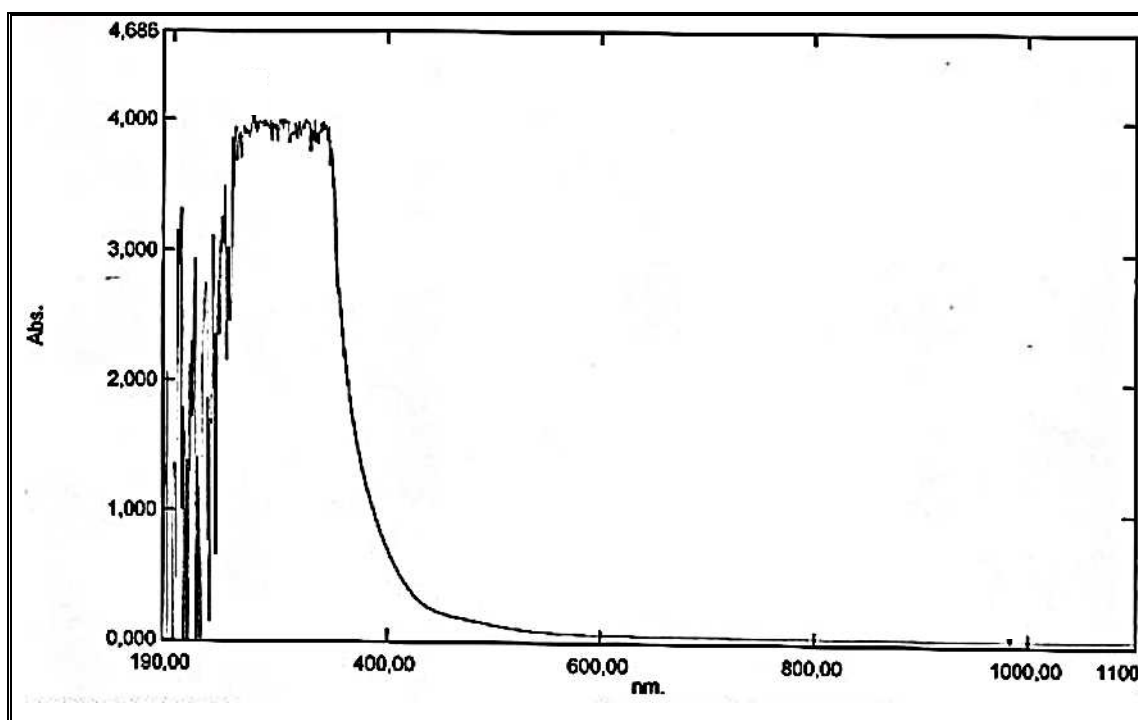


Fig.(3-49) UV-Vis spectrum of $[\text{Pt}_2(\text{L}^3)(\text{H}_2\text{O})_2\text{Cl}_4]\text{Cl}_4$ complex

Table (3-13) summarized electronic spectral data of $[\text{L}^3]$ and its Co(II), Ni(II), Cu(II), Pd(II) and Pt(IV) complexes:

Table (3-13) Electronic spectral data of [L³] and its metal complexes

Compound	λ_{nm}	$\nu_{cm^{-1}}$	ϵ_{max} molar ⁻¹ cm ⁻¹	Assignment
[L ³]	251	39840	3974	$\pi \rightarrow \pi^*$
	296	33783		$n \rightarrow \pi^*$
[Co ₂ (L ³)Cl ₂]Cl ₂	310	32258	3995	ligand field
	571	17513	992	$^4A_2 \rightarrow ^4T_2$
	610	16393	1018	$^4A_2 \rightarrow ^4T_1^{(F)}$
	637	15698	1018	$^4A_2 \rightarrow ^4T_1^{(P)}$
[Ni ₂ (L ³)(H ₂ O) ₄ Cl ₂]Cl ₂	283	35335	3867	ligand field
	413	24213	229	$^3A_{2g} \rightarrow ^3T_{2g}$
	639	15649	88	$^3A_{2g} \rightarrow ^3T_{1g}^{(F)}$
	681	14684	92	$^3A_{2g} \rightarrow ^3T_{1g}^{(P)}$
[Cu ₂ (L ³)(H ₂ O) ₆]Cl ₄	299	33444	3842	ligand field
	535	18691	76	$^2B_{1g} \rightarrow ^2A_{1g}$
	623	16051	214	$^2B_{1g} \rightarrow ^1B_{2g}$
	722	13850	229	$^2B_{1g} \rightarrow ^2E_g$
[Pd ₂ (L ³)Cl ₂]Cl ₂	322	31055	3764	ligand field
	594	16694	564	$^1B_{1g} \rightarrow ^1B_{2g}$
[Pt ₂ (L ³)(H ₂ O) ₂ Cl ₄]Cl ₄	233	42918	2214	ligand field
	457	21881	78	$^1B_{2g} \rightarrow ^1A_{1g}$
	547	18281	86	$^1B_{2g} \rightarrow ^1B_{1g}$

(3.9) Magnetic susceptibility of synthesized complexes:

Magnetic moment has been determined in the solid state by faraday's method^(66, 67). The magnetic properties of these complexes should provide a testing ground for the oxidation state of the complexes, therefore provides a way of counting the number of unpaired electrons. This should help in predicting the bonding model and electronic structure. The magnetic susceptibility for complexes was measured at room temperature **Table (3–14)**, the effective magnetic moment (μ_{eff} / B.M.) is given by

$$\mu_{\text{eff}} = 2.828\sqrt{X_A} \text{ T}$$

Where:

[T= Absolute temperature (25+273=298)]

[X_A= Atomic susceptibility corrected from diamagnetic presence]

The magnetic susceptibility was calculated according to the example shown below:

For the complex [Co₂(L¹)Cl₂]Cl₂

$$X_g(\text{Gram susceptibility}) = 7.6373 \times 10^{-6}$$

$$X_M(\text{Molar susceptibility}) = X_g \text{ M. Wt.}$$

$$= 6.952 \times 10^{-6} \times 768.54 = 5343.479 \times 10^{-6}$$

$$X_A(\text{Atom susceptibility}) = X_M - D$$

$$= 5343.479 \times 10^{-6} - (-255.56 \times 10^{-6})$$

$$= 5599.039 \times 10^{-6}$$

$$\mu_{\text{eff}} = 2.828 \sqrt{X_A} \text{ T}$$

$$\mu_{\text{eff}} = 2.828 (5599.039 \times 10^{-6} \times 298)^{1/2}$$

$$\mu_{\text{eff}} = 3.652 \text{ B.M}$$

Table (3–14) Magnetic susceptibility of synthesized complexes

Complexes	$X_g \times 10^{-6}$ Gram Susceptibility	$X_M \times 10^{-6}$ Molar Susceptibility	$X_A \times 10^{-6}$ Atom Susceptibility	$\mu_{\text{eff. B. M. expt.}}$	$\mu_{\text{eff. B. M. calc.}}$	Suggested Structure
$[\text{Co}_2(\text{L}^1)\text{Cl}_2]\text{Cl}_2$	6.952	5343.479	5599.039	3.652	3.88	tetrahedral
$[\text{Co}_2(\text{L}^2)\text{Cl}_2]\text{Cl}_2$	6.707	5343.480	5599.040	3.652	3.88	tetrahedral
$[\text{Co}_2(\text{L}^3)\text{Cl}_2]\text{Cl}_2$	6.265	5342.982	5598.542	3.652	3.88	tetrahedral
$[\text{Ni}_2(\text{L}^1)(\text{H}_2\text{O})_4\text{Cl}_2]\text{Cl}_2$	2.520	2185.739	2437.019	2.410	2.45	octahedral
$[\text{Ni}_2(\text{L}^2)(\text{H}_2\text{O})_4\text{Cl}_2]\text{Cl}_2$	2.396	2145.458	2396.738	2.390	2.45	octahedral
$[\text{Ni}_2(\text{L}^3)(\text{H}_2\text{O})_4\text{Cl}_2]\text{Cl}_2$	2.219	2111.484	2362.764	2.373	2.45	octahedral
$[\text{Cu}_2(\text{L}^1)(\text{H}_2\text{O})_6]\text{Cl}_4$	1.000	883.030	1128.200	1.639	1.73	octahedral
$[\text{Cu}_2(\text{L}^2)(\text{H}_2\text{O})_6]\text{Cl}_4$	0.969	882.778	1127.948	1.639	1.73	octahedral
$[\text{Cu}_2(\text{L}^3)(\text{H}_2\text{O})_6]\text{Cl}_4$	0.911	881.055	1126.225	1.638	1.73	octahedral
$[\text{Pd}_2(\text{L}^1)\text{Cl}_2]\text{Cl}_2$	0.00	0.00	0.00	Diamagnetic	0.00	Square planar
$[\text{Pd}_2(\text{L}^2)\text{Cl}_2]\text{Cl}_2$	0.00	0.00	0.00	Diamagnetic	0.00	Square planar
$[\text{Pd}_2(\text{L}^3)\text{Cl}_2]\text{Cl}_2$	0.00	0.00	0.00	Diamagnetic	0.00	Square planar
$[\text{Pt}_2(\text{L}^1)(\text{H}_2\text{O})_2\text{Cl}_4]\text{Cl}_4$	0.00	0.00	0.00	Diamagnetic	0.00	octahedral
$[\text{Pt}_2(\text{L}^2)(\text{H}_2\text{O})_2\text{Cl}_4]\text{Cl}_4$	0.00	0.00	0.00	Diamagnetic	0.00	octahedral
$[\text{Pt}_2(\text{L}^3)(\text{H}_2\text{O})_2\text{Cl}_4]\text{Cl}_4$	0.00	0.00	0.00	Diamagnetic	0.00	octahedral

(3.10) Molar conductivity for the synthesized complexes:

Molar conductivity can be attributed as one of the best evidences to suggest the charge of complexes from its electrolyte solutions, the molar conductance of different type of electrolytes⁽⁶⁸⁾ is summarized in **Table (3-15)**, the molar conductance of synthesized complexes in (DMF) are summarized in **Table (3-16)**. The conductance of the cobalt(II), nickel(II) and palladium(II) complexes of all ligands were in the range (130-173 S.cm² .mole⁻¹) indicating the 1:2 ratio electrolyte nature. While the conductance of the complexes of copper(II) and platinum(IV) are in the range (277-295 S.cm².mole⁻¹) indicating (1:4) ratio electrolyte nature⁽⁶⁷⁾.

Table (3-15) Molar conductivity of different complex solutions

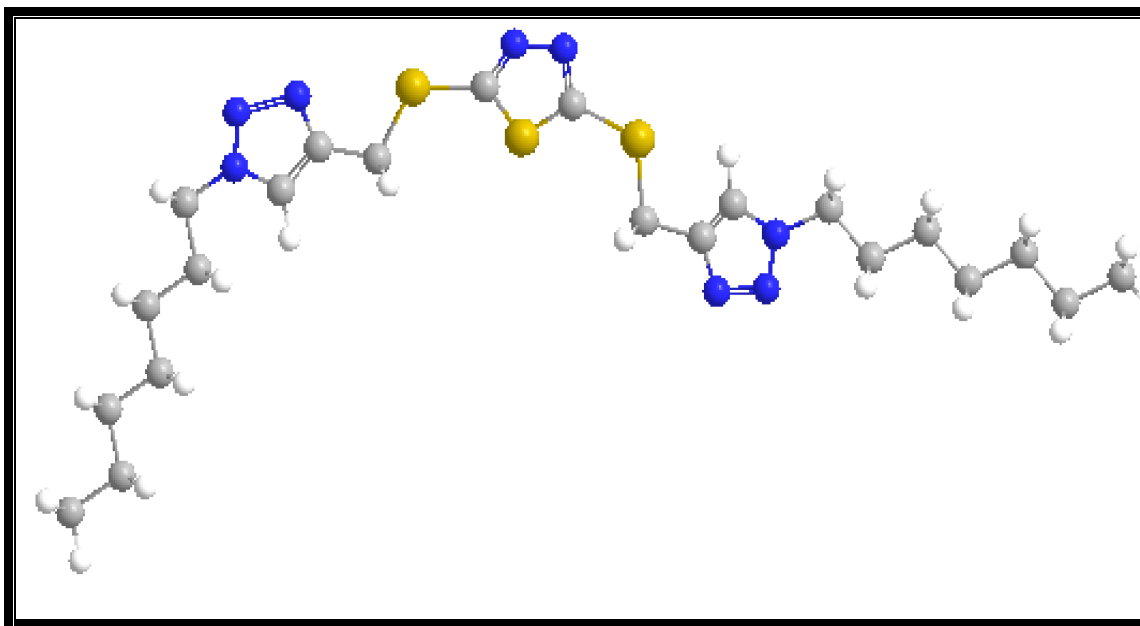
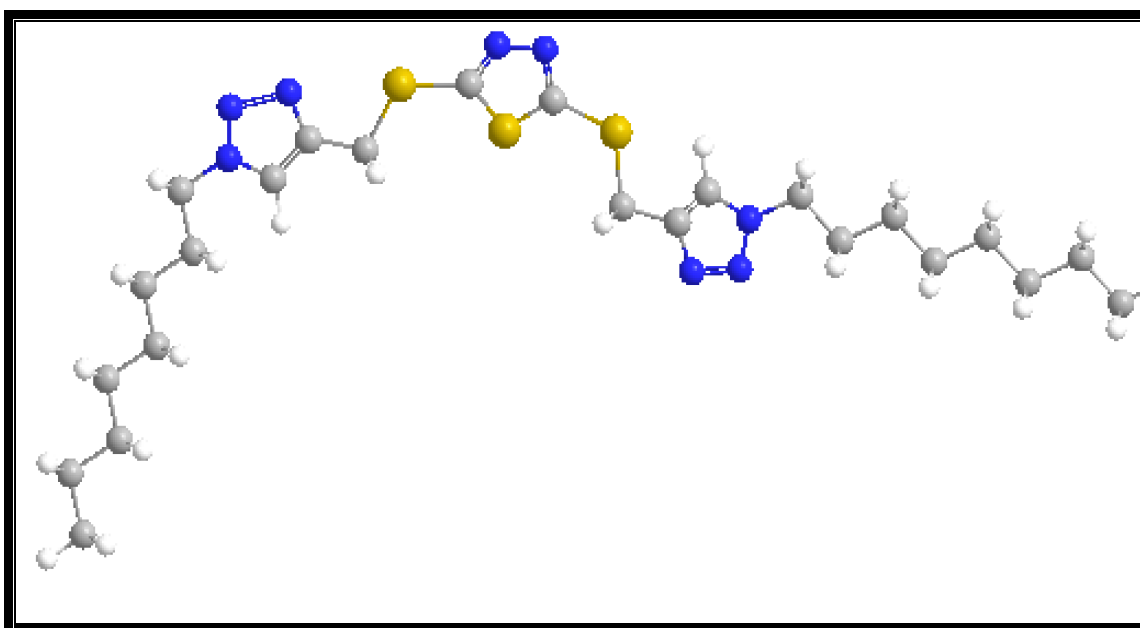
Solvent	Non-electrolyte	Type of electrolyte			
		1:1	1:2	1:3	1:4
Water	0.0	120	240	360	380
Methyl cyanide	0-30	120-160	220-300	340-420	500
Nitromethane	0-20	75-95	150-180	220-260	290-330
DMF	0-30	65-90	130-170	200-240	300
Ethanol	0-20	35-45	70-90	120	160

Table (3-16) conductivity of complexes dissolved in (DMF)

No.	Compound	Conductivity ($S.cm^2.mol^{-1}$)	Ratio of L:Cl ⁻	Suggested Structure
1.	$[Co_2(L^1)Cl_2]Cl_2$	145	1:2	tetrahedral
2.	$[Co_2(L^2)Cl_2]Cl_2$	142	1:2	tetrahedral
3.	$[Co_2(L^3)Cl_2]Cl_2$	140	1:2	tetrahedral
4.	$[Ni_2(L^1)(H_2O)_4Cl_2]Cl_2$	173	1:2	octahedral
5.	$[Ni_2(L^2)(H_2O)_4Cl_2]Cl_2$	170	1:2	octahedral
6.	$[Ni_2(L^3)(H_2O)_4Cl_2]Cl_2$	169	1:2	octahedral
7.	$[Cu_2(L^1)(H_2O)_6]Cl_4$	288	1:4	octahedral
8.	$[Cu_2(L^2)(H_2O)_6]Cl_4$	284	1:4	octahedral
9.	$[Cu_2(L^3)(H_2O)_6]Cl_4$	277	1:4	octahedral
10.	$[Pd_2(L^1)Cl_2]Cl_2$	130	1:2	Square planar
11.	$[Pd_2(L^2)Cl_2]Cl_2$	130	1:2	Square planar
12.	$[Pd_2(L^3)Cl_2]Cl_2$	131	1:2	Square planar
13.	$[Pt_2(L^1)(H_2O)_2Cl_4]Cl_4$	295	1:4	octahedral
14.	$[Pt_2(L^2)(H_2O)_2Cl_4]Cl_4$	294	1:4	octahedral
15.	$[Pt_2(L^3)(H_2O)_2Cl_4]Cl_4$	290	1:4	octahedral

(3-11) Suggested structures of ligands & complexes :**(3.11.1) Suggested structure of ligands:**

From the FT-IR, UV-Vis, ^1H , ^{13}C NMR spectral data, in addition C.H.N.S elemental analyses the suggested structures of $[\text{L}^1]$, $[\text{L}^2]$ and $[\text{L}^3]$ ligands show in **Fig.(3-50)**, **(3-51)** & **(3-52)**

**Fig.(3-50) $[\text{L}^1]$ ligand structure****Fig.(3-51) $[\text{L}^2]$ ligand structure**

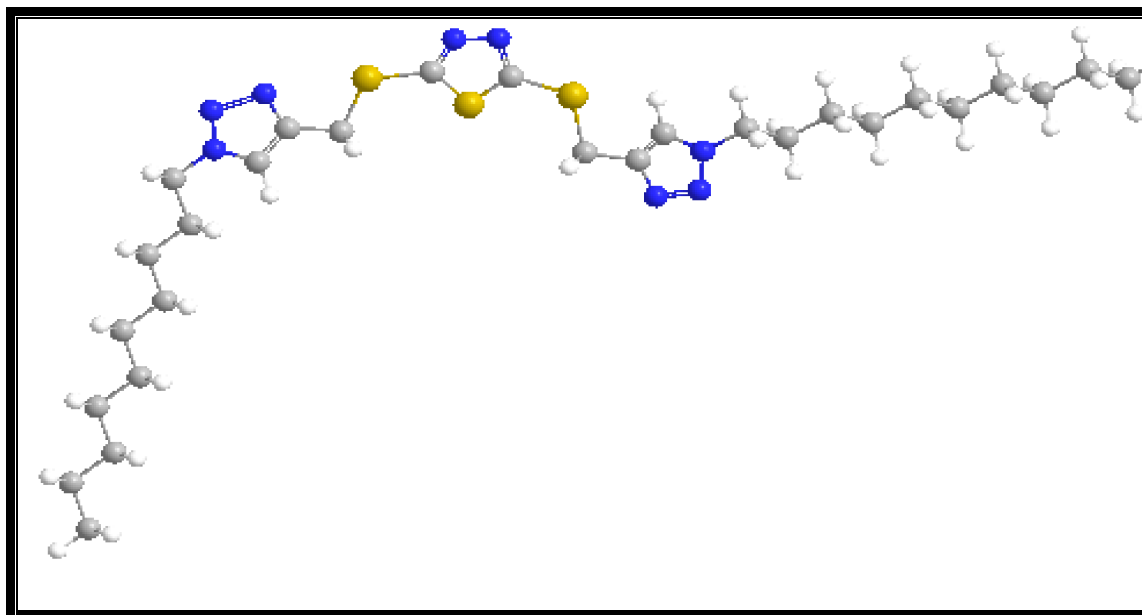


Fig.(3-52) [L³] ligand structure

(3.11.2) Suggested structures of the ligands:

From FT-IR, UV-Vis spectra of complexes, magnetic measurements and molar conductivity the suggested structures of complexes were Td for cobalt complexes, Oh for nickel & copper complexes, Sp for palladium complexes and Oh for platinum complexes **Fig. (3-53), (3-54), (3-55), (3-56) and (3-57)** respectively:

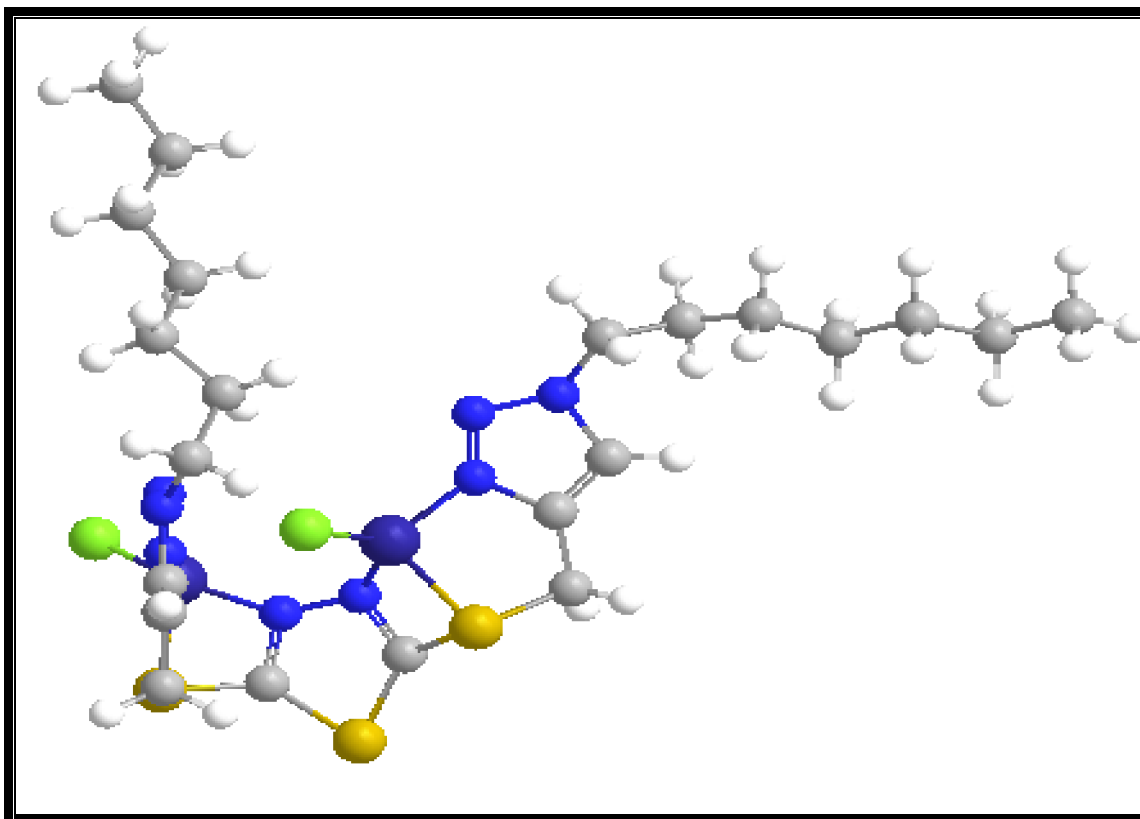


Fig.(3-53) suggested structure of $[\text{Co}_2\text{L}^1\text{Cl}_2]^{2+}$ complex

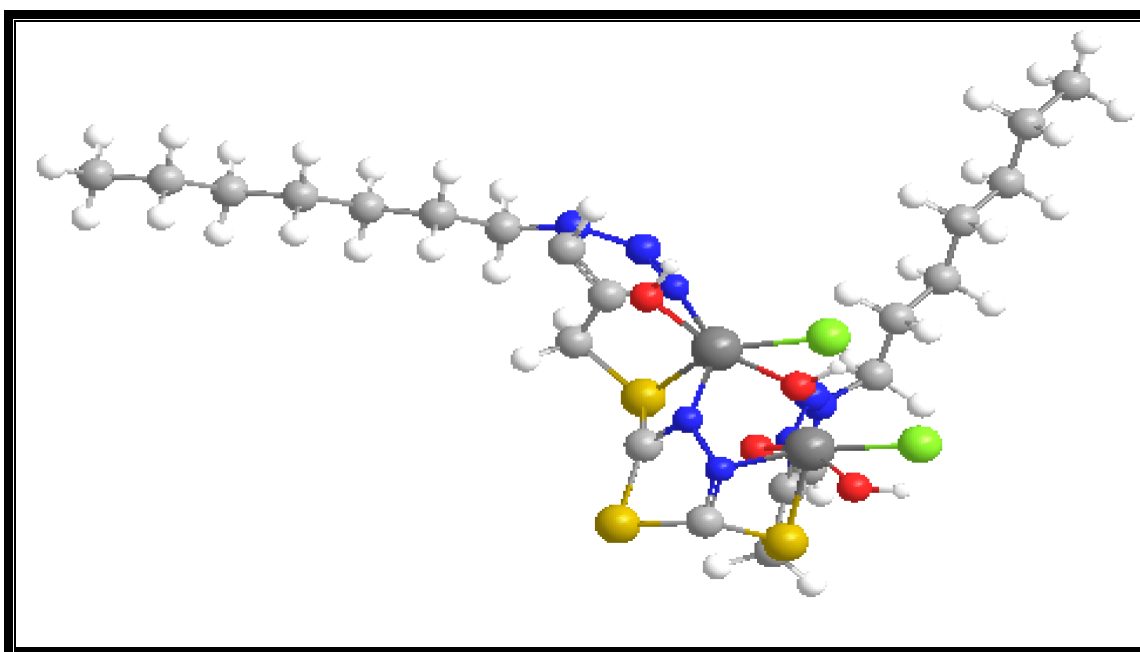


Fig.(3- 54) Suggested structure of $[\text{Ni}_2(\text{L}^1)(\text{H}_2\text{O})_4\text{Cl}_2]^{2+}$ complex

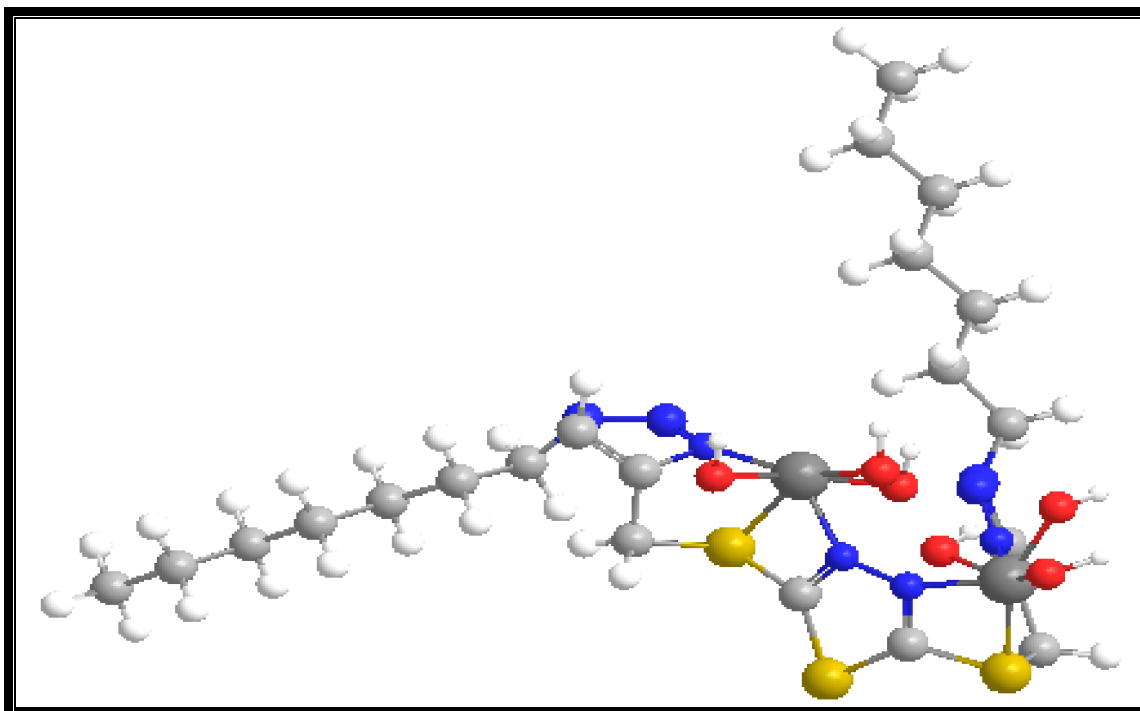


Fig.(3-55) Suggested structure of $[\text{Cu}_2\text{L}^16\text{H}_2\text{O}]^{4+}$ complex

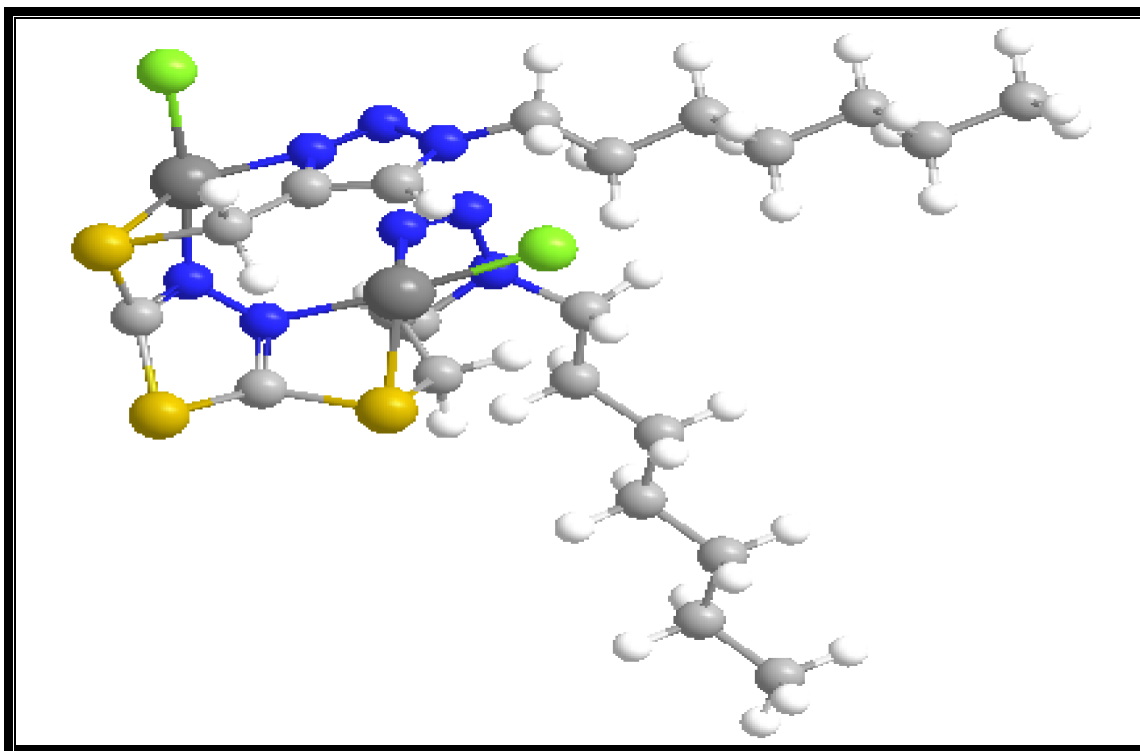


Fig.(3-56) Suggested structure of $[\text{Pd}_2\text{L}^12\text{Cl}]^{2+}$ complex

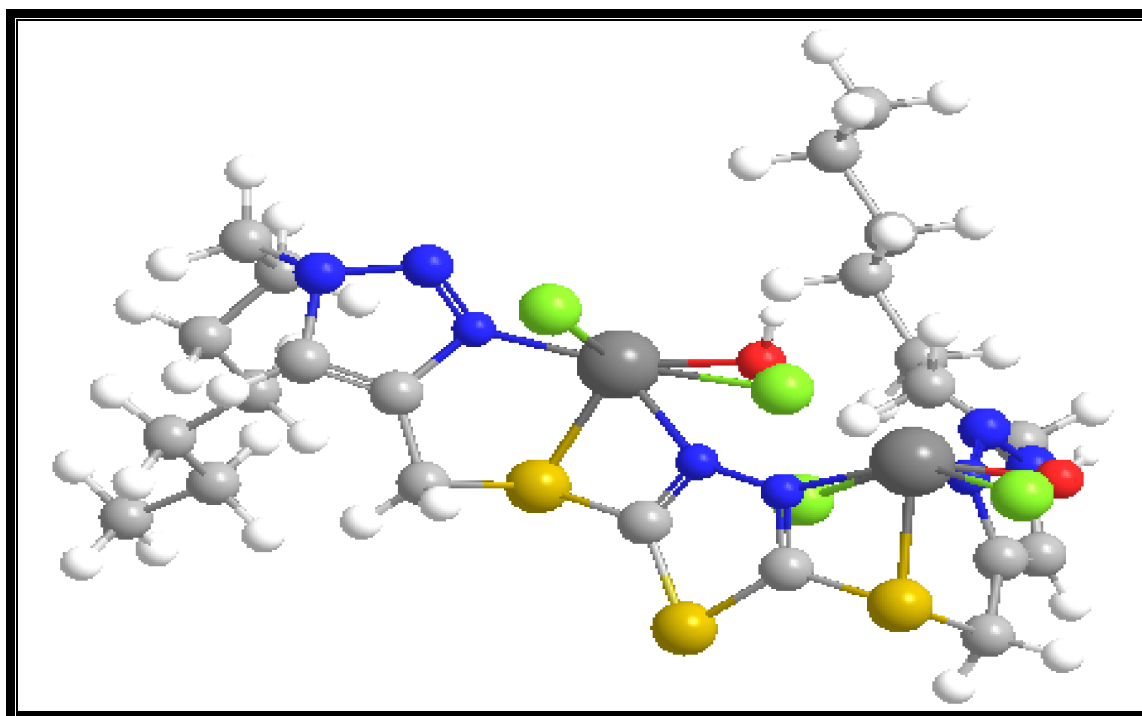


Fig.(3-57) Suggested structure of [Pt₂L₂H₂O₄Cl]⁴⁺ complex



Chapter Three

RESULTS AND DISCUSSION



REFERENCES

References:

1. G. Mishra, A.K.Singh and K. Jyoti, *International J. of ChemTech Research*, **3**, 3, 1380-1393, (2011).
2. R. Dua, S. Shrivastava, S.K. Sonwane and S.K. Srivastava, *J. of Advan. Biol. Res.*, **5**, 3, 120-144, (2011).
3. W. Samee and O. Vajragupta, *Afr. J. of Pharm. Pharmacol.*, **5**, 4, 477-485, (2011).
4. A. H. A. Al-Amiery, S. A. Mahmood, R. M. Mohamed and M. A. Mohammed, *J. Chem. Pharm. Res.*, **2**, 3, 120-126, (2010)
5. J. K. Gupta, R. K. Yadav, R. Dudhe and P. K. Sharma, *Int.J. PharmTech Res.*, **2**, 2, 1493-1507, (2010).
6. J. Salimon, N. Salih, A. Hameed, H. Ibraheem and E. Yousif, *J. of Appl. Sci. Res.*, **6**, 7, 866-870, (2010).
7. M. Barboiu, M. Cimpoesu, C. Guran and C. T. Supumn, *J. of Synthesis and Biological Activity of Metal Complexes*, **3**, 5, 227-232, (1996).
8. B. C. Tzeng, Y.L. Wu, G. H. Lee and S. M. Peng, *New J. of Chem.*, **31**, 199-201, (2007).
9. N. Turan, Z. Ering and M. Sekercl, *J. of Chem. Pak.*, **32**, 5, 630-637, (2010).
10. J. A. Obaleye, J. F. Adediji and M. A. Adebayo, *J. of Molecules*, **16**, 5861-5874, (2011).
11. C. G. Oliva, N. Jagerovic, P. Goya, I. Alkorta, J. Elguero, R. Cuberes and A. Dordal, *J. of ARKAT USA*, **2**, 127-147, (2010).
12. M. Martinelli, T. Milcent, S. Ongeri and B. Crousse, *Beilstein J. of Org. Chem.*, **4**, 19, (2008).
13. P. Li and L. Wang, *J. of Letters in Org. Chem.*, **4**, 1, 23-26, (2007).

14. L. H. Lu, J. H. Wu and C. H. Yang, *J. of the Chinese Chemical Society*, **55**, 414-417, (2008).
15. B. M. J. M. Suijkerbuijk, B. N. H. Aerts, H. P. Dijkstra, M. Lutz and A. L. Spek, *J. of Dalton Trans.*, **2007**, 1273-1276, (2007).
16. B. Beyer, C. Ulbricht, D. Escudero, C. Friebe, A. Winter, L. Gonzalez and U. S. Schubert, *J. of Organometallics*, **28**, 18, 5487-5488, (2009).
17. M. J. Prushan, Ph.D thesis, **Drexel University**, (2001).
18. P. M. Reddy, R. Rohini, E. R. Krishna, A. Hu and V. Ravinder, *Int. J. Mol. Sci*, **13**, 4982-4992, (2012).
19. Z. H. Chohan, H. Pervez, A. Rauf and C. T. Supuran, *J. of Metal Based Drugs*, **8**, 5, 263-267, (2002).
20. A. A. Al-Amiery, A. A. H. Kadhum and A. B. Mohamad, *J. of Bioinorganic Chem. and Appl.*, 1-6, (2012).
21. R.V. Singh, N. Fahmi and M. K. Biyala, *J. of the Iranian Chem. Soci.*, **2**, 1, 40-46, (2005).
22. S. O. P. Kuzmanović and L. S. Vojinović, *J. of APTEFF*, **34**, 1-148, (2003).
23. S. Hussain, J. Sharma and M. Amir, *E-J. of Chem. CODEN ECJHAO*, **5**, 4, 963-968, (2008).
24. J. Salimon, N. Salih, E. Yousif, A. Hameed and H. Ibraheem, *Australian J. of Basic and Appl. Sci.*, **4**, 7, 2016-2021, (2010).
25. J. Ruiz, V. Rodriguez, C. Haro, A. Espinosa, J. Pérez and C. Janiak, *J. of Dalton Trans.*, **39**, 2390-3301, (2010).
26. F. Bentiss, M. Outirite, M. Lagrene´e, M. Saadi and L. El Ammari, *Acta Cryst.*, **E68**, 360-361, (2012).
27. S.Kumar, D.N.Dhar and P.N.Saxena, *J. of Sci. and Ind. Res.*, **68**, 181-187, (2009).

28. J. Khan, R. Rashid, N. Rashid, Z. A. Bhatti, N. Bukhari, M. A. Khan and Q. Mahmood, *J. of Sarhad J. Agric.*, **26**, 1, 65-68, (2010).
29. J. F. Adediji, S. A. Amolegbe and L. Amudat, *J. of Chem. and Pharm. Res.*, **4**, 3, 1511-1518, (2012).
30. E. L. Chang, C. Simmers and D. A. Knight, *J. of Pharmaceuticals*, **3**, 1711-1728, (2010).
31. H. Yorimitsu and K. Oshima, *J. of Pure Appl. Chem.*, **78**, 2, 441–449, (2006).
32. C. M. Menzies and P. J. Squattrito, *Inorg. Chimica Acta*, **314**, 194-200, (2001).
33. S. C. Nayak, P. K. Das, and K. K. Sahoo, *J. of Chem. Pap*, **57**, 2, 91-96, (2003).
34. M. Amirnasr, A. H. Mahmoudkhani, A. Gorji, S. Dehghanpour and H. R. Bijanzadeh, *J. of Polyhedron*, **21**, 2733-2742, (2002).
35. U. Beckmann and S. Brooker, *Coordination Chemistry Reviews*, **245**, 17-29, (2003).
36. Elza Nelkenbaum, Moshe Kapon, Moris S. Eisen, *J. of Organometallic Chem.*, **690**, 2297–2305, (2005).
37. M. I .F. Garcia, B. F. Ferná'ndez, M. Fondo, A. M. G. Deibe, E. G. Fo'rneas, M. R. Bermejo, J. Sanmartin and A.M. Gonzalez, *Inorganica Chimica Acta*, **304** , 144-149, (2000).
38. G. A. Santillan, and C. J. Carrano, *J. of Inorg. Chem.*, **47**, 3, 930-939, (2008).
39. A. S. Ferwanah, A.M. Awadallah, B. M. Awad, N. M. El-Halabi and R. Boese, *Inorganica Chimica Acta*, **358**, 4511–4518, (2005).
40. A. A. M. Aly, M. A. Ghandour and M. S. AL-Fakeh, *Turk J. Chem.*, **36**, 69-79, (2012).

41. C. Marzano, M. Pellei, F. Tisato and C. Santini, *J. of Anti-Cancer Agents in Medicinal Chemistry*, **9**, 2, 185-211, (2009).
42. B. S. Creaven, M. F. Mahon, J. McGinley and A. Moore, *J. of Inorg. Chem. Com.*, **9**, 231-234, (2006).
43. A. S. Abu-Surrah, H. H. Al-Sa'doni, M.Y. Abdalla, *J. of Cancer Therapy*, **6**, 1-10, (2008).
44. M. Sodeoka and Y. Hamashima, *J. of Pure Appl. Chem.*, **78**, 2, 477-494, (2006).
45. A. M. Asiri and S. A. Khan, *J. of Molecules*, **15**, 4784-4791, (2010).
46. J. R. Khusnutdinova, N. P. Rath, and L. M. Mirica, *J. of Angew. Chem. Int.*, **50**, 5532-5536, (2011).
47. A. J. Thomson, *Platinum Metals Rev.*, **21**, 1, 2-15, (1977).
48. T. Boulikas, A. Pantos, E. Bellis, and P. Christofis, *J. of Cancer Therapy*, **5**, 537-583, (2007).
49. S. Kanda, T. Koizumi, Y. Komatsu, S. Yoshikawa, M. Okada, O. Hatayama, M. Yasuo, K. Tsushima, K. Urushihata, K. Kubo, M. Sasabayashi and A. Takamizawa, *J. of Anticancer Research*, **27**, 3005-3008, (2007).
50. I. Kostova, *J. of Recent Patents on Anti-Cancer Drug Discovery*, **1**, 1-22, (2006).
51. M. V. Almeida, A. P. S. Fontes, R. N. Berg, E. T. César, E. C. A. Felício, and J. D. S. Filho, *J. of Molecules*, **7**, 405-411, (2002).
52. N. J. Wheate, and J. G. Collins, *J. of Coordination Chemistry Reviews*, **241**, 133-145, (2003).
53. A. Bakalova, H. Varbanov, R. Buyukliev, G. Momekov, D. Ivanov and I. Doytchinova, *J. of Inorg. Chem. Com.*, **11**, 209-216, (2011).
54. D. B. Dell'Amico, L. Labella and F. Marchetti, *J. of Molecules*, **16**, 6082-6091, (2011).

55. R. M. Silverstein, and G. C. Bassler “*Spectrometric Identification of Organic Compounds*”.6th. ed., John Wiley and Sons (1998).
56. K.Nakamoto, "*Infraredspectra of inorganic and coordination compounds*" 4th edition. Wiley, intr., New York (1996).
57. A. B. P. Lever, “*Inorganic Electronic Spectroscopy 2nd Edition*”, New York (1984).
58. G. Stanescu, and A.Trutia, *J. of Romanian Reports in Physics*, **57**, 2, 223–228, (2005).
59. Y. Sasak, *J. of Bull. Inst. Chem. Res., Kyoto Univ.*, **58**, 2, (1980).
60. A. Romerosa, C. S. Bello, M. S. Ruiz, A. Caneschi, V. McKee, M. Peruzzini, L. Sorace and F. Zanobini, *J. of Dalton Trans.*, **2003**, 3233-3239, (2003).
61. M.Tas, M.Yagan, H. Bati, B. Bati and O. Buyukgungor, *Indian J. of Chem.*, **47A**, 37-42, (2008).
62. I. T. Lim and K. Y. Choi, *Int. J. Mol. Sci.*, **12**, 2232-2241, (2011).
63. G. Mathew, R. Krishnan, M. Antony and M.S. Suseelan, *E-J. of CODEN ECJHAO*, **8**, 3, 1346-1354, (2011).
64. S.A. Shaker, *E-J. of CODEN ECJHAO*, **7SI**, 580-586, (2010).
65. G. Gencheva, D. Tsekova, G. Gochev, G. Momekov, G. Tyuliev, V. Skumryev, M. Karaivanova, and P. R. Bontchev, *J. of Metal-Based Drugs*, **2007**, 1-13, (2007).
66. F. A. Cotton, G. Wilkinson, "*Advanced Inorganic Chemistry*" 4th Edition, John Wiley and Sons (1980).
67. A. H. D. AL-Qhadeer, Ph.D thesis, **Baghdad University**, (2006).
68. S. A. Kettle “*Coordination Compound*” Thomas Nelson and Sons, London, p.3, 186, 212 (1975).



جمهورية العراق
وزارة التعليم العالي والبحث العلمي
جامعة كربلاء
كلية العلوم / قسم الكيمياء

**تحضير و تشخيص معقدات ثنائية النواة مع
ليكاندات جديدة غير متجانسة الحلقة مشتقة من
٥،٢-ثنائي-مركبتوا، ٣،٤-ثايدايزول بواسطة
كيمياء النقرة**

رسالة مقدمة إلى

مجلس كلية العلوم - جامعة كربلاء

وهي جزء من متطلبات نيل درجة الماجستير في الكيمياء

من قبل

أثير مهدي مدلول الرماحي

بكلوريوس علوم كيمياء (٢٠٠٣) الجامعة المستنصرية

بأشراف

أ.م. الدكتورة

ايمان طالب كريم

٢٠١٢ م

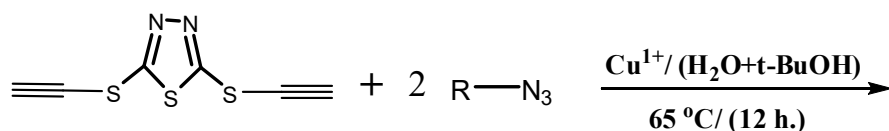
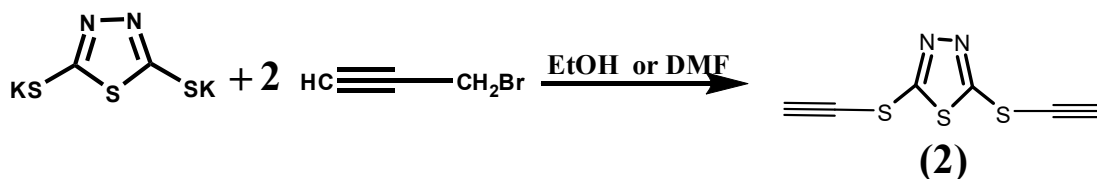
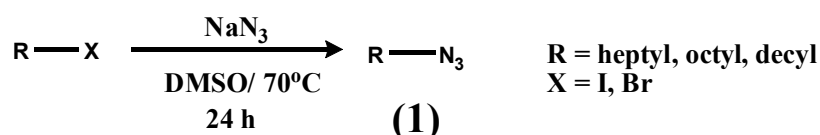
أ.م. الدكتور

عاشور حمود داود آل-غدير

١٤٣٣ هـ

الخلاصة:

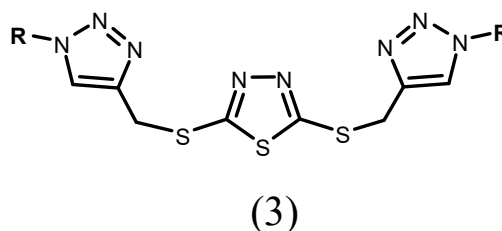
تضمن العمل تحضير وتشخيص ثلاث ليكاندات غير متجانسة الحلقة يحتوي كل ليكاند على ثلاث حلقات غير متجانسة اثنان منها ه حلقات الترايزول والحلقة الوسطية هي حلقة الثايدازول، حضرت الليكاندات من خلال تحضير مشتقين رئيسيين هما ازيد الالكيل الذي حضر من خلال مفاعلة هاليد الالكيل مع ازيد الصوديوم والمشتق الثاني هو تحضير الكاين طرفي من خلال اضافة البروبرجيل برومايد الى ملح البوتاسيوم للمركب ٢،٥-ثنائي مركبتوثايدازول وبعد ذلك جمع المشتقين من خلال كيمياء النقرة وبوجود كعامل مساعد والمخطط التالي يلخص المعادلة العامة للتحضير:



(3a) when R = Heptyl

(3b) when R = Octyl

(3c) when R = Decyl



استخدمت مطيافية الاشعة تحت الحمراء وفوق البنفسجية-المرئية وطيف الرنين النووي المغناطيسي كما اجري التشخيص الكمي الدقيق للعناصر اضافة الى فحص ذوبانية الليكاندات المحضرة بعدد من المذيبات المختلفة.

تم تحضير معقدات هذه الليكاندات مع ايونات الكوبلت والنيكل والنحاس والبلاديوم الثنائية اضافة الى ايون البلاتين الرباعي. شخّصت المعقدات المحضرة بمطيافية الاشعة تحت الحمراء وفوق البنفسجية-المرئية اضافة الى قياسات الحساسية المغناطيسية والتوصيلية الكهربائية المولارية وفحص ذوبانية المعقدات المحضرة بعدد من المذيبات المختلفة. ومن خلال القياسات اعلاه تم اقتراح الاشكال الفراغية للمعقدات وكانت كالشكل التالي:

رباعية السطوح لمعقدات الكوبلت الثنائي مع جميع الليكاندات ومربعة مستوية لمعقدات البلاديوم الثنائية مع جميع الليكاندات، أما معقدات النيكل والنحاس الثنائية والبلاتين الرباعي فهي ثمانية السطوح مع جميع الليكاندات:

